CARLOS ALEXANDRE GOMES RIBEIRO

IDENTIFICAÇÃO DE REGIÕES GENÔMICAS RELACIONADAS À SECA E DEFICIÊNCIA DE FÓSFORO VIA ANÁLISE DE LIGAÇÃO E MAPEAMENTO ASSOCIATIVO EM MILHO TROPICAL

Tese apresentada à Universidade Federal de Viçosa, como parte das exigências do Programa de Pós-Graduação em Genética e Melhoramento, para obtenção do título de Doctor Scientiae.

VIÇOSA
MINAS GERAIS - BRASIL
2015

Ficha catalográfica preparada pela Biblioteca Central da Universidade Federal de Viçosa - Câmpus Viçosa

T
R484i
2015

Ribeiro, Carlos Alexandre, 1985-
Identificação de regiões genômicas relacionadas á seca e deficiência de fósforo via análise de ligação e mapeamento associativo em milho tropical / Carlos Alexandre Ribeiro. – Viçosa, MG, 2015.
ix, 89f. : il. (algumas color.) ; 29 cm.

Orientador: Everaldo Gonçalves de Barros.
Tese (doutorado) - Universidade Federal de Viçosa.
Inclui bibliografia.

1. Milho - Melhoramento genético. 2. Genética vegetal. 3. Mapeamento genético. 4. Milho - Consumo hídrico. 5. Milho - Efeito do fósforo. I. Universidade Federal de Viçosa. Departamento de Biologia Geral. Programa de Pós-graduação em Genética e Melhoramento. II. Título.

CDD 22. ed. 633.15

CARLOS ALEXANDRE GOMES RIBEIRO

IDENTIFICAÇÃO DE REGIÕES GENÔMICAS RELACIONADAS À SECA E DEFICIÊNCIA DE FÓSFORO VIA ANÁLISE DE LIGAÇÃO E MAPEAMENTO ASSOCIATIVO EM MILHO TROPICAL

Tese apresentada à Universidade Federal de Viçosa, como parte das exigências do Programa de Pós-Graduação em Genética e Melhoramento, para obtenção do título de Doctor Scientiae.

APROVADA: 22 de outubro de 2015.

Dr. Luciano da Costa e Silva	Prof. Rodrigo Oliveira de Lima
Dra. Claudia Teixeira Guimarães (Coorientadora)	Dra. Sylvia Morais de Sousa Tinoco

Prof. Everaldo Gonçalves de Barros
(Orientador)

A meus pais Duílio e Rosa

À minha irmã Maria Virgínia e meu avô Carmo

AGRADECIMENTOS

Agradeço primeiramente a Deus por me proporcionar a oportunidade de crescimento pessoal e profissional através da experiência adquirida em mais uma importante etapa em minha vida.

À Universidade Federal de Viçosa, especialmente ao Programa de Pós-Graduação em Genética e Melhoramento pela oportunidade de realizar o curso.

À CAPES e ao CNPq pela concessão do financiamento dos estudos.

À Embrapa Milho e Sorgo que contribuiu diretamente aos estudos efetuados através da logística disponibilizada.

Ao Generation Challenge Program pelo financiamento das atividades de pesquisa.

Ao Professor Everaldo Gonçalves de Barros, não só pela orientação, mas pela amizade e pelo exemplo de profissionalismo e dedicação.

À minhas coorientadoras Claudia Teixeira Guimarães e Maria Marta Pastina que participaram intensamente do desenvolvimento da pesquisa. Muito obrigado pelos conselhos e pela confiança depositada durante esses anos.

Ao meu coorientador da Universidade de Cornell (EUA), Edward Buckler pela oportunidade, pelo exemplo e pelos ensinamentos.

Aos conselheiros, funcionários, professores e pesquisadores da Universidade Federal de Viçosa e Embrapa Milho e Sorgo pelo apoio e valiosa contribuição científica e profissional durante o desenvolvimento do trabalho, em especial a Gislene pela significativa contribuição na execução dos trabalhos.

Aos meus colegas, amigos e familiares que me acompanharam nessa jornada, participando direta ou indiretamente deste trabalho e sem dúvida foram fundamentais em todas as etapas.

À Juliana pelo apoio constante, companheirismo, carinho e compreensão.

Aos meus pais Duílio e Rosa, à minha irmã Maria Virgínia, e ao meu avô Carmo que nunca deixaram de me apoiar e me incentivar em todas as etapas da minha vida.

SUMÁRIO

RESUMO

RIBEIRO, Carlos Alexandre Gomes, D.Sc., Universidade Federal de Viçosa, outubro de 2015. **Identificação de regiões genômicas relacionadas à seca e à deficiência de fósforo via análise de ligação e mapeamento associativo em milho tropical**. Orientador: Everaldo Gonçalves de Barros. Coorientadores: Claudia Teixeira Guimarães e Maria Marta Pastina.

Estresses abióticos são aqueles impostos pelas condições edafo-climáticas ao longo do ciclo de uma cultura, que afetam seu desenvolvimento. Dentre os estresses abióticos que reduzem significativamente a produção de grãos do milho, podemos destacar a seca e a deficiência de fósforo. A compreensão dos mecanismos genéticos e fisiológicos em resposta a esses estresses pode fornecer ferramentas importantes para aumentar a tolerância e a produtividade das culturas, por meio da seleção assistida ou da transgenia. Estratégias de mapeamento de QTLs (Quantitative Trait Loci) e mapeamento associativo vêm sendo amplamente utilizadas com o objetivo de dissecar características complexas com elevado efeito de background genético e influência ambiental, tornando-os passíveis de seleção. Assim, o presente trabalho utilizou essas duas estratégias de mapeamento para identificar regiões genômicas envolvidas na resposta do milho à seca e à deficiência de fósforo. No mapeamento de QTLs, foi utilizada uma abordagem de modelos mistos em duas populações de milho tropical sob condições contrastantes de disponibilidade de água, sendo avaliados: produção de grãos, altura de planta e intervalo de florescimento. Altura de plantas e intervalo de florescimento foram incluídos como cofatores, contribuindo para melhorar a precisão na identificação de QTLs para a produção de grãos. Dezessete regiões genômicas foram identificadas para produção de grãos com ou sem co-fatores, além de dez QTLs para altura de planta e sete para intervalo de florescimento detectados nas duas populações de mapeamento. Em geral, ambos os pais de cada população contribuíram com alelos favoráveis. O efeito dos cofatores foi mais expressivo na população derivada do cruzamento L1761121 x L521237. Nessa população, QTLs para intervalo de florescimento nos cromossomos 3, 4 e 9 foram co-localizados com QTLs para produção de grãos, exceto quando o intervalo de florescimento foi incluído como co-fator no modelo, indicando que fatores genéticos comuns possam controlar ambas as características nessas regiões. Em quatro regiões genômicas nos cromossomos 1, 3, 6 e 8, foram detectados QTLs para produção de grãos coincidentes em ambas as populações, que também foram consistentemente identificados em outros estudos, sugerindo uma estabilidade desses QTLs em diferentes ambientes

e background genéticos, com uso potencial no melhoramento assistido. A deficiência de fósforo (P) é um problema recorrente principalmente em solos tropicais. A proliferação e o desenvolvimento do sistema radicular são estratégias para maximizar a exploração do solo, aumentando a eficiência na aquisição de P pelas plantas. Esse estresse abiótico foi abordado por meio do mapeamento associativo em um painel composto por 561 linhagens de milho tropical. O painel foi genotipado com marcadores SNPs gerados pela genotipagem por sequenciamento (GBS) e fenotipado para características de morfologia radicular e aquisição de P em solução nutritiva sob baixa e alta concentração de P. Modelos lineares mistos corrigidos para os efeitos de estrutura de populações e de parentesco permitiram a identificação de 136 SNPs associados com um conjunto de seis características, considerando a significância de $-\log_{10}$ (P-valor) ≥ 5. O decaimento médio do desequilíbrio de ligação foi de 1000 pares de bases, demonstrando uma alta diversidade genética das linhagens. Os SNPs significativos foram bem distribuídos em todos os cromossomos, confirmando a complexidade genética das características de morfologia radicular e de aquisição de P. O SNP apresentando a maior probabilidade de associação (S8_89092905) foi localizado dentro do gene GRMZM2G044531 no cromossomo 8, que codifica uma provável proteína da família AGC quinase. Esse SNP aumenta o comprimento e a área superficial das raízes, principalmente sob baixa concentração de P, com influência mínima no diâmetro radicular. Além disso, a uma distância de 127,4 kbp desse SNP, um outro SNP (S8_88964594), posicionado no gene GRMZM2G057116, que codifica um fator de transcrição da família WRKY, foi também associado com tais características fenotípicas. Apesar desses SNPs estarem fisicamente distantes, eles compartilham um alto desequilíbrio de ligação ($r^2 = 0,77$), superior ao valor médio encontrado ($r^2 = 0,18$) da região de 610 kbp onde eles estão localizados. Tais informações associadas com a natureza desses genes preditos, os tornam candidatos para futuros estudos de validação. Integrando os resultados desses dois estudos, uma região no cromossomo 8 entre os bins 8.02 e 8.03 merece destaque por terem sido detectados QTLs para produção de grãos sob estresse hídrico em duas populações e SNPs significativamente associados com morfologia. Assim, essa região genômica é altamente recomendada como alvo tanto para o melhoramento assistido quanto para a busca por genes candidatos, visando desenvolver genótipos de milho adaptados e produtivos em condições de estresses.

ABSTRACT

RIBEIRO, Carlos Alexandre Gomes, D.Sc., Universidade Federal de Viçosa, October, 2015. **Identification of genomic regions related to drought and phosphorus deficiency by linkage analysis and association mapping in tropical maize**. Adviser: Everaldo Gonçalves de Barros. Co-advisers: Claudia Teixeira Guimarães e Maria Marta Pastina.

Abiotic stresses are those imposed by soil and climatic conditions throughout the cycle of a culture that affect their development and production stability. Among the abiotic stresses that significantly reduce maize grain yield, we can highlight the drought and phosphorus deficiency. Understanding the genetic and physiological mechanisms in response to these stresses can provide important tools to increase tolerance and crop productivity, through assisted selection or genetic modification. QTL (Quantitative Trait Loci) and association mapping strategies have been widely used in order to dissect complex traits with high genetic background effect and environmental effect, making them eligible for selection. Thus, the present study used these two mapping strategies to identify loci that are involved in maize response to drought and phosphorus deficiency. In the QTL mapping it was used a mixed model approach in two populations of tropical maize in contrasting conditions of water availability, in which we evaluated grain yield, plant height and anthesis-silking interval. The traits plant height and anthesis-silking interval were included as cofactors in QTL model, contributing to improved precision in the QTL identification for grain yield. Seventeen genomic regions were identified for grain yield with or without co-factors, additionally ten QTLs for plant height and seven for anthesis-silking interval were also detected in both mapping populations. In general, both parents of each population contributed with favorable alleles. The effect of cofactors was more marked in the population derived from the cross L1761121 x L521237. In this population, QTL for anthesis-silking interval on chromosomes 3, 4 and 9 were co-located with QTLs for grain yield, except when the anthesis-silking interval was included as co-factor in the model, indicating that common genetic factors may control both traits in these regions. On four genomic regions on chromosomes 1, 3, 6 and 8, QTLs were detected for grain yield in both populations, which have also been consistently identified in other studies, suggesting stability of these QTLs in different environments and genetic background, with potential use in assisted breeding. Phosphorus deficiency (P) is a recurring problem mainly in tropical soils. The proliferation and development of the root system are strategies to maximize the soil exploitation, increasing P acquisition efficiency by plants. This abiotic stress was addressed

through association mapping on a panel of 561 tropical maize inbreed lines. The panel was genotyped with SNP markers generated by genotyping-by-sequencing (GBS) and phenotyped for root morphology traits and P acquisition in nutrient solution under low and high P concentration. Mixed linear models corrected for population structure and kinship effects allowed the identification of 136 SNPs associated with a set of six traits considering the significance of $-\log_{10}$ (P-value) ≥ 5. The average decay of linkage disequilibrium was 1000 base pairs, showing a high genetic diversity in this panel. The significant SNPs were well distributed in all chromosomes, confirming the genetic complexity of root morphology traits and P acquisition. The SNP presenting the highest association probability (S8_89092905) was placed inside the GRMZM2G044531 gene on chromosome 8, which encodes a putative AGC kinase family protein. This SNP increases the root length and surface area, particularly under low P concentration with minimal influence on root diameter. Furthermore, at a distance of 127.4 kbp upstream, another SNP (S8_88964594) placed inside the gene GRMZM2G057116, encoding a putative WRKY transcription factor, also associated with such phenotypic traits. Despite these SNPs are physically distant, they share high linkage disequilibrium ($r^2 = 0.77$), higher than the average found ($r^2 = 0.18$) of 610 kbp region where they are located. Such information associated with the nature of these predicted genes, makes them candidates for future validation studies. Integrating the results of these two studies, a region on chromosome 8 between the bins 8.02 and 8.03 was noteworthy for have detected QTLs for grain yield under water stress in two populations and SNPs significantly associated with root morphology. Thus, this genomic region is highly recommended as target for marker-assisted breeding and for search of candidate genes in order to develop maize genotypes adapted and productive under stress conditions.

INTRODUÇÃO GERAL

Importância do milho

O milho (Zea mays L. spp. mays) é uma gramínea da família Poaceae, sendo o cereal mais produzido no mundo, com produção mundial estimada em um bilhão de toneladas do grão para a safra 2014/15 (USDA, 2015). O Brasil ocupa a terceira posição no ranking dos maiores produtores mundiais, atrás dos Estados Unidos e da China, e a segunda posição entre os maiores exportadores do grão, atrás apenas dos Estados Unidos. A produção brasileira de milho, considerando a primeira e a segunda safra de 2014/2015, foi de 84,7 milhões de toneladas ocupando uma área de 15,7 milhões de hectares, com uma produtividade média de 5,4 toneladas por hectare (CONAB, 2015).

O milho é um dos produtos de maior destaque do setor agrícola nacional, devido as suas amplas formas de utilização, que incluem a alimentação animal, que representa a maior parte do consumo desse cereal (70%), principalmente para aves e suínos; a alimentação humana; a indústria, com a produção de solventes, vitaminas, conservantes, estabilizadores e adoçantes; a produção de óleo e de biocombustível.

Além da sua importância econômica e social, o milho é uma das espécies cultivadas mais bem estudadas do ponto de vista genético, fisiológico e bioquímico. O genoma do milho foi completamente sequenciado, cujo tamanho varia de 2,3 a 2,7 Gb (giga bases), ao longo de 10 cromossomos, contendo mais de 30.000 genes (Schnable et al., 2009). Assim, os estudos genéticos em milho têm contribuído significativamente para o entendimento da estrutura, função e inter-relações moleculares, apesar da sua complexidade genômica, composto por cerca de 80% de elementos transponíveis.

Efeito do estresse à seca na estabilidade de produção

Estresses abióticos são aqueles impostos pelas condições edafo-climáticas ao longo do ciclo de uma cultura, que afetam seu desenvolvimento e a estabilidade da produção (Verslues et al., 2006). A produção agrícola, em diversas partes do mundo, é diretamente afetada por fenômenos climáticos adversos cada vez mais frequentes como, alterações na temperatura, pluviosidade, umidade do solo, radiação solar, dentre outros. Dentre os principais fatores abióticos que interferem na produção, destaca-se o déficit hídrico que ocorre quando a perda de água pela planta excede a capacidade de absorção pela raiz, provocando danos irreversíveis à planta (Jaleel

et al., 2007). Sob condições de deficiência hídrica, um dos primeiros efeitos é a redução da turgescência da célula e alterações dos processos fisiológicos dependentes do turgor, como o crescimento celular (Taiz e Zeiger, 2004). A severidade do efeito causado pelo déficit hídrico dependerá da intensidade e da duração do estresse, além do quão adaptada está a cultura ou o genótipo para tolerar o estresse.

Além disso, como a ocorrência da seca em condições naturais é de difícil previsão, e muitas vezes associada a outros estresses como o calor e deficiência de nutrientes, dificulta ainda mais a mensuração desses efeitos em campo, o que implica em novos desafios frente às constantes alterações climáticas. Durante o déficit hídrico, a diminuição na disponibilidade de água afeta a taxa de transpiração bem como o transporte de metabólitos, que acarreta a diminuição da captação de nutrientes, como nitrogênio e fósforo, e a alteração na concentração desses compostos em diferentes órgãos da planta (Ge et al., 2012). Assim, quanto maior for o estresse hídrico, menor será a captação desses nutrientes.

Mecanismos de adaptação à seca em milho

Diversos mecanismos morfológicos são acionados nas plantas para adaptação ao estresse à seca (Farooq et al., 2009). Esses mecanismos podem ser classificados em: escape, evitação (avoidance) e tolerância. O escape está relacionado com o encurtamento do ciclo de vida permitindo que as plantas se reproduzam antes que o ambiente apresente limitação hídrica. Características como tempo de floração reduzido são relacionadas com uma melhor adaptação ao déficit hídrico, onde um menor ciclo de vida pode favorecer o escape (Araus et al., 2012). A evitação consiste em mecanismos voltados a redução da perda de água pela planta como o controle da transpiração pelo estômato e a manutenção da captação de água pelo sistema radicular (Kavar et al., 2008). Adaptações morfológicas como aumento de suberização do caule e da raiz, formação de cutículas mais espessas nas folhas ou alteração em sua composição como heteroplastia, abscisão foliar, redução no tamanho das folhas e redução do crescimento da parte aérea em relação ao sistema radicular são fundamentais para uma maior tolerância ao déficit hídrico (Taiz e Zeiger, 2004). Estruturas como tricomas foliares também apresentam uma função importante ao reduzir a transpiração e a temperatura das folhas por refletir a luz solar (Farooq et al., 2009). Os mecanismos de tolerância estão relacionados à defesa da planta a partir do aparecimento do déficit hídrico. Tolerância a seca é definida como a capacidade relativa de sustentar ou conservar a função da

planta em um estado de desidratação, sendo, às vezes, visto como a segunda linha de defesa, após os mecanismos de evitação (Blum, 2005). Os mecanismos de escape e evitação são muito mais conhecidos nas plantas do que mecanismos de tolerância, um dos principais exemplos de mecanismos de tolerância é a remobilização das reservas de carboidrato do caule para o enchimento de grãos sob estresse hídrico (Blum, 1998). Este processo permite o enchimento de grãos de forma eficaz, quando toda a fotossíntese da planta é inibida pelo estresse, desde que quantidade suficiente de carboidrato tenha sido armazenada antes do enchimento de grãos (Blum, 2005).

Além dos mecanismos morfológicos, mecanismos bioquímicos e fisiológicos alternativos são ativados em função da baixa disponibilidade de água no solo e/ou alta demanda evaporativa que retardam o aparecimento do déficit hídrico. Com o aumento da severidade do estresse hídrico, a fotossíntese e a transpiração são atingidas devido, principalmente, à regulação dos estômatos (Kumar et al., 1994). As células-guarda dos estômatos necessitam de água para sua abertura e fechamento, promovendo as trocas gasosas. O fechamento estomático diminui a entrada de CO_2, tornando-o pouco disponível para a assimilação na fotossíntese, reduzindo a eficiência da fotossíntese e acumulando energia nos centros de reação dos fotossistemas, o que resulta na formação de espécies reativas de oxigênio (ROS) que causam desintegração de membranas causada pelo estresse oxidativo (Tambussi et al., 2000).

Apesar do déficit hídrico causar efeitos negativos à produção ao longo de todo o desenvolvimento da cultura, em milho são elencados três importantes estádios de desenvolvimento, onde essa deficiência acarreta danos mais severos. Os estádios de desenvolvimento críticos são: i) iniciação floral e desenvolvimento da inflorescência, quando o número potencial de grãos é determinado (estádio v3); ii) período de fertilização, quando deve-se evitar a desidratação do grão de pólen e garantir o desenvolvimento do tubo polínico, sendo fixado o potencial de produção; e iii) enchimento de grãos, quando ocorre a deposição de matéria seca, sendo determinado o peso dos grãos (Magalhaes e Duraes, 2006).

Em milho, características como altura de planta e intervalo de florescimento estão correlacionadas com produção de grãos em condições de estresse hídrico. Sob estresse hídrico o crescimento radicular é beneficiado comparado a parte aérea de modo a favorecer a captação de água. Em situações onde o estresse é mais severo o crescimento da parte aérea é completamente interrompido, consequentemente a produção de grãos é afetada, uma vez que a planta necessita

alcançar uma estatura suficiente para ter um nível adequado de fotoassimilados (Lu et al., 2012). Embora a base da vulnerabilidade do milho no período de florescimento não seja entendida por completo, evidências indicam que as linhagens mais adaptadas favorecem a estrutura reprodutiva em detrimento da parte vegetativa sob déficit hídrico (Setter et al., 2011). Em condições de estresse em geral ocorre um atraso na emergência do estilo-estigma resultando em dessincronia de florescimento dos órgãos reprodutores masculino e feminino, ocasionando o aborto de grãos (Cattivelli et al., 2008).

Bases moleculares da resposta ao estresse à seca

Vários estudos vêm contribuindo para identificação de regiões genômicas relacionadas com a resposta ao estresse hídrico em milho (Agrama e Moussa, 1996; Malosetti et al., 2008; Messmer et al., 2009; Messmer et al., 2011; Almeida et al., 2013). Características como produção de grãos, altura de planta e intervalo de florescimento são frequentemente avaliadas em estratégias de mapeamento genético visando a identificação e a utilização de QTLs (Quantitative Trait Loci) no intuito de elevar a tolerância de genótipos em um contexto de melhoramento de plantas. Cinco QTLs para a redução do intervalo entre o florescimento masculino e feminino foram introgredidos por retrocruzamento assistido em linhagens elites de milho sensíveis à seca, resultando em uma maior estabilidade de produção em comparação a linhagens não melhoradas em condições de estresse hídrico severo (Ribaut e Ragot, 2007). No entanto, a vantagem produtiva diminuiu sob estresses menos intensos, desaparecendo quando o estresse causou uma redução na produção menor que 40%. Apesar de várias regiões genômicas identificadas, ainda é limitado o conhecimento a respeito da resposta ao estresse com relação aos genes envolvidos.

Estudos funcionais envolvendo a caracterização molecular do papel fisiológico de genes relacionados ao estresse hídrico em diferentes estágios de resposta podem ajudar a elucidar os mecanismos regulatórios envolvidos com a resposta ao estresse. O ácido abscísico (ABA) é um regulador central de diversas respostas de plantas para estresses ambientais tendo papel importante na integração de sinais após a percepção do estresse (Tran et al., 2007). O déficit hídrico tende a aumentar a concentração de ABA que promove o fechamento dos estômatos, limitando a difusão de CO_2 de espaços intercelulares para o interior dos cloroplastos durante a seca exercendo influência no desenvolvimento da semente (Cornic, 2000; Setter e Parra, 2010).

Quinases e fosfatases têm sido descritas como enzimas importantes na transdução de sinais em resposta ao estresse osmótico em plantas, como membros da família MAPK (Mitogen-Activated Protein Kinases) dependentes de Ca^{2+} e as SnRK (SNF1 related kinases), que atuam como um regulador do fechamento estomático em resposta ao ABA (Mustilli et al., 2002; Brock et al., 2010). Plantas com redução ou aumento na expressão de genes que codificam muitas destas quinases, são mais ou menos tolerantes ao estresse hídrico, respectivamente (Mustilli et al., 2002). Estes resultados demonstram a importância das quinases nos mecanismos de tolerância à seca, colocando-as como candidatas para estudo e potencial aplicação no desenvolvimento de genótipos tolerantes à seca.

Efeito do estresse por deficiência de fósforo na estabilidade de produção

O Cerrado brasileiro possui uma das maiores áreas potencialmente cultiváveis no mundo, cujo solo é ácido por natureza. Solos ácidos limitam a produção agrícola em 30 a 40% das terras cultivadas mundiais (Haug, 1984). A baixa fertilidade natural desses solos, juntamente com uma combinação de compostos minerais tóxicos como o alumínio e o manganês, inibem o crescimento radicular, limitando o desenvolvimento das plantas. Por outro lado, o bioma Cerrado apresenta diversas vantagens agronômicas no que tange à topografia, ao clima e às condições físicas do solo, assumindo, por isso, um papel importante na agricultura nacional.

Uma das principais limitações à produção agrícola nos solos ácidos é a baixa disponibilidade de fósforo (P), cuja difusão é fortemente limitada pela sua fixação com óxidos de alumínio e de ferro na fração argila (Shen et al., 2011). Assim, o P é um dos nutrientes com o menor índice de eficiência de uso pelas plantas, sendo que apenas 5% dos fertilizantes aplicados são efetivamente absorvidos pelas plantas. Portanto, altas dosagens de adubação fosfatada são necessárias para suprir os requerimentos das culturas. O P é um dos nutrientes minerais mais importantes para o crescimento e desenvolvimento das plantas, sendo o segundo nutriente mais limitante para a produção de grãos depois do nitrogênio (Vance e Chiou, 2011). Reduções de até 50% no rendimento das culturas têm sido observadas sob deficiência de P em relação a áreas de fertilização contínua (Baligar e Fageria, 1997). Por outro lado, uma grande proporção de agricultores de baixa renda não tem acesso aos fertilizantes fosfatados, comprometendo assim a produção agrícola nessas áreas (Sharpley et al., 2001; Lynch, 2011).

Mecanismos de adaptação à deficiência de fósforo

As plantas utilizam vários mecanismos de adaptação à baixa disponibilidade de P, que podem ser classificados em dois grupos principais: eficiência de aquisição e eficiência de utilização interna (Vance et al., 2003; Parentoni e Souza Júnior, 2008). A eficiência de aquisição é definida como a quantidade de nutriente absorvido pela planta dividido pela quantidade de nutriente suprido à cultura (Moll et al., 1982). A eficiência de utilização interna está relacionada com a quantidade de produto (grãos) produzido por unidade de nutriente (Good et al., 2004), envolvendo, principalmente a reciclagem, a translocação e o armazenamento de fósforo na planta (Schachtman et al., 1998; Baligar et al., 2001; Shenoy e Kalagudi, 2005).

A eficiência na aquisição de P apresentou maior influência na eficiência no uso de P do que a eficiência de utilização interna em genótipos de milho tropical (Parentoni e Souza Júnior, 2008). Como o P possui baixa mobilidade no solo, a principal estratégia para sua aquisição consiste em maximizar a exploração do solo por meio da proliferação e da extensão do sistema radicular (Ramaekers et al., 2010). Assim, genótipos mais eficientes na aquisição de P apresentaram pelos radiculares longos e densos (Lynch, 2007), raízes laterais mais longas (Zhu e Lynch, 2004), maior ramificação e área de superfície radicular (Lynch, 2007). Além das mudanças na morfologia radicular, outros mecanismos estão envolvidos na adaptação a baixa disponibilidade de P como a exsudação de ácidos orgânicos e de outros compostos orgânicos de baixo peso molecular para a rizosfera e associação das raízes com microrganismos, como fungos micorrízicos arbusculares (Vance et al., 2003; Ramaekers et al., 2010; Lynch, 2011).

A compreensão dos mecanismos genéticos associados com a morfologia radicular pode auxiliar na seleção de linhagens com eficiência de aquisição de P em condições de baixa disponibilidade desse nutriente por potencializar a exploração do solo (Lynch, 2007). Na maioria dos solos, as camadas superiores são as que possuem maior biodisponibilidade de P. Dentre as adaptações das plantas com o intuito de aumentar a superfície de absorção de P, as alterações na morfologia de pelos radiculares são aquelas com menor custo energético (Gahoonia e Nielsen, 2004; Kochian et al., 2004; Haling et al., 2013). Assim, uma estratégia promissora para contribuir para minimizar os efeitos da deficiência de P em solos seria explorar a diversidade genética para características radiculares e para parâmetros de eficiência na aquisição de P (Wissuwa et al., 2009). Apesar da sua importância, características radiculares raramente são utilizadas como critérios de seleção devido a sua difícil avaliação, principalmente em condições de campo.

Bases moleculares da resposta ao estresse por deficiência de P

Genes que controlam o desenvolvimento radicular também podem ser alvos para a seleção com propósito de aumentar a tolerância à deficiência hídrica e de fósforo. Características como comprimento total radicular e área de superfície total têm sido correlacionadas tanto com maior tolerância a seca (Li et al., 2015) quanto para melhor aquisição de P (De Souza et al., 2012), demonstrando uso potencial de seleção considerando ambos os estresses. No entanto, a seleção de genótipos com base em características radiculares não vem sendo realizada em função das dificuldades na avaliação fenotípica.

Morfologia de raiz é uma característica complexa em milho, sendo controlada por vários genes (Tuberosa et al., 2002; Ramaekers et al., 2010). Apesar de vários QTLs associados com a morfologia do sistema radicular e com a aquisição de P terem sido identificados em solução nutritiva e em condições de campo (Zhu et al., 2005a; b; Chen et al., 2008), apenas um número limitado de genes candidatos foram associados com tais características. Um QTL de efeito maior controlando absorção de P (Pup1) foi identificado em arroz, explicando cerca de 80% da sua variação fenotípica (Wissuwa et al., 2002), sendo também associado com um aumento na área superficial da raiz em condições de baixo P (Wissuwa e Ae, 2001). Phosphorus-starvation tolerance 1 (PSTOL1) foi identificado como um gene responsável pelos efeitos do Pup1, que codifica uma proteína quinase envolvida no crescimento inicial da raiz e na absorção de P, aumentando também a produção de grãos em variedades em arroz cultivadas sob deficiência de P (Gamuyao et al., 2012). Recentemente, quatro homólogos do gene PSTOL1 de milho foram co-localizados com QTLs relacionados com características radiculares e índices de eficiência de aquisição de P em solução nutritiva sob estresse de P (Azevedo et al., 2015). Outros genes associados com a morfologia da raiz foram identificados em milho, tais como roothairless (rth1) (Wen et al., 2005), brittle stalk-2-like protein 3 (bk2L3) (Brady et al., 2007), e rootless concerning crown and seminal roots (rtcs) (Taramino et al., 2007).

Mapeamento por meio de ligação e associação para análise de características quantitativas

Os primeiros estudos identificando associações entre variações fenotípicas e marcas genéticas foram baseados em marcadores morfológicos e citológicos. A partir do desenvolvimento de marcadores moleculares como RFLP (Restriction Fragment Length Polymorphism), AFLP

(Amplified Fragment Length Polymorphism), SSR (Simple Sequence Repeats) e SNP (Single-Nucleotide Polymorphism), o mapeamento genético começou a ser amplamente utilizado na decomposição de características genéticas complexas em seus componentes mendelianos. A grande disponibilidade de marcadores com densa cobertura dos genomas, aliada aos procedimentos estatísticos avançados, tem permitido a identificação de regiões genômicas associadas com características de interesse agronômico para a maioria das espécies vegetais.

O mapeamento de QTLs baseado em análises de ligação genética é realizado em populações estruturadas derivadas de cruzamento entre dois genótipos contrastantes para a característica de interesse, seguido por ciclos de autofecundação ou de retrocruzamentos, como retrocruzamento, F_2 e RILs (Recombinant Inbred Lines). O grau de associação entre marcadores moleculares e variações fenotípicas é um indicativo da frequência de recombinação entre o marcador e o QTL, quanto menor a frequência de recombinação entre os locos, maior será o grau de associação. A baixa frequência de recombinação entre locos não é garantia de proximidade física entre locos, pois outros fatores como proximidade do centrômero tendem a diminuir a frequência de recombinação. Alguns dos métodos utilizados para o mapeamento de QTL são os modelos lineares baseado em ANOVA e regressão linear, mapeamento por intervalo simples, mapeamento por intervalo composto (Jansen e Stam, 1994) e mapeamento por múltiplos intervalos (Kao et al., 1999).

O mapeamento por associação ou mapeamento associativo é baseado no desequilíbrio de ligação (DL), utilizando populações naturais, coleções de germoplasma ou conjunto de genótipos elites. O DL ou também chamado desequilíbrio de fase gamética é uma associação não aleatória de alelos em uma população, ou seja, é a ocorrência de gametas com frequências diferentes daquelas esperadas sob segregação independente. O DL pode ser afetado pela deriva genética, estrutura populacional, seleção natural ou artificial, epistasia e pelo sistema reprodutivo. A eficácia do mapeamento por associação depende da possibilidade de corrigir o desequilíbrio de ligação oriundo da ligação física propriamente dita do desequilíbrio de ligação decorrente da estrutura populacional (Remington et al., 2001). A estrutura populacional é vista como a segunda principal causa de associação entre marcadores e caracteres fenotípicos, presente na maioria das populações vegetais apresentando algum grau de estruturação ou subdivisão (Flint-Garcia et al., 2003; Mackay e Powell, 2007). O grau de parentesco entre os indivíduos do painel também deve ser considerado no mapeamento por associação, principalmente quando se utilizam painéis envolvendo

germoplasmas melhorados, descendentes de um pequeno grupo de linhagens fundadoras (Yu et al., 2006). O controle dos falsos positivos provenientes da estrutura de população e do parentesco entre indivíduos permite uma maior precisão na identificação de regiões potenciais relacionadas com a característica de interesse, favorecendo a busca pelos genes alvo com maior segurança.

O mapeamento associativo tem como vantagens a análise de múltiplos alelos, representando um conjunto de genótipos ou mesmo a espécie, ao contrário de apenas dois alelos avaliados nas populações biparentais. As populações segregantes são demoradas para obtenção e envolvem um custo para o desenvolvimento, ao passo que um painel para mapeamento associativo requer apenas uma coleção de genótipos. A resolução do mapeamento genético (QTL e associativo) depende da recombinação entre o marcador e o loco que controla a característica de interesse. Desta forma, no caso das análises de ligação baseadas em populações experimentais, uma menor resolução é observada, devido ao menor número de gerações de recombinação comparado com populações não estruturadas, onde muitas gerações de recombinação ocorreram entre marcador e QTL, considerando o histórico de recombinação das linhagens avaliadas (Yu e Buckler, 2006).

Uma das limitações do mapeamento por desequilíbrio de ligação é a baixa confiabilidade na detecção de alelos raros na população, principalmente se eles possuírem um pequeno efeito sobre a característica. Nos casos de alelos raros, as populações biparentais seriam mais adequadas para o mapeamento, pois seriam feitos cruzamentos controlados em que a população experimental herdaria o alelo de interesse. Por estas razões, é possível afirmar que esses são métodos complementares e que uma estratégia interessante seria utilizar o mapeamento por associação para refinar a localização do QTL previamente identificado através da análise de ligação em populações estruturadas, assim contribuindo de uma forma mais precisa para uma melhor compreensão da estrutura genética.

REFERÊNCIAS BIBLIOGRÁFICAS

AGRAMA, H. A. S.; MOUSSA, M. E. Mapping QTLs in breeding for drought tolerance in maize (Zea mays L). **Euphytica,** v. 91, n. 1, p. 89-97, 1996. ISSN 0014-2336. Disponível em: < <Go to ISI>://WOS:A1996VP38000010 >.

ALMEIDA, G. D. et al. QTL mapping in three tropical maize populations reveals a set of constitutive and adaptive genomic regions for drought tolerance. **Theoretical and Applied Genetics,** v. 126, n. 3, p. 583-600, Mar 2013. ISSN 0040-5752. Disponível em: < <Go to ISI>://WOS:000315441800003 >.

ARAUS, J. L.; SERRET, M. D.; EDMEADES, G. O. Phenotyping maize for adaptation to drought. **Frontiers in Physiology,** v. 3, 2012. ISSN 1664-042X. Disponível em: < <Go to ISI>://WOS:000209173000299 >.

AZEVEDO, G. C. et al. Multiple interval QTL mapping and searching for PSTOL1 homologs associated with root morphology, biomass accumulation and phosphorus content in maize seedlings under low-P. **BMC Plant Biology,** v. 15, Jul 7 2015. ISSN 1471-2229. Disponível em: < <Go to ISI>://WOS:000357561900003 >.

BALIGAR, V. C.; FAGERIA, N. K. Nutrient use efficiency in acid soils: nutrient management and plant use efficiency. In: Moniz, A. C.; Furlani, A. M. C.; Schaffertm, R. E.; Rosolem, C. A. e Canatarella, H. (Ed.). **Plant–soil interactions at low pH: sustainable agriculture and forestry roduction**. 1997. p. 75–97.

BALIGAR, V. C.; FAGERIA, N. K.; HE, Z. L. Nutrient use efficiency in plants. **Communications in Soil Science and Plant Analysis,** v. 32, n. 7-8, p. 921-950, 2001. ISSN 0010-3624. Disponível em: < <Go to ISI>://WOS:000170101800002 >.

BLUM, A. Improving wheat grain filling under stress by stem reserve mobilisation (Reprinted from Wheat: Prospects for global improvement, 1998). **Euphytica,** v. 100, n. 1-3, p. 77-83, 1998. ISSN 0014-2336. Disponível em: < <Go to ISI>://WOS:000073208800011 >.

BLUM, A. Drought resistance, water-use efficiency, and yield potential - are they compatible, dissonant, or mutually exclusive? **Australian Journal of Agricultural Research,** v. 56, n. 11, p. 1159-1168, 2005. ISSN 0004-9409. Disponível em: < <Go to ISI>://WOS:000233570500006 >.

BRADY, S. M. et al. Combining expression and comparative evolutionary analysis. The COBRA gene family. **Plant Physiology,** v. 143, n. 1, p. 172-187, Jan 2007. ISSN 0032-0889. Disponível em: < <Go to ISI>://WOS:000243350600019 >.

BROCK, A. K. et al. The Arabidopsis Mitogen-Activated Protein Kinase Phosphatase PP2C5 Affects Seed Germination, Stomatal Aperture, and Abscisic Acid-Inducible Gene Expression. **Plant Physiology,** v. 153, n. 3, p. 1098-1111, Jul 2010. ISSN 0032-0889. Disponível em: < <Go to ISI>://WOS:000279400200017 >.

CATTIVELLI, L. et al. Drought tolerance improvement in crop plants: An integrated view from breeding to genomics. **Field Crops Research,** v. 105, n. 1-2, p. 1-14, Jan 2 2008. ISSN 0378-4290. Disponível em: < <Go to ISI>://WOS:000252464800001 >.

CHEN, J. Y. et al. QTL mapping of phosphorus efficiency and relative biologic characteristics in maize (Zea mays L.) at two sites. **Plant and Soil,** v. 313, n. 1-2, p. 251-266, Dec 2008. ISSN 0032-079X. Disponível em: < <Go to ISI>://WOS:000260961600020 >.

COMPANHIA NACIONAL DE ABASTECIMENTO - CONAB. **Acompanhamento da Safra Brasileira: Grãos - Safra 2014/2015 - Décimo segundo levantamento**. Disponível em: <http://www.conab.gov.br/>. Acesso em 20 de setembro de 2015.

CORNIC, G. Drought stress inhibits photosynthesis by decreasing stomatal aperture - not by affecting ATP synthesis. **Trends in Plant Science,** v. 5, n. 5, p. 187-188, May 2000. ISSN 1360-1385. Disponível em: < <Go to ISI>://WOS:000086954500002 >.

DE SOUSA, S. M. et al. A role for root morphology and related candidate genes in P acquisition efficiency in maize. **Functional Plant Biology**, v. 39, n. 10-11, p. 925-935, 2012. ISSN 1445-4408. Disponível em: < <Go to ISI>://WOS:000310380800011 >.

FAROOQ, M. et al. Plant drought stress: effects, mechanisms and management. In: LICHTFOUSE, E. et al. (eds.). Sustainable Agriculture: Springer, 2009. 29: 185-212.

FLINT-GARCIA, S. A.; THORNSBERRY, J. M.; BUCKLER, E. S. Structure of linkage disequilibrium in plants. **Annual Review of Plant Biology,** v. 54, p. 357-374, 2003. ISSN 1040-2519. Disponível em: < <Go to ISI>://WOS:000185094100014 >.

GAHOONIA, T. S.; NIELSEN, N. E. Root traits as tools for creating phosphorus efficient crop varieties. **Plant and Soil,** v. 260, n. 1-2, p. 47-57, Mar 2004. ISSN 0032-079X. Disponível em: < <Go to ISI>://WOS:000221763000005 >.

GAMUYAO, R. et al. The protein kinase Pstol1 from traditional rice confers tolerance of phosphorus deficiency. **Nature,** v. 488, n. 7412, p. 535-+, Aug 23 2012. ISSN 0028-0836. Disponível em: < <Go to ISI>://WOS:000307761600042 >.

GE, T. D. et al. Effects of drought stress on phosphorus and potassium uptake dynamics in summer maize (Zea mays) throughout the growth cycle. **Acta Physiologiae Plantarum**, v. 34, n. 6, p. 2179-2186, Nov 2012. ISSN 0137-5881. Disponível em: < <Go to ISI>://WOS:000310165900012 >.

GOOD, A. G.; SHRAWAT, A. K.; MUENCH, D. G. Can less yield more? Is reducing nutrient input into the environment compatible with maintaining crop production? **Trends in Plant Science,** v. 9, n. 12, p. 597-605, Dec 2004. ISSN 1360-1385. Disponível em: < <Go to ISI>://WOS:000226018700009 >.

HALING, R. E. et al. Root hairs improve root penetration, rootsoil contact, and phosphorus acquisition in soils of different strength. **Journal of Experimental Botany,** v. 64, n. 12, p. 3711-3721, Sep 2013. ISSN 0022-0957. Disponível em: < <Go to ISI>://WOS:000323578700014 >.

HAUG, A. Molecular Aspects of Aluminum Toxicity. **Crc Critical Reviews in Plant Sciences,** v. 1, n. 4, p. 345-373, 1984. ISSN 0735-2689. Disponível em: < <Go to ISI>://WOS:A1984SS33300004 >.

JALEEL, C. A. et al. Responses of antioxidant defense system of Catharanthus roseus (L.) G. Don. to paclobutrazol treatment under salinity. **Acta Physiologiae Plantarum,** v. 29, n. 3, p. 205-209, Jun 2007. ISSN 0137-5881. Disponível em: < <Go to ISI>://WOS:000249586400004 >.

JANSEN, R. C.; STAM, P. High-Resolution of Quantitative Traits into Multiple Loci Via Interval Mapping. **Genetics,** v. 136, n. 4, p. 1447-1455, Apr 1994. ISSN 0016-6731. Disponível em: < <Go to ISI>://WOS:A1994NB82100021 >.

KAO, C. H.; ZENG, Z. B.; TEASDALE, R. D. Multiple interval mapping for quantitative trait loci. **Genetics,** v. 152, n. 3, p. 1203-1216, Jul 1999. ISSN 0016-6731. Disponível em: < <Go to ISI>://WOS:000081341900031 >.

KAVAR, T. et al. Identification of genes involved in the response of leaves of Phaseolus vulgaris to drought stress. **Molecular Breeding,** v. 21, n. 2, p. 159-172, Feb 2008. ISSN 1380-3743. Disponível em: < <Go to ISI>://WOS:000251868400003 >.

KOCHIAN, L. V.; HOEKENGA, O. A.; PINEROS, M. A. How do crop plants tolerate acid soils? - Mechanisms of aluminum tolerance and phosphorous efficiency. **Annual Review of Plant Biology,** v. 55, p. 459-493, 2004. ISSN 1040-2519. Disponível em: < <Go to ISI>://WOS:000222766000018 >.

KUMAR, A.; SINGH, D. P.; SINGH, P. Influence of Water-Stress on Photosynthesis, Transpiration, Water-Use Efficiency and Yield of Brassica-Juncea L. **Field Crops Research,** v. 37, n. 2, p. 95-101, May 1994. ISSN 0378-4290. Disponível em: < <Go to ISI>://WOS:A1994PC82400002 >.

LI, R. et al. Genetic variation for maize root architecture in response to drought stress at the seedling stage. **Breeding Science,** v. 65, n. 4, p. 298-307, Sep 2015. ISSN 1344-7610.

LU, Y. L. et al. Comparative LD mapping using single SNPs and haplotypes identifies QTL for plant height and biomass as secondary traits of drought tolerance in maize. **Molecular Breeding,** v. 30, n. 1, p. 407-418, Jun 2012. ISSN 1380-3743. Disponível em: < <Go to ISI>://WOS:000304646100033 >.

LYNCH, J. P. Roots of the second green revolution. **Australian Journal of Botany,** v. 55, n. 5, p. 493-512, 2007. ISSN 0067-1924. Disponível em: < <Go to ISI>://WOS:000248796000001 >.

LYNCH, J. P. Root Phenes for Enhanced Soil Exploration and Phosphorus Acquisition: Tools for Future Crops. **Plant Physiology,** v. 156, n. 3, p. 1041-1049, Jul 2011. ISSN 0032-0889. Disponível em: < <Go to ISI>://WOS:000292294100008 >.

MACKAY, I.; POWELL, W. Methods for linkage disequilibrium mapping in crops. **Trends in Plant Science,** v. 12, n. 2, p. 57-63, Feb 2007. ISSN 1360-1385. Disponível em: < <Go to ISI>://WOS:000244826000004 >.

MAGALHAES, P. C.; DURAES, F. O. M. **Fisiologia da Produção de milho**. Embrapa Milho e Sorgo. Sete Lagoas, 2006. 10 p.

MALOSETTI, M. et al. A multi-trait multi-environment QTL mixed model with an application to drought and nitrogen stress trials in maize (Zea mays L.). **Euphytica,** v. 161, n. 1-2, p. 241-257, May 2008. ISSN 0014-2336. Disponível em: < <Go to ISI>://WOS:000254877800021 >.

MESSMER, R. et al. Drought stress and tropical maize: QTLs for leaf greenness, plant senescence, and root capacitance. **Field Crops Research,** v. 124, n. 1, p. 93-103, Oct 9 2011. ISSN 0378-4290. Disponível em: < <Go to ISI>://WOS:000296595800010 >.

MESSMER, R. et al. Drought stress and tropical maize: QTL-by-environment interactions and stability of QTLs across environments for yield components and secondary traits. **Theoretical and Applied Genetics,** v. 119, n. 5, p. 913-930, Sep 2009. ISSN 0040-5752. Disponível em: < <Go to ISI>://WOS:000269153000013 >.

MOLL, R. H.; KAMPRATH, E. J.; JACKSON, W. A. Analysis and Interpretation of Factors Which Contribute to Efficiency of Nitrogen-Utilization. **Agronomy Journal,** v. 74, n. 3, p. 562-564, 1982. ISSN 0002-1962. Disponível em: < <Go to ISI>://WOS:A1982NW34300036 >.

MUSTILLI, A. C. et al. Arabidopsis OST1 protein kinase mediates the regulation of stomatal aperture by abscisic acid and acts upstream of reactive oxygen species production. **Plant Cell,** v. 14, n. 12, p. 3089-3099, Dec 2002. ISSN 1040-4651. Disponível em: < <Go to ISI>://WOS:000179936800010 >.

PARENTONI, S. N.; SOUZA JÚNIOR, C. L. Phosphorus acquisition and internal utilization efficiency in tropical maize genotypes. **Pesquisa Agropecuaria Brasileira,** v. 43, n. 7, p. 893-901, Jul 2008. ISSN 0100-204X. Disponível em: < <Go to ISI>://WOS:000258821200014 >.

RAMAEKERS, L. et al. Strategies for improving phosphorus acquisition efficiency of crop plants. **Field Crops Research,** v. 117, n. 2-3, p. 169-176, Jun 3 2010. ISSN 0378-4290. Disponível em: < <Go to ISI>://WOS:000278304600001 >.

REMINGTON, D. L. et al. Structure of linkage disequilibrium and phenotypic associations in the maize genome. **Proceedings of the National Academy of Sciences of the United States of America,** v. 98, n. 20, p. 11479-11484, Sep 25 2001. ISSN 0027-8424. Disponível em: < <Go to ISI>://WOS:000171237100090 >.

RIBAUT, J. M.; RAGOT, M. Marker-assisted selection to improve drought adaptation in maize: the backcross approach, perspectives, limitations, and alternatives. **Journal of Experimental Botany,** v. 58, n. 2, p. 351-360, Jan 2007. ISSN 0022-0957. Disponível em: < <Go to ISI>://WOS:000243992800024 >.

SCHACHTMAN, D. P.; REID, R. J.; AYLING, S. M. Phosphorus uptake by plants: From soil to cell. **Plant Physiology,** v. 116, n. 2, p. 447-453, Feb 1998. ISSN 0032-0889. Disponível em: < <Go to ISI>://WOS:000072021600001 >.

SCHNABLE, P. S. et al. The B73 Maize Genome: Complexity, Diversity, and Dynamics. **Science,** v. 326, n. 5956, p. 1112-1115, Nov 20 2009. ISSN 0036-8075. Disponível em: < <Go to ISI>://WOS:000271951000044 >.

SETTER, T. L.; PARRA, R. Relationship of Carbohydrate and Abscisic Acid Levels to Kernel Set in Maize under Postpollination Water Deficit. **Crop Science,** v. 50, n. 3, p. 980-988, May-Jun 2010. ISSN 0011-183X. Disponível em: < <Go to ISI>://WOS:000276961900027 >.

SETTER, T. L. et al. Genetic association mapping identifies single nucleotide polymorphisms in genes that affect abscisic acid levels in maize floral tissues during drought. **Journal of Experimental Botany,** v. 62, n. 2, p. 701-716, Jan 2011. ISSN 0022-0957. Disponível em: < <Go to ISI>://WOS:000285625500024 >.

SHARPLEY, A. N.; MCDOWELL, R. W.; KLEINMAN, P. J. A. Phosphorus loss from land to water: integrating agricultural and environmental management. **Plant and Soil,** v. 237, n. 2, p. 287-307, Dec 2001. ISSN 0032-079X. Disponível em: < <Go to ISI>://WOS:000172862000010 >.

SHEN, J. B. et al. Phosphorus Dynamics: From Soil to Plant. **Plant Physiology,** v. 156, n. 3, p. 997-1005, Jul 2011. ISSN 0032-0889. Disponível em: < <Go to ISI>://WOS:000292294100003 >.

SHENOY, V. V.; KALAGUDI, G. M. Enhancing plant phosphorus use efficiency for sustainable cropping. **Biotechnology Advances,** v. 23, n. 7-8, p. 501-513, Nov 2005. ISSN 0734-9750. Disponível em: < <Go to ISI>://WOS:000232631900003 >.

TAIZ, L.; ZEIGER, E. **Fisiologia Vegetal**. Porto Alegre: Artmed, 2004. 719 p.

TAMBUSSI, E. A. et al. Oxidative damage to thylakoid proteins in water-stressed leaves of wheat (Triticum aestivum). **Physiologia Plantarum,** v. 108, n. 4, p. 398-404, Apr 2000. ISSN 0031-9317. Disponível em: < <Go to ISI>://WOS:000087013400009 >.

TARAMINO, G. et al. The maize (Zea mays L.) RTCS gene encodes a LOB domain protein that is a key regulator of embryonic seminal and post-embryonic shoot-borne root initiation. **Plant Journal,** v. 50, n. 4, p. 649-659, May 2007. ISSN 0960-7412. Disponível em: < <Go to ISI>://WOS:000246398400009 >.

TRAN, L. S. P. et al. Functional analysis of AHK1/ATHK1 and cytokinin receptor histidine kinases in response to abscisic acid, drought, and salt stress in Arabidopsis. **Proceedings of the National Academy of Sciences of the United States of America,** v. 104, n. 51, p. 20623-20628, Dec 18 2007. ISSN 0027-8424. Disponível em: < <Go to ISI>://WOS:000251885000084 >.

TUBEROSA, R. et al. Mapping QTLs regulating morpho-physiological traits and yield: Case studies, shortcomings and perspectives in drought-stressed maize. **Annals of Botany,** v. 89, p. 941-963, Jun 2002. ISSN 0305-7364. Disponível em: < <Go to ISI>://WOS:000176402100015 >.

UNITED STATES DEPARTMENT OF AGRICULTURE - USDA. **World Agricultural Supply and Demand Estimates**. Office of the Chief Economist. 40. Disponível em: www.usda.gov/oce/commodity/projections/. Acesso em 20 de setembro de 2015.

VANCE, C. P.; CHIOU, T. J. Phosphorus Focus Editorial. **Plant Physiology,** v. 156, n. 3, p. 987-988, Jul 2011. ISSN 0032-0889. Disponível em: < <Go to ISI>://WOS:000292294100001 >.

VANCE, C. P.; UHDE-STONE, C.; ALLAN, D. L. Phosphorus acquisition and use: critical adaptations by plants for securing a nonrenewable resource. **New Phytologist,** v. 157, n. 3, p. 423-447, Mar 2003. ISSN 0028-646X. Disponível em: < <Go to ISI>://WOS:000181333500004 >.

VERSLUES, P. E. et al. Methods and concepts in quantifying resistance to drought, salt and freezing, abiotic stresses that affect plant water status. **Plant Journal,** v. 45, n. 4, p. 523-539, Feb 2006. ISSN 0960-7412. Disponível em: < <Go to ISI>://WOS:000234919800005 >.

WEN, T. J. et al. The roothairless1 gene of maize encodes a homolog of sec3, which is involved in polar exocytosis. **Plant Physiology,** v. 138, n. 3, p. 1637-1643, Jul 2005. ISSN 0032-0889. Disponível em: < <Go to ISI>://WOS:000230414800042 >.

WISSUWA, M.; AE, N. Further characterization of two QTLs that increase phosphorus uptake of rice (Oryza sativa L.) under phosphorus deficiency. **Plant and Soil,** v. 237, n. 2, p. 275-286, Dec 2001. ISSN 0032-079X. Disponível em: < <Go to ISI>://WOS:000172862000009 >.

WISSUWA, M.; MAZZOLA, M.; PICARD, C. Novel approaches in plant breeding for rhizosphere-related traits. **Plant and Soil,** v. 321, n. 1-2, p. 409-430, Aug 2009. ISSN 0032-079X. Disponível em: < <Go to ISI>://WOS:000268192400017 >.

WISSUWA, M. et al. Substitution mapping of Pup1: a major QTL increasing phosphorus uptake of rice from a phosphorus-deficient soil. **Theoretical and Applied Genetics,** v. 105, n. 6-7, p. 890-897, Nov 2002. ISSN 0040-5752. Disponível em: < <Go to ISI>://WOS:000179685700012 >.

YU, J. M. et al. A unified mixed-model method for association mapping that accounts for multiple levels of relatedness. **Nature Genetics,** v. 38, n. 2, p. 203-208, Feb 2006. ISSN 1061-4036. Disponível em: < <Go to ISI>://WOS:000234953200015 >.

YU, J. M.; BUCKLER, E. S. Genetic association mapping and genome organization of maize. **Current Opinion in Biotechnology,** v. 17, n. 2, p. 155-160, Apr 2006. ISSN 0958-1669. Disponível em: < <Go to ISI>://WOS:000237135800008 >.

ZHU, J. M.; KAEPPLER, S. M.; LYNCH, J. P. Mapping of QTL controlling root hair length in maize (Zea mays L.) under phosphorus deficiency. **Plant and Soil,** v. 270, n. 1-2, p. 299-310, Mar 2005a. ISSN 0032-079X. Disponível em: < <Go to ISI>://WOS:000230397000028 >.

ZHU, J. M.; KAEPPLER, S. M.; LYNCH, J. P. Mapping of QTLs for lateral root branching and length in maize (Zea mays L.) under differential phosphorus supply. **Theoretical and Applied Genetics,** v. 111, n. 4, p. 688-695, Aug 2005b. ISSN 0040-5752. Disponível em: < <Go to ISI>://WOS:000231313100008 >.

ZHU, J. M.; LYNCH, J. P. The contribution of lateral rooting to phosphorus acquisition efficiency in maize (Zea mays) seedlings. **Functional Plant Biology,** v. 31, n. 10, p. 949-958, 2004. ISSN 1445-4408. Disponível em: < <Go to ISI>://WOS:000224481200001 >.

CAPÍTULO 1

Multi-environment QTL mixed models adjusted for phenological covariates for drought stress in tropical maize

C. A. G. Ribeiro, M. M. Pastina, L. J. M. Guimarães, L. Tomé, S. N. Parentoni, J. V. Magalhaes, E. G. de Barros, C. T. Guimaraes

C. A. G. Ribeiro
Departamento de Genética e Melhoramento, Universidade Federal de Viçosa, Viçosa, Minas Gerais, 36570-000, Brazil

E. G. de Barros
Programa de Pós-Graduação em Ciências Genômicas e Biotecnologia, Universidade Católica de Brasília, Brasília, Distrito Federal, 70330-710, Brazil

C. A. G. Ribeiro · M. M. Pastina · L. J. M. Guimarães · L. Tomé · S. N. Parentoni · J. V. Magalhaes · C. T. Guimaraes

Embrapa Maize and Sorghum, Sete Lagoas, Minas Gerais, 35701–970, Brazil
e-mail: claudia.guimaraes@embrapa.br

Abstract

Selection of quantitative trait loci (QTL) for grain yield under water stress is still barely applied in breeding programs. This is mainly due to the high genetic complexity of this trait, which involves a large number of genes with high genetic background and environmental influences. In order to understand the genetic basis underlying the drought-related traits and their genotype-environment interaction, we performed QTL mapping using mixed models to analyze two tropical maize populations under two water regimes. Both mapping population were $F_{2:3}$, derived from the cross between the inbred lines L2321 x L31212 (MP1) and L1761121 x L521237 (MP2). Plant height and anthesis-silking interval were included as cofactors in the QTL model for grain yield, improving significantly the accuracy of the QTL mapping. Seventeen genomic regions were identified for grain yield with or without cofactors, additionally ten QTLs for plant height and seven for anthesis-silking interval was also detected in both mapping populations. Both parents in each cross contributed with favorable alleles. In the MP2, QTLs for anthesis-silking interval (ASI) on chromosomes 3, 4 and 9, bins 3.04, 4.05 and 9.04, respectively, were co-localized with QTLs for grain yield, except when ASI was used as cofactor, indicating the effect of phenological trait in the grain yield, probably due to common genetic factors in these regions. Additionally, four genomic regions on chromosomes 1, 3, 6 and 8 harbored QTLs for grain yield coincident in both populations, which were also consistently identified in other studies, showing a great potential for use in marker-assisted breeding and to search for candidate genes aiming to improve drought tolerance in maize.

Keywords: QTL mapping, water stress, secondary traits, cofactor

Introduction

Maize (Zea mays) is the most produced cereal worldwide, and broadly used for human food and animal feed, as well as for many industrial purposes. Grain yield is widely affected by a range of abiotic stresses, highlighting drought as a major limiting factor (Cairns et al. 2013). Water stress occurs when the loss of water by plant exceeds the capacity of water absorption, causing irreversible damages to the plant, which ranges from mild to total yield losses (Jaleel et al. 2007). As the majority of maize is cultivated under rain fed conditions, its yield is highly affected by the climate changes, demanding drought tolerant genotypes (Ali et al. 2012; Lobell et al. 2014). Furthermore, with the constant increase of the world food demand, the agriculture has to be expanded to marginal areas, with an inadequate water supply, emphasizing the need for genetic improved varieties with the ability to withstand in water deficit conditions.

Drought tolerance is a complex trait, which is highly dependent on the evaluation methods (Blum 2005; Collins et al. 2008). Water deficit results in negative effects along the plant development, and different morpho-physiological mechanisms are involved in plant adaptation and yield stability under stress conditions (Lu et al. 2011). The root development is favored over shoot to increase the root expansion, reaching deeper soil layers under water deficit (Ribaut et al. 2009). Drought stress decreases the photosynthetic rates, compromising the accumulation of assimilates causing yield losses (Shah and Paulsen 2003). In maize, floral initiation, fertilization and grain filling are the most sensitive growth phases for drought stress to reduce grain yield (Grant et al. 1989; Ribaut et al. 1997; Messmer et al. 2009).

In breeding programs, secondary traits, highly correlated with yield have been used for indirect selection, due to the greater heritability under stress conditions. For example, plant height could reflect, at some level, the response to water deficit, being useful for indirect selection (Lu et al. 2012). Anthesis-silking interval (ASI) has been inversely correlated with drought tolerance in maize, with promising results for breeding purposes (Ribaut et al. 2004). The marker-assisted introgression of five quantitative trait loci (QTLs) reducing ASI in a maize elite inbred line sensitive to drought was efficient to improve grain yield under severe water stress, but no difference was detected at low levels of water deficit (Ribaut and Ragot 2007).

Expressive gains in grain yield were reached under drought stress by conventional breeding in maize but the genetic basis underlying this trait still remains unclear (Almeida et al. 2013). QTL

mapping in bi-parental populations is a useful approach to dissect and to understand the genetic components of complex traits (Hao et al. 2010). Several studies have reported QTLs for drought tolerance in maize (Agrama and Moussa 1996; Almeida et al. 2013; Malosetti et al. 2008; Messmer et al. 2011; Messmer et al. 2009), rice (Dixit et al. 2012; Lanceras et al. 2004; Venuprasad et al. 2012), sorghum (Harris et al. 2007; Sabadin et al. 2012), and wheat (Kadam et al. 2012; Mathews et al. 2008; Quarrie et al. 2005), among other crops. The phenotypic traits used in these studies were based on grain yield, plant height, ASI, root morphology, stay-green, osmotic potential and dry matter. Despite widely investigated, QTLs identified for grain yield in drought conditions are barely applied in marker-assisted breeding programs, mainly due to the high influence of genetic background and environmental interaction (Banziger et al. 2006; Beyene et al. 2015).

The genotype by environment interaction strongly counteracts in the identification of stable genomic regions controlling genetic factors of traits. QTLs detected for these complex traits often explain a small proportion of phenotypic variance, including epistatic interactions (Beyene et al. 2015; Mathews et al. 2008). Mixed models have becoming increasingly used in order to increase accuracy in QTL mapping (Mathews et al. 2008). This approach allows modeling heterogeneous (co)variances (VCOV) for genetic and residual effects, which consequently improves the accuracy and reliability in QTL detection and estimates their effects in multiple environments (Boer et al. 2007; Malosetti et al. 2008; Sabadin et al. 2012). Furthermore, phenological traits have been used as cofactors to control confounding effects in the detection of QTLs for grain yield under drought stress. One strategy is to use it as covariable in the phenotypic model as performed in wheat using ear emergence time (Bennett et al. 2012) and maize with anthesis date (Almeida et al. 2013). In the other hand, QTLs detected for phenological traits could be used in the QTL model as applied in sorghum, in which QTLs for plant height and flowering time were used as cofactors to detect QTLs for grain yield associated with drought tolerance (Sabadin et al. 2012).

In the present study, we performed QTL mapping using mixed models in two tropical maize populations, in two years and two contrasting water supplies. Our goals were (1) to identify genomic regions related to grain yield, plant height and ASI with constant and specific effects across multiple environments, for each population; (2) to evaluate the influence of secondary traits as cofactor in the QTL detection for grain yield; and (3) to identify common QTL regions in both populations. The genomic regions selected can be used for the development of marker-assisted selection strategies in maize breeding programs.

Material and Methods

Plant material

Two $F_{2:3}$ tropical maize biparental populations were developed at Embrapa Maize and Sorghum for genetic mapping. The first mapping population (MP1) consisted of 97 $F_{2:3}$ families derived from the cross between the inbred lines L2321 (drought tolerant) and L31212 (drought sensitive). The second mapping population (MP2) consisted of 136 $F_{2:3}$ families derived from the cross between the elite inbred lines L1761121 (drought tolerant) and L521237 (drought sensitive).

Field experiments

The experiments were conducted at Embrapa Maize and Sorghum experimental station, located in Janaúba, Minas Gerais state, Brazil (15°47' S, 43°18' W, 516 m). The MP1 was evaluated in two years 2006 and 2007 under well-watered (WW) and water-stress (WS). Field experiments for the MP2 were conducted in 2012 and 2013 under WS condition only. WW conditions were fully irrigated during the whole crop cycle with a drip irrigation system, and the soil moisture was monitored based on the gravimetric method in three different depths (0-10, 10-30 and 30-50cm). The WS condition was achieved through the complete interruption of irrigation at 15 days before flowering (tassel booting), which allowed soil moisture depletion during flowering and post-flowering time. All trials were conducted in a dark-red latosol from June to October during the rain-free period.

The experiments were conducted in a randomized complete block design with three replicates for MP1 in 2006, and in an alpha lattice design with three replicates in 2007. For MP2, the experiment consisted of three sets (trials) with 48, 47 and 47 $F_{2:3}$ progenies each. Each trial was arranged as a randomized incomplete block design with three and two replicates in 2012 and 2013, respectively. Parental lines were included as common checks in each trial. The plots, for both populations, consisted of one 4-m long row, with 0.8 m between rows and 0.2 m between plants. Fertilization was based on the results of a soil test, and was applied as required, in accordance with local recommendation. Phytosanitary management was made according to the crop needs.

Plant height (PH) was measured as the distance from the ground surface to the top emerging leaf, based on a representative plant in each plot. Anthesis-silking interval (ASI), the difference between female and male flowering, was calculated as the number of days from the date of emerged silks on 50% of the plants in a plot minus the date that 50% of the plants with anther dehiscence in a plot (Bolanos and Edmeades 1996). For grain yield (GY), all grains of each plot were weighted and corrected for 13% of moisture, and converted to Kg ha^{-1}. The number of plants per plot was used as covariate in the statistical models adjustment for GY.

Genotypic data and linkage map

Genomic DNA was isolated from young leaves using the cetyltrimethylammonium bromide (CTAB) method (Saghai-Maroof et al. 1984). A set of 271 markers comprising 51 microsatellites (Simple Sequence Repeats, SSR) and 220 SNPs (Single nucleotide Polymorphism) were genotyped in the MP1 and 311 SNP markers were used for MP2. The SSR amplification reactions consisted of 30 ng of genomic DNA; 10 µM Tris-HCl pH 8.0; HCl 50 µM, 2 µM $MgCl_2$, 125 µM of each deoxynucleotide (dNTP); and 0.4 µM of each primer and one unit (1U) of Taq DNA polymerase in a final volume of 10 µL. The amplification cycles were an initial denaturation at 95 °C for 2 min, nine cycles using with touchdown of 1 °C in annealing temperature per cycle at 94 °C for 20 s, 68 °C for 20 s and 72 °C for 20 s, followed by 25 cycles at 94 °C for 20 s, 60 °C for 20 s, and 72 °C for 20 s and a final extension at 72 °C for five minutes. The amplified fragment were visualized in 10% polyacrylamide gels (29:1 acrylamide:bisacrylamide) in TBE buffer (0.89 M Tris-HCl, 0.02 M boric acid, 0.02 M EDTA, pH 8.0). After 2 hours electrophoresis at 200 V, the gels were incubated under constant stirring for 15 minutes in a fixing solution (10% ethanol, 0.5% acetic acid), 15 minutes in 0.2% silver nitrate solution and transferred to revealing solution (3% NaOH, 0.5% formaldehyde) until the bands showed. The gel image was captured under white light using Eagle Eye II (Stratagene®). SNP markers were generated using Kompetitive Allele-Specific Polymerase chain reaction (KASP assay) in the LGC Genomics Inc. (Teddington, UK). The sequences, genetic and genomic locations of SSR and SNP markers are available at the Maize Genetics and Genomics Database (http://www.maizegdb.org/data_center/locus).

Markers were tested for an expected segregation ratio of 1:2:1 using chi-square statistics ($\alpha \leq 0.05$), corrected for multiple tests based on Bonferroni's method and markers with segregation distortion were removed. The genetic map was constructed using the MAPMAKER/EXP 3.0b

software (Lincoln et al. 1992), with a minimum logarithm of odds (LOD) of 3.0 and a maximum distance between adjacent markers of 40 cM. The Kosambi mapping function (Kosambi 1944) was used to convert the recombination fractions into map distances. The physical and genetic positions of each marker were used to confirm the marker order along the linkage groups.

Phenotypic data analysis

For each mapping population, a multi-environment mixed model analysis was performed for all evaluated traits. Thus, for MP1, the following model was used (random effects are underlined):

$$y_{ijkl} = \mu + e_j + r_{k(j)} + \underline{b}_{l(jk)} + \underline{g}_{i(j)} + \varepsilon_{ijkl}$$

where y_{ijkl} is the phenotype of the i^{th} individual ($i = 1, \ldots, I$) in replicate k ($k = 1, \ldots, K$) of block l ($l = 1, \ldots, L$) within environment j ($j = 1, \ldots, J$); μ is the overall mean; e_j is the fixed effect of environments; $r_{k(j)}$ is the fixed effect of replicates within environment j ; $\underline{b}_{l(jk)}$ is the random effect of blocks within replicate k of environment j , assuming that the vector $\underline{b} = (\underline{b}_{1(11)}, \ldots, \underline{b}_{L(JK)})$ has a multivariate normal distribution with zero mean and variance-covariance (VCOV) matrix $\mathbf{B}_J$; $\underline{g}_{i(j)}$ is the random genetic effect of genotype i at environment j , assuming that the vector $\underline{\mathbf{g}} = (\underline{g}_{11}, \ldots, \underline{g}_{IJ})$ has a multivariate normal distribution with zero mean and VCOV matrix $\mathbf{G}_J \otimes \mathbf{I}_n$, in which $\otimes$ denotes the Kronecker product of matrices, and $\mathbf{I}_n$ is an identity matrix; and ε_{ijkl} is the random non-genetic effect, assuming that the vector $\underline{\boldsymbol{\varepsilon}} = (\underline{\varepsilon}_{1111}, \ldots, \underline{\varepsilon}_{IJKL})$ has a multivariate normal distribution with zero mean and VCOV matrix $\mathbf{R}_J$.

For MP2, the following model was used (random effects are underlined):

$$y_{ijklm} = \mu + e_j + t_{m(j)} + r_{k(jm)} + \underline{b}_{l(jkm)} + \underline{G}_{i(j)} + \varepsilon_{ijklm}$$

where y_{ijklm} is the phenotype of the i^{th} individual ($i = 1, \ldots, I$) in replicate k ($k = 1, \ldots, K$) of block l ($l = 1, \ldots, L$), in the trial m ($m = 1, \ldots, M$) within environment j ($j = 1, \ldots, J$); μ is the overall mean; e_j is the fixed effect of environments; $t_{m(j)}$ is the fixed effect of trial within environment j; $r_{k(jm)}$ is the fixed effect of replicates in the trial m , within environment j; $\underline{b}_{l(jkm)}$ is the random effect of blocks within replicate k in the trial m of environment j, assuming that the vector $\underline{b} = (\underline{b}_{1(111)}, \ldots, \underline{b}_{L(JKM)})$ has a multivariate normal distribution with zero mean and variance-

covariance (VCOV) matrix $\mathbf{B}_J$; $\underline{G}_{i(j)}$ is the random genetic effect of genotype i at environment j. Genotypes can be separated in two groups:

$$\underline{G}_{i(j)} = \begin{cases} \underline{g}_{i(j)} & i = 1, \dots, n_g \\ c_{i(j)} & i = n_g + 1, \dots, n_g + n_c \end{cases}$$

where n_g is the number of genotypes in the progeny ($i = 1, \dots, n_g$), n_c is the number of checks ($i = 1, \dots, n_g + n_c$), and $n = n_g + n_c$. The vector $\underline{\mathbf{g}} = (\underline{g}_{11}, \dots, \underline{g}_{IJ})$ has a multivariate normal distribution with zero mean and VCOV matrix $\mathbf{G}_J \otimes \mathbf{I}_n$, in which $\otimes$ denotes the Kronecker product of matrices, and $\mathbf{I}_n$ is an identity (co)variance matrix; $c_{i(j)}$ represents a fixed effect for check i within environment j, and ε_{ijkl} is the random non-genetic effect, assuming that the vector $\underline{\boldsymbol{\varepsilon}} = (\underline{\varepsilon}_{11111}, \dots, \underline{\varepsilon}_{IJKLM})$ has a multivariate normal distribution with zero mean and VCOV matrix $\mathbf{R}_J$. Although the effect of checks is not relevant for QTL mapping, its inclusion in the phenotypic model may help to control for non-genetic variation (Boer et al. 2007).

Pearson's correlation coefficients were calculated to determine relationships between traits. Broad-sense heritabilities (h^2) on the individual plant basis were estimated based on single-environment analyses, through the variance components for genetic (σ_g^2), block (σ_b^2) and residual (σ_ε^2) effects. Thus, the general formula was:

$$h^2 = \frac{\sigma_g^2}{\sigma_g^2 + \sigma_b^2 + \sigma_\varepsilon^2}$$

Different variance-covariance (VCOV) structures for the $\mathbf{G}_J$ matrix were compared via AIC (Akaike Information Criterion) (Akaike 1974) in order to identify the best model to fit phenotypic data in a mixed model framework across environments. Besides the identity matrix, which assumes homogeneity of genetic variances and no genetic correlation across environments, three different VCOV structures were also examined: i) Diagonal: heterogeneous genetic variances and no genetic correlations among environments; ii) Compound Symmetry: heterogeneous genetic variances and common genetic covariance across environments; and iii) Unstructured: heterogeneous genetic variances and specific covariances for each pair of environments. Similarly, different structures were also compared for the VCOV matrix of non-genetic residual effects ($\mathbf{R}_J$) to allow for residual heteroscedasticity as well as residual correlations between environments (Boer et al. 2007; Malosetti et al. 2008; Pastina et al. 2012). All models were fitted using Residual

Maximum Likelihood (REML) (Patterson and Thompson 1971) through software GenStat 16.1 (Payne et al. 2010).

QTL mixed model analysis

For the QTL mapping procedure, random genetic effects were regressed on genetic predictors representing functions of the conditional probabilities for the QTL genotype (Boer et al. 2007; Haley and Knott 1992; Jiang and Zeng 1997). Genetic predictors were estimated at all marker positions and at an additional grid of points with a maximum step size of 2.0 cM. The genotypic effect was partitioned into environment-specific additive and dominance QTL effects, and environment-specific residual genetic effect according to the equation:

$$g_{i(j)} = x_{\alpha_{iq}} \alpha_{qj} + x_{\delta_{iq}} \delta_{qj} + g^{*}_{i(j)}$$

where i is the genotype ($i = 1, \dots, n_g$), j is the environment ($j = 1, \dots, J$) and q is the genomic position under evaluation, $x_{\alpha_{iq}}$ is the genetic predictor of the additive effect for individual i and position q, α_{qj} is the environment-specific additive QTL effect, $x_{\delta_{iq}}$ is the genetic predictor of the dominance effect for individual i and position q, δ_{qj} is the environment-specific dominance QTL effect, and $g^{*}_{i(j)}$ represents the environment-specific genetic residual effect, after adjustment for the putative QTL effects. At marker positions, $x_{\alpha_{iq}}$ assumed the values +1, 0 and -1 and $x_{\delta_{iq}}$ takes the values 0, 1, 0 for genotypes AA, Aa, and aa, respectively. QTL genotypes are not directly observable, but additive genetic predictor can be calculated from the difference of conditional probabilities of genotypes QQ and qq and their correspondent flanking markers: Pr(QQ|flanking markers) - Pr(qq|flanking markers). The dominance genetic predictor can be calculated based on the conditional probability for QTL genotype Qq and the flanking makers: Pr(Qq|flanking markers) (Jiang and Zeng 1997; Malosetti et al. 2008).

The mixed-model QTL mapping procedure consisted of four steps. In the first step, a phenotypic mixed model was fitted including the selected VCOV structures for $\mathbf{G}_J$ and $\mathbf{R}_J$ matrices based on the lowest AIC value. In the second step, an interval mapping (IM) approach (Lander and Botstein 1989) was performed to scan for environment-specific QTL effects along the genome. As described above, the molecular marker information was addressed to the mixed-model framework as genetic predictors. In the third step, based on the putative QTLs identified through

the IM scan, a set of markers were selected to be included as cofactors in a multi-environment composite interval mapping model, CIM (Jansen and Stam 1994; Zeng 1994). Only the closest markers to the QTL peaks were used as cofactors, considering only one marker in a window size of 30 cM (centiMorgan). A genome-wide threshold (α) of 0.01 was used to select putative QTLs in both IM and CIM models. At the final step, a multi-QTL mapping model including all putative QTLs identified through the CIM scan was fitted, and the statistical significance of QTL main and environment-specific effects was assessed via the Wald test, considering a significance level of 5%. All the QTL mapping analyses were performed in the software Genstat v.16 (Payne et al. 2009), using Residual Maximum Likelihood (REML).

The proportion of the genetic variance explained by all QTLs identified in a specific environment was estimated as: $\mathrm{GV}_T = \left(\frac{\mathrm{GV}_R - \mathrm{GV}_F}{\mathrm{GV}_R}\right) \mathrm{X}\ 100$, where GV_T is the total genetic variance explained by all QTLs in the model, GV_R is the genetic variance of the reduced model, i.e. with no QTL effects, and GV_F is the genetic variance of the full model, including the whole set of QTLs. On the other hand, the genetic variance explained by each QTL was calculated as: $\mathrm{GV}_{QTL} = \left(\frac{\mathrm{GV}_{R_Q} - \mathrm{GV}_F}{\mathrm{GV}_R}\right) \mathrm{X}\ 100$, where GV_{QTL} is the genetic variance explained by the QTL, and GV_{R_Q} is the genetic variance of the reduced model without the QTL effect.

The QTL mapping procedure described above was applied for GY, PH and ASI in both mapping populations. Furthermore, PH and ASI were included as fixed effect covariables in the QTL mixed models fitted for GY. The phenological traits were tested independently as covariables and in combination.

Results

Phenotypic data

Phenotypic means, coefficient of variation, variance and heritability for GY, PH and ASI for both mapping populations are described in Table 1. The distribution of phenotypic data for each trait in each environment, as well as the phenotypic means of the parents are depicted in the histograms for both mapping populations, MP1 (Figure 1) and MP2 (Figure 2). The parental lines of MP1, L2321 and L31212, contrasted for GY, PH and ASI. The MP2 parents also contrasted for GY but presented a similar performance for PH and ASI under WS. As the MP2 parental lines are

elite breeding lines from Embrapa, the selection process culminated in less contrasting secondary traits, although phenotypic variations can be observed in the population. Variations in phenology are expected even if the parents of the mapping population do not show differences in the phenotypic means for the traits (Sabadin et al. 2012). Significant genetic variation in GY, PH and ASI were observed for both $F_{2:3}$ mapping populations with moderate to high broad sense heritability estimates.

In general, the mean values for all traits in MP1 were stable in both years, with an approximately 50% reduction in GY under WS compared to WW, ranging from 1,757 Kg.ha^{-1} (WS06) to 3,719 Kg.ha^{-1} (WW07). Heritability estimates for GY ranged from 0.36 (WW07) to 0.62 (WS06), whereas they were similar for PH under water-stress in 2006 (0.51) and 2007 (0.58). ASI presented low heritability estimates, 0.24 and 0.19 for WS06 and WW06 respectively, and a strong variation in the means, which ranged from 1.05 in WS07 to 0.1 in WW07 (Table 1). GY for MP1 was significantly correlated (p-value $\leq$ 0.001) among years and water regimes, varying from 0.29 to 0.54, with higher values for the same year or the water regime (Table S1). A similar correlation pattern was observed for PH, which ranged from 0.35 to 0.50 among environments. The correlations were lower (0.19 to 0.46) for ASI among environments, but significant between environments at 0.01 of probability, except for WW06 and WW07 (0.16). GY and PH were moderately correlated (p-value $\leq$ 0.001) within the same environments, and ASI was not significantly correlated with PH and GY, except with GY in WS07 (-0.32, p-value $\leq$ 0.001).

The MP2 was evaluated only under drought stress, with the average of GY in 2012 of 3654 Kg.ha^{-1} (h^2 = 0.44) and of 1578 Kg.ha^{-1} in 2013 (h^2 = 0.38). PH in 2012 was 164.4 cm greater then 145.9 cm in 2013 with the respective heritability of 0.37 and 0.43. The ASI mean was -0.37 in WS12 and 2.45 in WS13 with similar heritability estimates (Table 1). In general, the GY reduced in 2013 compared with 2012, followed by reduction in PH and increasing in ASI. However, no significant climate changes were observed between these years that could justify such yield difference (Figure S1). Phenotypic correlations for MP2 in 2012 and 2013 were significant at 0.001 of probability for GY (0.32), PH (0.39) and ASI (0.47) (Table S2). GY was significantly correlated (p-value $\leq$ 0.001) with PH (0.28) and ASI (-0.36) in 2012 as well as with PH (0.28) and ASI (-0.61) in 2013. No significant correlation was found for PH and ASI.

Multi-environment QTL analysis for MP1 (L2321 x L31212)

The genetic map constructed with 196 markers (166 SNPs and 30 SSRs) covered 1,816.8 cM of all 10 maize chromosomes with an average interval between adjacent markers of 9.8 cM. QTL analyses were carried out considering all four environments (WS06, WW06, WS07 and WW07) simultaneously for GY using PH and/or ASI as cofactors (Table 2 and Figure 3). An unstructured VCOV matrix associated to the genetic effects ($\mathbf{G}_J$) was selected based on AIC (Akaike 1974) for GY and an identity matrix the best structure for the non-genetic residual effects ($\mathbf{R}_J$). The inclusion of cofactors did not affect the chosen VCOV matrix. For PH the selected $\mathbf{G}_J$ and $\mathbf{R}_J$ matrices were an unstructured and a compound symmetry, respectively, and for ASI the selected matrix for $\mathbf{G}_J$ was a compound symmetry and for $\mathbf{R}_J$ a diagonal. The matrices properties are described in Material and Methods section.

Eleven QTLs were identified for GY with and without the cofactors, whereas five QTLs were mapped for PH and two for ASI (Table 2 and Figure 3). Out of the four QTLs mapped for GY without cofactors (bins 4.03, 5.03, 6.04 and 7.03), the ones located at bins 4.03 and 5.03 mapped close to QTLs for PH, losing their significance when PH was used as cofactors in the mixed model. In the other hand, QTLs for GY mapped at bins 1.09, 7.03 (103 cM) and 10.03 were detected only when PH was included as cofactor, either alone or with ASI, and expressed environmental specific effects. The QTL associated with GY at bin 10.05 was also identified using all combinations of PH and/or ASI as cofactors and new QTLs for GY were mapped using both cofactors (bins 2.08, 3.06 and 8.03, Table 2 and Figure 3). The QTL for GY(ASI) at bin 10.05 was the most significant with $-\log_{10}$ (p-value) of 3.36, whereas the QTL for GY(PH) at bin 10.03 explained the highest percentage of variance in 2007 under both conditions. In general, the QTLs for GY expressed effects predominantly due to dominance deviations, exhibited a pronounced QTL x Environment interactions (QEI) and were derived from both parents. The inclusion of the cofactors allowed the identification of novel QTLs for GY, with a higher influence of the PH as cofactor compared to ASI.

Multi-environment QTL analysis for MP2 (L1761121 x L521237)

The linkage map for the MP2 consisted of 267 SNP markers covering 1,277.2 cM of the maize genome with an average interval between adjacent markers of 5.0 cM. The VCOV matrices

with the best fit were an unstructured for $\mathbf{G}_J$ and a diagonal for $\mathbf{R}_J$ for all traits and conditions, with or without cofactors.

Ten QTLs were found for GY considering or not the cofactors, five QTLs were mapped for PH and five for ASI in the MP2 (Table 3 and Figure 4). All three QTLs for GY detected without cofactors on chromosomes 3, 4 and 9 were coincident with QTLs for ASI and lost their significance when ASI was used as cofactor in the mixed model for GY, but remained significant with PH as cofactor (Figure 4). On chromosome 2, one QTL for ASI at bin 2.02 seems to contribute with the significance of QTLs for GY using ASI as cofactor in this region. The differences in the QTL positions in this region can be addressed to the large interval between markers that encompass more than one bin. New genomic regions associated with GY were significant by using the cofactors, such as on chromosomes 6 and 8, without colocalization to the QTLs for PH or ASI.

The QTL for GY at bin 3.04 without cofactors explained the highest proportion of variance (24.3%) in WS13 showing additive and dominance main effects. All alleles associated with QTL for ASI increasing the anthesis-silking interval were derived from the drought sensitive parent. In general, the QTLs were donated by both parents and the additive effects were more prevalent than dominant effects, with more QTLs expressing main effects and less influenced by QEI in comparison to MP1.

Joint QTL results between populations

The coincidence among QTLs in both mapping populations was compared based on the confidence interval of the QTLs and the physical position of the makers in each linkage map (Figure 5). Four genomic regions harbored QTLs for GY in both mapping populations on chromosomes 1, 3, 6 and 8. QTLs with environment-specific dominance effect expressed in 2006 with and without water stress for GY with cofactors (PH and PH,ASI) in MP1 colocalized with a GY QTL with PH as cofactor in the MP2, showing additive and dominance main effects at bin 1.09. At bin 3.06, a main dominance effect QTL for GY(PH,ASI) in MP1 was coincident with an environment-specific additive effect QTL for GY(PH) in MP2. Despite the difference of the effect type, their LOD peak positions were very close to each other based on the physical distance with a narrow confidence interval. On chromosome 6 (bin 6.04), a GY QTL in MP1 colocalized with QTLs for GY using different phenological cofactors in the MP2. Most of these QTLs presented additive main effect, except GY(ASI) that showed an environment-specific additive effect. At bin

8.03, a GY(PH,ASI) QTL in the MP1 colocalized with QTLs for GY(ASI; PH,ASI) in the MP2, with all these QTLs showing environment-specific dominance effects.

Discussion

Multi-environment QTL based on mixed model analyses were carried out in two bi-parental $F_{2:3}$ maize populations. The drought stress imposed in the MP1 reduced the GY means by about 50% compared with well-watered condition in both years, which also reduced the genetic variance for GY and increase the genetic variance for ASI in the population, except in 2007. Drought stress tends to reduce the genetic variance for GY and increase the ASI (Messmer et al. 2009; Ribaut et al. 1997; Tuberosa et al. 2002). In general, the heritability estimates for GY were from moderate to high, ranging from 0.36 (WW07) to 0.62 (WS06). High heritability estimates were also found in other studies for grain yield in maize under drought stress and non-stress conditions (Lima et al. 2006; Lu et al. 2011; Messmer et al. 2009; Ribaut et al. 1997), ranging from 0.57 in WS condition (Messmer et al. 2009) to 0.83 in WW condition (Lu et al. 2011).

Out of 21 QTLs identified in both mapping populations for GY, three and five showed constant effects across environments for the MP1 and MP2, respectively, whereas the other QTLs showed significant interactions with environments (QEI). The number of QTLs exhibiting constant effect across environments was higher in MP2, probably because this population was evaluated only under stress conditions in two years. Almeida et al. (2013) have found a strong QEI using three tropical maize populations for QTL mapping under drought and control conditions. Boer et al. (2007) have also found a high QEI on chromosomes 4 and 7, highlighting the strong year effect in the chromosome 7 for GY. The majority of the GY QTLs associated with drought tolerance are environment- and population-specific with inconsistent effect sizes and direction, limiting their utilization in breeding programs (Almeida et al. 2013). Furthermore, information on stable QTL across diverse environments and with low genetic background effects is scarce (Li et al. 2010). QTL x Environment interactions are expected in grain yield under water stress and an evaluation of this interaction, in terms of presence, magnitude and form is strongly recommended in attempt to understand the genetic architecture of quantitative traits (Boer et al. 2007). Ignoring possible genetic correlation of QTL effects across environments may lead to erroneous decisions due to overoptimistic inferences in QTL detection (Korol et al. 1998; Piepho 2000). Selection for a QTL under strong QEI should not be a priority in a plant breeding process unless it can be shown that

they are particularly important in the target environment for the crop (Clarke et al. 1992; Sabadin et al. 2012).

Here, we used a multi-environment QTL analysis associated with mixed model including phenological covariates to adjust for genetic correlation among environments and the possible influence of the phenological traits, such as PH and ASI, as cofactors on the identification of GY QTL, helping in the discrimination of genetic causes underlying the QTL. For instance, in the MP2, QTLs for GY at bins 3.04 (43.9 - 103.4 Mb), 4.05 (122.8 - 170.5 Mb) and 9.04 (98.5 - 131.0 Mb) were colocalized with QTLs for ASI, which were not detected when ASI was included as cofactor in the model (Figure 4). These results suggest that these QTLs for grain yield can be related to variations in ASI, being resulted of pleiotropic QTL. In the chromosome 9, the SNP PZB01432.3, at the position 124 Mb, was significantly associated with ASI under water stress and control condition in a panel composed by 80 maize lines genotyped with 1006 SNPs (Hao et al. 2011). This genomic region in the chromosome 9 was coincident with one consensus QTL (cQTL) related with several flowering time traits in maize using meta-analysis (Chardon et al. 2004). This cQTL was flanked by the marker csu147 (105-107 Mb) that was also syntenic with three major QTLs affecting flowering time in rice, colocalized with the genes osZTL/LKP2_L2 and osELF3_L2 related to circadian clock (bin 9.04) (Chardon et al. 2004). Thus, a statistical approach based on the adoption of proper secondary traits as cofactors in the QTL models appears to be an efficient strategy to help in understanding the genetic basis behind GY under drought tolerance studies.

Among the QTLs for GY, three of these genomic regions have shown several overlaps in different populations (Almeida et al. 2013; Almeida et al. 2014; Cai et al. 2012; Hao et al. 2011; Hund et al. 2011; Messmer et al. 2009; Semagn et al. 2013). The bin 7.03 (130.0 - 165.1 Mbp) harbors QTLs for GY with and without phenological cofactors in the MP1, showing specific-environment additive effect that were colocalized with QTLs controlling axile roots in three populations (Hund et al. 2011) and QTLs for GY and ASI under water stress (Hao et al. 2011). The bin 10.05, at the positon 109.8 to 141.6 Mbp, QTLs for GY with either PH and/or ASI as cofactors showed specific-environment dominant effect and were colocalized with a meta-QTL containing five QTLs for GY under WS and WW conditions (Almeida et al. 2013). Additionally, a significant SNP was associated with GY under stress and control conditions (Hao et al. 2011). Finally, the region between the position 90.4 and 131.0 Mbp on chromosome 9 in the MP2

harbored QTLs for GY, GY(PH) and ASI showing additive effect that were colocalized with a significant SNP for ASI in water stress and well-watered conditions through two years (Hao et al. 2011), and a meta-QTL for GY and ASI containing three QTLs, detected across 18 maize populations (Semagn et al. 2013).

Combining the information from both populations, four genomic regions harbored coincident QTLs for grain yield. The coincident genomic region at bin 1.09, spanned a physical position from 223.1 to 289.6 Mbp for MP1 and 217.0 - 284.1 Mbp for MP2, with QTLs showing constant effect across water stress and control conditions. In this region, Almeida et al. (2013) identified a meta-QTL (276.0 - 285.3 Mbp) integrating three QTLs for GY under water stress and one QTL for well-watered using three maize subtropical bi-parental populations. A candidate gene at position 285.3 Mbp was associated with ABA metabolites in the silk organ in a panel of 350 maize lines, the significant SNP PZB01403.4 was located inside the predicted gene GRMZM2G124260, which encodes the enzyme aldehyde oxidase (ZmAO3) (Setter et al. 2011). ZmAO3 is closely related to rice and Arabidopsis aldehyde oxidases that are involved in metabolic pathway of abscisic acid (ABA) (Ibdah et al. 2009; Setter et al. 2011). ABA is a central regulator of diverse responses of plants to environmental stresses, integrating the molecular signals after stress perception (Tran et al. 2007). Water deficiency increases ABA concentration in reproductive tissues negatively influencing the seed development. The exogenous ABA application decreases the growth of the seed and cell division in endosperm in the first days after pollination before the starch synthesis stage (Setter and Parra 2010).

Another region harboring consistent GY QTLs was at bin 3.06, ranging from 178.2 to 208.2 Mbp in the MP1 and from 168.4 to 212.7 Mbp in the MP2. One QTL for total length of root crown evaluated in solid media under non-stress condition was mapped at 178.9 Mbp on chromosome 3 using a recombinant inbred line (RIL) derived from the cross between B73 and Mo17 (Burton et al. 2015). This genomic region was also detected for root length in a consensus QTL map from 15 QTL studies in maize (Hund et al. 2011). According to these authors, QTLs controlling different root traits during all development stages in four populations were mapped at bin 3.06. Significant SNPs, PZB01919.1 and PZA02317.9, located at 178.2 and 198.5 Mbp on chromosome 3, respectively, were associated with grain yield under water stress in a panel composed by 80 maize lines genotyped with 1006 SNPs (Hao et al. 2011).

Four QTLs for grain yield were colocalized at bin 6.04, within the region 91.9 - 212.7 Mbp, being one GY QTL without cofactors for MP1 and three GY QTLs using cofactors for MP2. QTLs for root dry weight, total root surface area and total root length evaluated under field conditions at flowering time were mapped between bins 6.02 - 6.04 using 187 advanced-backcrosses (Cai et al. 2012). Two SNPs, PZA03555.1 and PZA03750.2, significantly associated with GY-WW and GY-WS, respectively, were mapped within the candidate gene Dehydrin 1, located at 137.3 Mbp on chromosome 6 (Hao et al. 2011). Dehydrins are proteins that typically accumulate upon exposure to dehydration stress (Ceccardi et al. 1994).

The region on chromosome 8 (bin 8.03), spanning from 14.7 to 105.8 Mbp, overlapped QTLs for GY using phenological cofactors in both mapping populations. QTLs for grain yield mapped in two populations derived from the parents Ye478 and Wu312 under field conditions and over two years (Liu et al. 2011) were also coincident with this genomic region.

Our mapping populations were evaluated on a representative location of the Brazilian semi-arid region, although the great amount of QTLs with constant effect across environment showing often additive effects, possible changes in their expression is expected, leading to further validation in the target environment in order to ensure about potential breeding applications in other areas. A detailed characterization and validation of these genomic regions through the further fine mapping studies will help in dissect and identification the putative genes contributing to the phenotypic variation and the molecular markers linked to the QTL can be used as a starting point for marker-assisted selection in molecular breeding strategies in order to improve drought tolerance in maize.

Acknowledgments

The authors would like to acknowledge the Conselho Nacional de Desenvolvimento Científico e Tecnológico (CNPq) and Coordenação de Aperfeiçoamento de Pessoal de Nível Superior (CAPES) for the PhD fellowship to the first author (CAGR); Embrapa Maize and Sorghum and Generation Challenge Programme for the financial support.

References

Agrama HAS, Moussa ME (1996) Mapping QTLs in breeding for drought tolerance in maize (Zea mays L). Euphytica 91:89-97

Akaike H (1974) New Look at Statistical-Model Identification. Ieee T Automat Contr Ac 19:716-723

Ali Q, Ahsan M, Tahir MHN, Khaliq I, Kashif M, Elahi M, Farooq J, Khan NH, Naveed MT, Ali F, Saeed U, Anwar M (2012) An overview of genomics assisted improvement of drought tolerance in maize (Zea mays L.): QTL approaches. Afr J Biotechnol 11:12839-12848

Almeida GD, Makumbi D, Magorokosho C, Nair S, Borem A, Ribaut JM, Banziger M, Prasanna BM, Crossa J, Babu R (2013) QTL mapping in three tropical maize populations reveals a set of constitutive and adaptive genomic regions for drought tolerance. Theor Appl Genet 126:583-600

Almeida GD, Nair S, Borem A, Cairns J, Trachsel S, Ribaut JM, Banziger M, Prasanna BM, Crossa J, Babu R (2014) Molecular mapping across three populations reveals a QTL hotspot region on chromosome 3 for secondary traits associated with drought tolerance in tropical maize. Mol Breeding 34:701-715

Banziger M, Setimela PS, Hodson D, Vivek B (2006) Breeding for improved abiotic stress tolerance in maize adapted to southern Africa. Agr Water Manage 80:212-224

Beyene Y, Semagn K, Mugo S, Tarekegne A, Babu R, Meisel B, Sehabiague P, Makumbi D, Magorokosho C, Oikeh S, Gakunga J, Vargas M, Olsen M, Prasanna BM, Banziger M, Crossa J (2015) Genetic Gains in Grain Yield Through Genomic Selection in Eight Bi-parental Maize Populations under Drought Stress. Crop Sci 55:154-163

Blum A (2005) Drought resistance, water-use efficiency, and yield potential - are they compatible, dissonant, or mutually exclusive? Aust J Agr Res 56:1159-1168

Boer MP, Wright D, Feng LZ, Podlich DW, Luo L, Cooper M, van Eeuwijk FA (2007) A mixed-model quantitative trait loci (QTL) analysis for multiple-environment trial data using environmental covariables for QTL-by-environment interactions, with an example in maize. Genetics 177:1801-1813

Bolanos J, Edmeades GO (1996) The importance of the anthesis-silking interval in breeding for drought tolerance in tropical maize. Field Crop Res 48:65-80

Burton AL, Johnson J, Foerster J, Hanlon MT, Kaeppler SM, Lynch JP, Brown KM (2015) QTL mapping and phenotypic variation of root anatomical traits in maize (Zea mays L.). Theor Appl Genet 128:93-106

Cai HG, Chen FJ, Mi GH, Zhang FS, Maurer HP, Liu WX, Reif JC, Yuan LX (2012) Mapping QTLs for root system architecture of maize (Zea mays L.) in the field at different developmental stages. Theor Appl Genet 125:1313-1324

Cairns JE, Crossa J, Zaidi PH, Grudloyma P, Sanchez C, Araus JL, Thaitad S, Makumbi D, Magorokosho C, Banziger M, Menkir A, Hearne S, Atlin GN (2013) Identification of

Drought, Heat, and Combined Drought and Heat Tolerant Donors in Maize. Crop Sci 53:1335-1346

Ceccardi TL, Meyer NC, Close TJ (1994) Purification of a Maize Dehydrin. Protein Expres Purif 5:266-269

Chardon F, Virlon B, Moreau L, Falque M, Joets J, Decousset L, Murigneux A, Charcosset A (2004) Genetic architecture of flowering time in maize as inferred from quantitative trait loci meta-analysis and synteny conservation with the rice genome. Genetics 168:2169-2185

Clarke JM, Depauw RM, Townleysmith TF (1992) Evaluation of Methods for Quantification of Drought Tolerance in Wheat. Crop Sci 32:723-728

Collins NC, Tardieu F, Tuberosa R (2008) Quantitative trait loci and crop performance under abiotic stress: Where do we stand? Plant Physiol 147:469-486

Dixit S, Swamy BPM, Vikram P, Ahmed HU, Cruz MTS, Amante M, Atri D, Leung H, Kumar A (2012) Fine mapping of QTLs for rice grain yield under drought reveals sub-QTLs conferring a response to variable drought severities. Theor Appl Genet 125:155-169

Grant RF, Jackson BS, Kiniry JR, Arkin GF (1989) Water Deficit Timing Effects on Yield Components in Maize. Agron J 81:61-65

Haley CS, Knott SA (1992) A Simple Regression Method for Mapping Quantitative Trait Loci in Line Crosses Using Flanking Markers. Heredity 69:315-324

Hao ZF, Li XH, Liu XL, Xie CX, Li MS, Zhang DG, Zhang SH (2010) Meta-analysis of constitutive and adaptive QTL for drought tolerance in maize. Euphytica 174:165-177

Hao ZF, Li XH, Xie CX, Weng JF, Li MS, Zhang DG, Liang XL, Liu LL, Liu SS, Zhang SH (2011) Identification of Functional Genetic Variations Underlying Drought Tolerance in Maize Using SNP Markers. J Integr Plant Biol 53:641-652

Harris K, Subudhi PK, Borrell A, Jordan D, Rosenow D, Nguyen H, Klein P, Klein R, Mullet J (2007) Sorghum stay-green QTL individually reduce post-flowering drought-induced leaf senescence. J Exp Bot 58:327-338

Hund A, Reimer R, Messmer R (2011) A consensus map of QTLs controlling the root length of maize. Plant Soil 344:143-158

Ibdah M, Chen YT, Wilkerson CG, Pichersky E (2009) An Aldehyde Oxidase in Developing Seeds of Arabidopsis Converts Benzaldehyde to Benzoic Acid. Plant Physiol 150:416-423

Jaleel CA, Gopi R, Manivannan P, Panneerselvam R (2007) Responses of antioxidant defense system of Catharanthus roseus (L.) G. Don. to paclobutrazol treatment under salinity. Acta Physiol Plant 29:205-209

Jansen RC, Stam P (1994) High-Resolution of Quantitative Traits into Multiple Loci Via Interval Mapping. Genetics 136:1447-1455

Jiang CJ, Zeng ZB (1997) Mapping quantitative trait loci with dominant and missing markers in various crosses from two inbred lines. Genetica 101:47-58

Kadam S, Singh K, Shukla S, Goel S, Vikram P, Pawar V, Gaikwad K, Khanna-Chopra R, Singh N (2012) Genomic associations for drought tolerance on the short arm of wheat chromosome 4B. Funct Integr Genomic 12:447-464

Korol AB, Ronin YI, Nevo E (1998) Approximate analysis of QTL-environment interaction with no limits on the number of environments. Genetics 148:2015-2028

Kosambi DD (1944) The estimation of map distances from recombination values. Ann Eugen 12:172-175. doi:10.1111/j.1469-1809.1943.tb02321.x

Lanceras JC, Pantuwan G, Jongdee B, Toojinda T (2004) Quantitative trait loci associated with drought tolerance at reproductive stage in rice. Plant Physiol 135:384-399

Lander ES, Botstein D (1989) Mapping Mendelian Factors Underlying Quantitative Traits Using Rflp Linkage Maps. Genetics 121:185-199

Li W-J, Liu Z-Z, Shi Y-S, Song Y-C, Wang T-Y, Xu C-W, Li Y (2010) Detection of Consensus Genomic Region of QTLs Relevant to Drought-Tolerance in Maize by QTL Meta-Analysis and Bioinformatics Approach. Acta Agronomica Sinica 36:1457-1467

Lima MDA, de Souza CL, Bento DAV, de Souza AP, Carlini-Garcia LA (2006) Mapping QTL for grain yield and plant traits in a tropical maize population. Mol Breeding 17:227-239

Lincoln SE, Daly MJ, Lander ES (1992) Constructing genetic maps with Mapmaker Exp 3.0. 3rd ed. Whitehead Institute for Biometrical Research, Cambridge, MA.

Liu JC, Cai HG, Chu Q, Chen XH, Chen FJ, Yuan LX, Mi GH, Zhang FS (2011) Genetic analysis of vertical root pulling resistance (VRPR) in maize using two genetic populations. Mol Breeding 28:463-474

Lobell DB, Roberts MJ, Schlenker W, Braun N, Little BB, Rejesus RM, Hammer GL (2014) Greater Sensitivity to Drought Accompanies Maize Yield Increase in the US Midwest. Science 344:516-519

Lu YL, Hao ZF, Xie CX, Crossa J, Araus JL, Gao SB, Vivek BS, Magorokosho C, Mugo S, Makumbi D, Taba S, Pan GT, Li XH, Rong TZ, Zhang SH, Xu YB (2011) Large-scale screening for maize drought resistance using multiple selection criteria evaluated under water-stressed and well-watered environments. Field Crop Res 124:37-45

Lu YL, Xu J, Yuan ZM, Hao ZF, Xie CX, Li XH, Shah T, Lan H, Zhang SH, Rong TZ, Xu YB (2012) Comparative LD mapping using single SNPs and haplotypes identifies QTL for plant height and biomass as secondary traits of drought tolerance in maize. Mol Breeding 30:407-418

Malosetti M, Ribaut JM, Vargas M, Crossa J, van Eeuwijk FA (2008) A multi-trait multi-environment QTL mixed model with an application to drought and nitrogen stress trials in maize (Zea mays L.). Euphytica 161:241-257

Mathews KL, Malosetti M, Chapman S, McIntyre L, Reynolds M, Shorter R, van Eeuwijk F (2008) Multi-environment QTL mixed models for drought stress adaptation in wheat. Theor Appl Genet 117:1077-1091

Messmer R, Fracheboud Y, Banziger M, Stamp P, Ribaut JM (2011) Drought stress and tropical maize: QTLs for leaf greenness, plant senescence, and root capacitance. Field Crop Res 124:93-103

Messmer R, Fracheboud Y, Banziger M, Vargas M, Stamp P, Ribaut JM (2009) Drought stress and tropical maize: QTL-by-environment interactions and stability of QTLs across environments for yield components and secondary traits. Theor Appl Genet 119:913-930

Pastina MM, Malosetti M, Gazaffi R, Mollinari M, Margarido GRA, Oliveira KM, Pinto LR, Souza AP, van Eeuwijk FA, Garcia AAF (2012) A mixed model QTL analysis for sugarcane multiple-harvest-location trial data. Theor Appl Genet 124:835-849

Patterson HD, Thompson R (1971) Recovery of Inter-Block Information When Block Sizes Are Unequal. Biometrika 58:545-&

Payne RW, Harding SA, Murray DA, Soutar DM, Baird DB, Glaser AI, Channing IC, Welham SJ, Gilmour AR, Thompson R, Webster R (2010) GenStat release 13 reference manual, part 2 directives. VSN International, Hemel Hempstead

Piepho HP (2000) A mixed-model approach to mapping quantitative trait loci in barley on the basis of multiple environment data. Genetics 156:2043-2050

Quarrie SA, Steed A, Calestani C, Semikhodskii A, Lebreton C, Chinoy C, Steele N, Pljevljakusic D, Waterman E, Weyen J, Schondelmaier J, Habash DZ, Farmer P, Saker L, Clarkson DT, Abugalieva A, Yessimbekova M, Turuspekov Y, Abugalieva S, Tuberosa R, Sanguineti MC, Hollington PA, Aragues R, Royo A, Dodig D (2005) A high-density genetic map of hexaploid wheat (Triticum aestivum L.) from the cross Chinese Spring X SQ1 and its use to compare QTLs for grain yield across a range of environments. Theor Appl Genet 110:865-880

Ribaut JM, Betrán J, Monneveux P, Setter T (2009) Drought tolerance in maize. In: Bennetzen JL, Hake SC (eds) Handbook of maize: its biology, 1st edn. Springer, New York, pp 311–344

Ribaut JM, Hoisington D, Banziger M, Setter T, Edmeades G (2004) Genetic dissection of drought tolerance in maize: a case study. In: NGUYEN HT, BLUM A (Ed.). Physiology and Biotechnology Integration for Plant Breeding. New York, 2004. cap. 15, p.571-609. ISBN 0-8247-4802-6.

Ribaut JM, Jiang C, GonzalezdeLeon D, Edmeades GO, Hoisington DA (1997) Identification of quantitative trait loci under drought conditions in tropical maize .2. Yield components and marker-assisted selection strategies. Theor Appl Genet 94:887-896

Ribaut JM, Ragot M (2007) Marker-assisted selection to improve drought adaptation in maize: the backcross approach, perspectives, limitations, and alternatives. J Exp Bot 58:351-360

Sabadin PK, Malosetti M, Boer MP, Tardin FD, Santos FG, Guimaraes CT, Gomide RL, Andrade CLT, Albuquerque PEP, Caniato FF, Mollinari M, Margarido GRA, Oliveira BF, Schaffert RE, Garcia AAF, van Eeuwijk FA, Magalhaes JV (2012) Studying the genetic basis of drought tolerance in sorghum by managed stress trials and adjustments for phenological and plant height differences. Theor Appl Genet 124:1389-1402

Saghai-Maroof MA, Soliman KM, Jorgensen RA, Allard RW (1984) Ribosomal DNA Spacer-Length Polymorphisms in Barley - Mendelian Inheritance, Chromosomal Location, and Population-Dynamics. P Natl Acad Sci-Biol 81:8014-8018

Semagn K, Beyene Y, Warburton ML, Tarekegne A, Mugo S, Meisel B, Sehabiague P, Prasanna BM (2013) Meta-analyses of QTL for grain yield and anthesis silking interval in 18 maize populations evaluated under water-stressed and well-watered environments. Bmc Genomics 14

Setter TL, Parra R (2010) Relationship of Carbohydrate and Abscisic Acid Levels to Kernel Set in Maize under Postpollination Water Deficit. Crop Sci 50:980-988

Setter TL, Yan JB, Warburton M, Ribaut JM, Xu YB, Sawkins M, Buckler ES, Zhang ZW, Gore MA (2011) Genetic association mapping identifies single nucleotide polymorphisms in genes that affect abscisic acid levels in maize floral tissues during drought. J Exp Bot 62:701-716

Shah NH, Paulsen GM (2003) Interaction of drought and high temperature on photosynthesis and grain-filling of wheat. Plant Soil 257:219-226

Tran LSP, Urao T, Qin F, Maruyama K, Kakimoto T, Shinozaki K, Yamaguchi-Shinozaki K (2007) Functional analysis of AHK1/ATHK1 and cytokinin receptor histidine kinases in response to abscisic acid, drought, and salt stress in Arabidopsis. P Natl Acad Sci USA 104:20623-20628

Tuberosa R, Salvi S, Sanguineti MC, Landi P, MacCaferri M, Conti S (2002) Mapping QTLs regulating morpho-physiological traits and yield: Case studies, shortcomings and perspectives in drought-stressed maize. Ann Bot-London 89:941-963

Venuprasad R, Bool ME, Quiatchon L, Cruz MTS, Amante M, Atlin GN (2012) A large-effect QTL for rice grain yield under upland drought stress on chromosome 1. Mol Breeding 30:535-547

Zeng ZB (1994) Precision Mapping of Quantitative Trait Loci. Genetics 136:1457-1468

Tables

Table 1. Mean, minimum (Min), maximum (Max), coefficient of variation (CV), estimates of genetic (σ_g^2), block (σ_b^2) and error (σ_ε^2) variances and heritability (h^2) for Grain Yield (Kg.ha^{-1}), Plant Height (cm) and Anthesis-Silking Interval (days) in both $F_{2:3}$ maize mapping populations (MP1 and MP2)

Population	Trait	Environment	Mean	Min	Max	CV	σ_g^2	σ_b^2	σ_ε^2	h^2
MP1	GY	WS06	1757	0	6938	50.83	457154	-	277772	0.62
		WW06	3334	153.2	8855	35.52	692684	54613	382179	0.61
		WS07	2041	0	7307	55.05	633271	184404	313022	0.56
		WW07	3719	772.7	7751	30.7	369273	285031	358018	0.36
	PH	WS06	129.5	85	175	9.5	74.87	17.45	54.36	0.51
		WW06	138.7	75	190	10.2	82.03	-	66.42	0.55
		WS07	134	100	185	10.4	110.07	22.75	56.81	0.58
		WW07	142.8	100	185	9.7	105.52	24.62	56.26	0.57
	ASI	WS06	0.68	-2	5	162.5	0.289	-	0.929	0.24
		WW06	0.47	-2	4	205.1	0.178	-	0.756	0.19
		WS07	1.05	-3	8	188.4	2.805	0.148	1.045	0.70
		WW07	0.10	-3	4	1360	1.0351	-	0.929	0.53
MP2	GY	WS12	3654	0	7330	32.38	468799	40785	550608	0.44
		WS13	1578	306.1	3578	41.37	149099	20730	220528	0.38
	PH	WS12	164.4	120	205	8.197	68.1	-	116.3	0.37
		WS13	145.9	105	200	9.207	75.64	-	99.43	0.43
	ASI	WS12	-0.37	-6	6	-458.1	1.45	-	1.388	0.51
		WS13	2.45	-5	11	105.8	3.472	-	3.158	0.52

WW and WS represent well-watered and water-stressed environments, respectively, followed by the last two digits of the year of evaluation: 06 (2006), 07 (2007), 12 (2012) and 13 (2013). - represents that the variance for block effects was not significant and not included in the model to estimate heritability.

Table 2. QTL effects obtained from the mixed model approach for multiple environments in a $F_{2:3}$ maize population derived from the cross: L2321 x L31212.

Trait (covariate)	Chr (bin) [a]	Pos (cM)	Confidence Interval (cM)	Confidence Interval (Mb) [b]	Markers [c]	Type of QTL Effect	QTL Effects (%GV_{QTL}) WS06	WW06	WS07	WW07	$\overline{SE}$
GY	4.03	22.1	16.1 - 34.7	7.3 - 29.2	PHM2388.27 - PHM2159.8	δ_k	514.1 (7.7)	388 (0.0)	513.9 (6.8)	131 (0.0)	191.7
	5.03	97.8	95.0 - 120.9	28.2 - 58.2	umc1705 - PZA00805.1	δ	-342.7 (6.0)	-342.7 (0.0)	-342.7 (3.3)	-342.7 (1.8)	132.3
	6.04	86.8	77.5 - 107.1	108.5 - 128.4	nc010 - PHM12794.48	α	-214.4 (0.6)	-214.4 (2.3)	-214.4 (0.0)	-214.4 (5.6)	91.4
	7.03	136.7	97.1 - 157.6	130.0 - 165.1	umc1015 - PZA00795.1	α_k	-161.7 (2.8)	26.5 (1.2)	126.2 (0.0)	191.7 (0.3)	131.2
						%GV_T	18.0	1.5	5.3	8.1	
GY(PH)	1.09	251.5	229.1 - 265.5	223.1 - 289.6	PHM15871.11 - PZB01227.6	δ_k	440.4 (5.9)	570.3 (10.0)	114.6 (0.0)	93.6 (0.0)	163.6
	7.03	103.1	78.4 - 127.6	135.5 - 165.1	PZA01542.1 - PZA00795.1	α_k	-21.5 (0.0)	296.2 (6.8)	90.5 (0.0)	353 (13.9)	122.4
	10.03	29.9	25.9 - 33.9	84.0 - 87.3	PZB00409.1 - PZA00814.1	δ_k	-286.6 (2.3)	-200.0 (0.0)	-610.1 (14.4)	-618.4 (20.1)	162.6
	10.05	82.0	66.0 - 91.5	124.3 - 141.6	PZA03196.1 - PZA03603.1	δ_k	-321 (0.0)	-199.6 (0.0)	293.4 (0.8)	-20.3 (0.0)	215.0
						%GV_T	9.5	11.5	7.2	29.0	
GY(ASI)	10.05	84.0	74.0 - 91.5	124.3 - 141.6	PZA03196.1 - PZA03603.1	δ_k	-322.7 (0.4)	-129.7 (0.0)	192.3 (0.0)	-170.3 (0.6)	210.7
						%GV_T	0.4	0.0	0.0	0.6	
GY(PH,ASI)	1.09	249.5	231.1 - 263.5	223.1 - 289.6	PHM15871.11 - PZB01227.6	δ_k	489.2 (10.8)	520.6 (12.3)	210.8 (0.0)	169.8 (1.2)	153.7
	2.08	102.1	94.7 - 132.5	192.6 - 218.3	PHM3055.9 - PZA02012.7	δ_k	258.9 (1.5)	68.7 (0.0)	-52 (2.1)	91.3 (0.0)	160.6
	3.06	194.5	181.1 - 215.1	178.2 - 208.2	PHM17210.5 - PZA02516.1	δ	-228.1 (1.3)	-228.1 (9.3)	-228.1 (2.1)	-228.1 (10.0)	123.1
	4.03	18.1	0 - 38.6	3.5 - 29.2	PHM2438.28 - PZA02457.1	α_k	-129.2 (15.8)	-14.4 (3.0)	-257.8 (8.9)	-258.8 (9.5)	110.3
	7.03	103.1	78.4 - 154.7	130.0 - 165.1	umc1015 - PZA00795.1	α_k	-78.1 (5.0)	229 (10.6)	8.3 (0.0)	224.8 (8.7)	129.6
	8.03	16.9	0 - 35.6	14.7 - 105.8	PZA02955.3 - PHM4134.8	δ_k	-123.7 (0.0)	249.5 (6.8)	37.5 (0.0)	89.8 (0.1)	112.2
	10.03	29.9	25.9 - 37.9	84.0- 87.3	PZB00409.1 - PZA00814.1	δ	-346.2 (0.0)	-346.2 (0.0)	-346.2 (6.8)	-346.2 (12.9)	133.5
	10.05	82.0	66.0 - 91.5	124.3 - 141.6	PZA03196.1 - PZA03603.1	δ_k	-149.1 (0.3)	-60.1 (0.0)	295.5 (0.0)	-29.2 (0.0)	208.4
						%GV_T	23.9	24.7	15.8	43.3	

Table 2. Continued

Trait (covariate)	Chr (bin) [a]	Pos (cM)	Confidence Interval (cM)	Confidence Interval (Mb) [b]	Markers [c]	Type of QTL Effect	QTL Effects (%GV_{QTL}) WS06	WW06	WS07	WW07	$\overline{SE}$
PH	2.04	0.0	0.0 - 13.7	29.2 - 35.3	bnlg381 - PZA01993.7	α_k	-1.61 (9.7)	-2.17 (13.8)	-3.59 (5.4)	-5.48 (8.1)	1.4
	3.04	92.4	75.1 - 107.3	2.7 - 143.9	PHM2776.11 - PHM1745.16	δ_k	-1.55 (0.6)	-5.07 (11.4)	2.52 (0.0)	-1.56 (0.0)	2.2
	4.03	7.4	0.0 - 54.2	3.9 - 66.9	PHM2438.28 - PZA03597.1	α	3.38 (12.5)	3.38 (19.6)	3.38 (13.4)	3.38 (16.7)	1.1
	5.03	136.9	117.6 - 147.6	58.2 - 78.4	PZA00805.1 - PZA02818.6	δ	4.27 (4.5)	4.27 (23.4)	4.27 (0.4)	4.27 (7.15)	1.9
	10.04	51.2	21.9 - 57.2	16.2 - 117.6	PZA02961.6 - PZA01089.1	δ_k	1.67 (0.0)	-1.88 (2.8)	2.30 (0.0)	5.30 (0.0)	2.0
						%GV_T	23.6	63.3	14.4	24	
ASI	1.02	53.8	44.6 - 65.8	22.6 - 28.4	bnlg109 - PZB02058.1	α_k	0.10	0.12	-0.51	-0.37	0.15
						δ_k	0.56 (18.3)	0.08 (0.0)	0.45 (7.3)	0.24 (8.6)	0.23
	10.04	62.1	45.5 – 84.0	109.8 - 141.6	PZA01292.1 - PZA03603.1	α_k	-0.33	-0.08	0.03	0.31	0.18
						δ_k	0.24 (9.7)	-0.06 (31.3)	-0.32 (10.5)	-0.62 (8.8)	0.26
						%GV_T	21.8	21.2	14.3	14.2	

GY: Grain Yield; PH: Plant Height; ASI: Anthesis-Silking Interval; Chr: chromosome; Pos: QTL position; [a] Bin was defined based on the position of the QTL; [b] Physical positions of the markers flanking the confidence interval; [c] Markers flanking the confidence interval; α : additive effect; δ : dominance effect; α_k : environment-specific QTL additive effect; δ_k : environment-specific QTL dominance effect; WS06: water-stressed condition in 2006; WW06: well-watered condition in 2006; WS07: water-stressed condition in 2007; WW07: well-watered condition in 2007. %GV_T : percentage of genetic variance explained by all QTLs per trait. %GV_{QTL} : percentage of genetic variance explained by each individual QTL. $\overline{SE}$: Average standard errors.

Table 3. QTL effects obtained from the mixed model approach for multiple environments in a $F_{2:3}$ maize population derived from the cross: L1761121 x L521237

Trait (covariable)	Chr (bin) [a]	Pos (cM)	Confidence Interval (cM)	Confidence Interval (Mb) [b]	Markers [c]	Type of QTL Effect	QTL Effects (%GV_{QTL})				$\overline{SE}$
							WS12		WS13		
GY	3.04	38.0	33.2 - 43.0	43.9 - 103.4	PZA03070.9 - PZA02299.16	α	264.1	(4.4)	264.1	(24.3)	58.29
						δ	-212.7		-212.7		77.79
	4.06	59.3	43.2 - 74.7	122.8 - 170.5	PZB00093.7 - PHM3155.14	α	-243.8	(7.5)	-243.8	(15.4)	64.83
						δ	376.2		376.2		118.51
	9.04	64.5	46.3 - 77.1	90.4 - 131.0	PZA03596.1 - PHM3502.17	α_k	-69.4	(0.0)	171.4	(5.0)	87.25
						%GV_T		8.5		46.9	
GY(PH)	1.09	110.6	93.6 - 144.9	217.0 - 284.1	PZA03741.1 - PZA02087.2	α	107.7	(5.8)	107.7	(10.1)	48.57
						δ	-207.3		-207.3		70.5
	3.04	43.0	30.9 - 60.5	43.9 - 160.0	PZA03070.9 - PHM9914.11	α	197.8	(5.2)	197.8	(16.7)	52.52
						δ	-191.1		-191.1		69.48
	3.06	98.4	80.2 - 130.5	168.4 - 212.7	PHM1959.26 - PZB01457.1	α_k	-92.9	(2.3)	136.9	(6.0)	70.36
	4.06	57.3	38.0 - 72.7	37.2 - 170.5	PZA01751.2 - PHM3155.14	α	-255.5	(8.5)	-255.5	(15.2)	57.31
						δ	297.9		297.9		106.13
	6.05	72.9	47.7 - 92.6	125.1 - 149.3	PZA01591.1 - PZA02436.1	α	164.7	(0.6)	164.7	(10.3)	53.18
	9.04	66.5	48.3 - 77.1	98.5 - 131.0	PZB01899.1 - PHM3502.17	α	-201	(0.0)	-201	(11.5)	58.49
						%GV_T		19.9		69.7	
GY(ASI)	2.03	41.6	19.9 - 53.6	6.5 - 27.8	PZA01935.10 - PZA03568.1	δ_k	-388.2	(5.2)	40.8	(0.7)	107.4
	4.07	72.7	40.0 - 100.4	37.2 - 194.1	PZA01751.2 - PZB01461.1	δ	221	(0.5)	221	(19.4)	66.73
	6.04	28.9	18.3 - 63.0	91.9 - 141.1	PHM8909.12 - PZA02478.7	α_k	251.1	(6.2)	90.6	(8.9)	68.54
	8.03	40.8	38.6 - 44.4	64.4 - 100.6	PZA00793.2 - PZA03135.1	δ_k	214.5	(3.2)	119.9	(14.6)	88.92
						%GV_T		17.7		35	

Table 3. Continued

Trait (covariable)	Chr (bin) [a]	Pos (cM)	Confidence Interval (cM)	Confidence Interval (Mb) [b]	Markers [c]	Type of QTL Effect	QTL Effects (%GV_{QTL})				$\overline{SE}$
							WS12		WS13		
GY(PH,ASI)	2.02	29.9	17.9 - 53.6	6.5 - 27.8	PZA01935.10 - PZA03568.1	δ_k	-336.5	(8.4)	38.2	(4.46)	99.26
	3.05	66.8	52.5 - 80.2	142.8 - 164.8	PZA00920.1 - PZA01396.1	α	177.9	(0.2)	177.9	(20.7)	39.01
	4.05	47.3	34.0 - 76.7	17.5 - 170.5	PHM687.25 - PHM3155.14	α	-154.4	(0.9)	-154.4	(13.3)	41.46
	6.04	47.7	18.8 - 65.0	91.9 - 141.1	PHM8909.12 - PZA02478.7	α	153.0	(0.4)	153.0	(14.2)	43.28
	8.03	40.8	38.0 - 44.3	64.4 - 100.6	PZA00793.2 - PZA03135.1	δ_k	174.7	(2.3)	-163.2	(17.0)	82.25
						%GV_T		18.3		64.5	
PH	1.04	48.3	42.3 - 68.0	148.6 - 206.2	PZA03200.2 - PHM14614.22	α	4.23	(11.8)	4.23	(11.6)	1.0
	1.07	81.6	77.6 - 88.5	208.1 - 217.0	PZA01019.1 - PZA03741.1	δ_k	-2.37	(2.5)	3.59	(4.4)	1.8
	4.08	100.7	76.7 - 121.7	172.3 - 242.3	PZA01477.3 - PHM4125.11	α	-2.25	(1.2)	-2.25	(1.7)	1.1
	6.06	100.6	88.6 - 116.7	149.3 - 163.3	PZA02436.1 - PZA00889.2	α_k	-3.43	(8.2)	-7.76	(24.0)	1.5
	8.02	13.3	0.0 - 25.9	5.1 - 18.5	PZA01623.3 - PHM5158.13	δ_k	-1.00	(0.0)	-5.31	(7.3)	1.8
						%GV_T		17.0		46.3	
ASI	1.07	77.6	64.0 - 83.6	183.8 - 212.4	PHM5622.21 - PHM1438.34	α	-0.50	(11.1)	-0.50	(9.6)	0.14
	2.02	14.1	0.0 - 29.9	1.2 - 13.8	PHM4951.8 - PZA00108.4	α	-0.64	(10.9)	-0.64	(5.0)	0.15
	3.04	33.2	30.9 - 43.0	43.9 - 103.4	PZA03070.9 - PZA02299.16	α_k	-0.18	(1.4)	-0.92	(12.8)	0.18
	4.05	55.3	43.2 - 72.7	122.8 - 170.5	PZB00093.7 - PHM3155.14	δ_k	-0.62	(11.8)	-1.45	(7.2)	0.39
	9.04	64.5	50.3 - 77.1	98.5 - 131.0	PZB01899.1 - PHM3502.17	α	-0.87	(15.5)	-0.87	(16.1)	0.17
						%GV_T		51.1		56.5	

GY: Grain Yield; PH: Plant Height; ASI: Anthesis-Silking Interval; Chr: chromosome; Pos: QTL position; [a] Bin was defined based on the position of the QTL; [b] Physical positions of the markers flanking the confidence interval; [c] Markers flanking the confidence interval; α : additive effect; δ : dominance effect; α_k : environment-specific QTL additive effect; δ_k : environment-specific QTL dominance effect; WS12: water-stressed condition in 2012; WS13: water-stressed condition in 2013. %GV_T : percentage of genetic variance explained by all QTLs per trait. %GV_{QTL} : percentage of genetic variance explained by each individual QTL. $\overline{SE}$: Average standard errors.

Figures

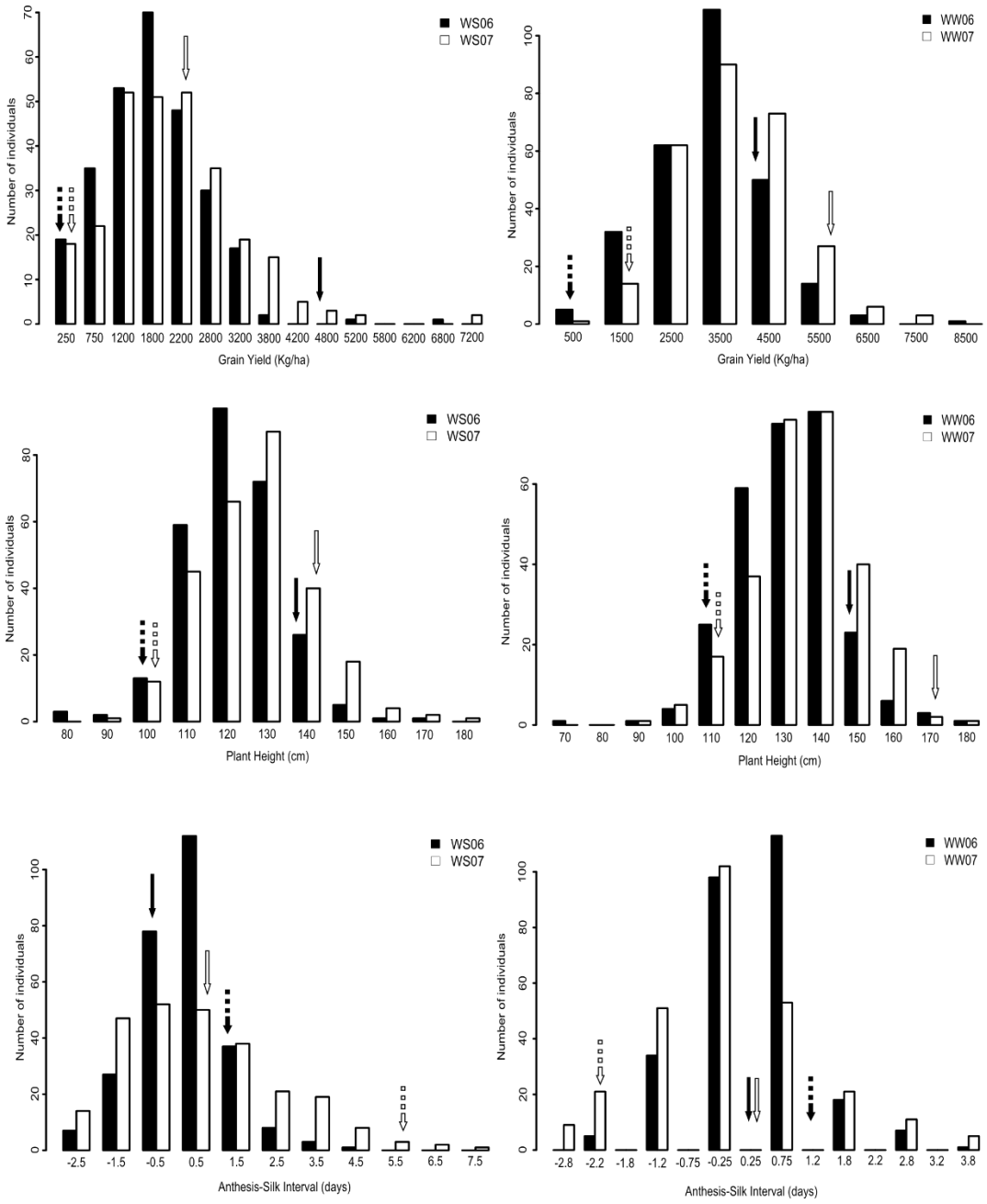

Figure 1. Histograms of the distribution of grain yield ($Kg.ha^{-1}$), plant height (cm) and anthesis-silking interval (days) under water-stressed (WS) and well-watered (WW) conditions in 2006 (06) depicted in black and 2007 (07) depicted in white, across 97 $F_{2:3}$ individuals. Solid arrows represent the phenotypic means for parent L2321 (drought tolerant) and dotted arrows for parent L31212 (drought sensitive).

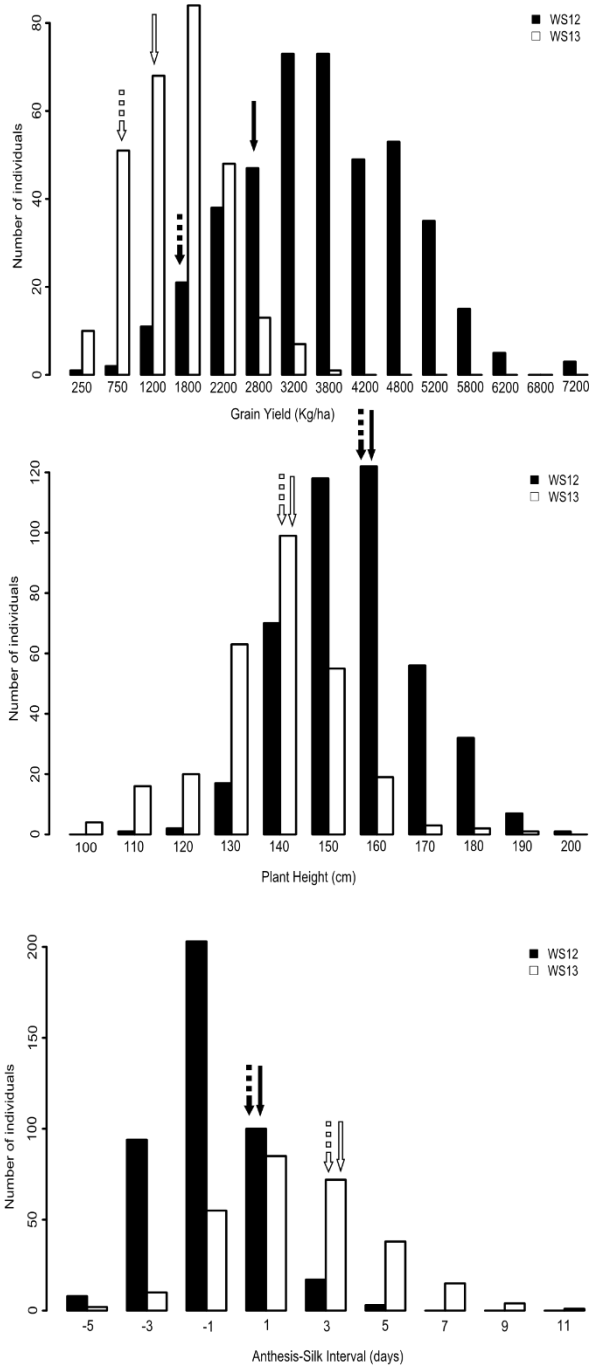

Figure 2. Histograms of the distribution of grain yield (Kg/ha), plant height (cm) and anthesis-silking interval (days) under water-stressed (WS) conditions in 2012 (12) depicted in black and 2013 (13) depicted in white, across 136 $F_{2:3}$ individuals. Solid arrows represent the phenotypic means for the parental L1761121 (drought tolerant) and dotted arrows for the parental L521237 (drought sensitive).

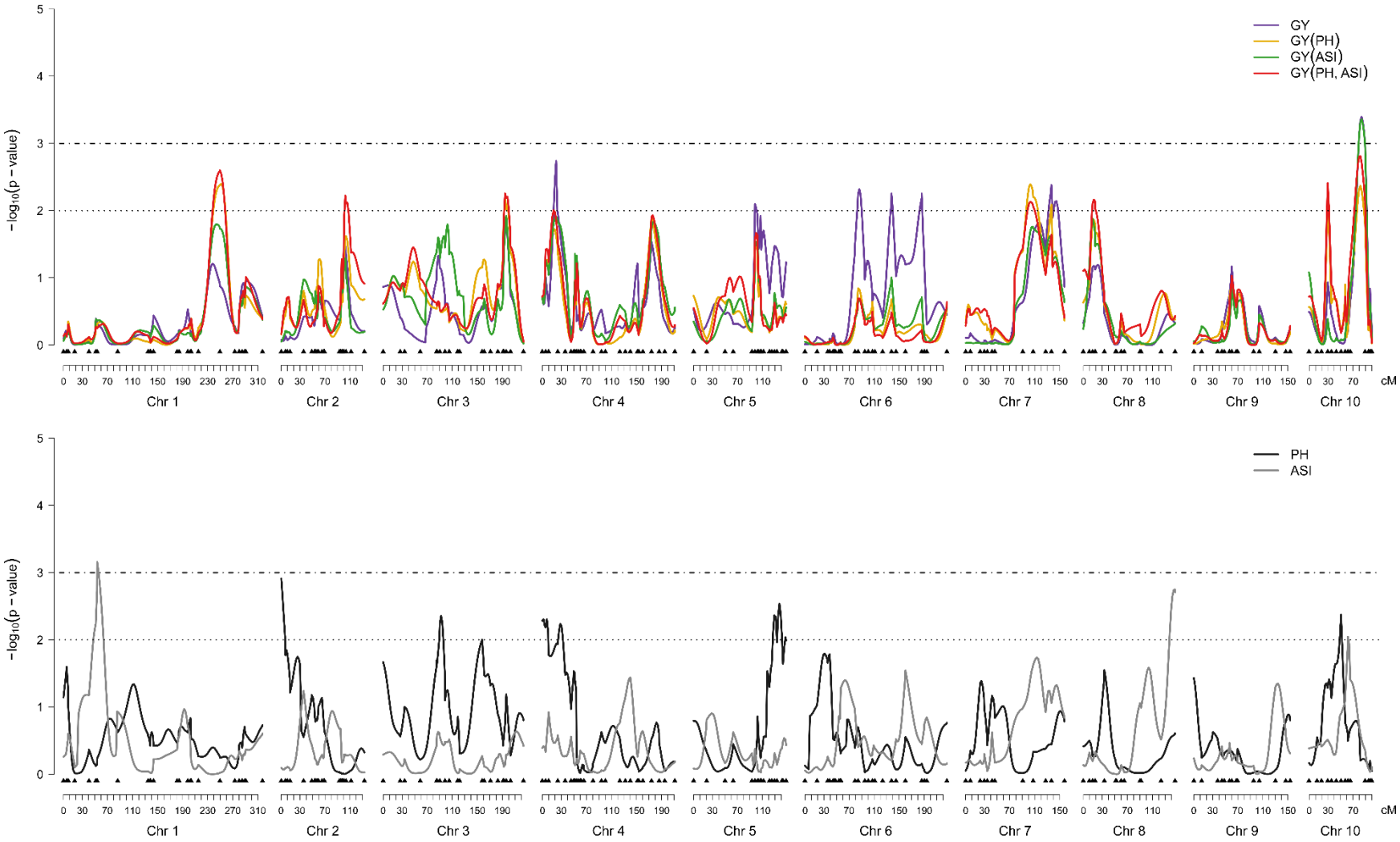

Figure 3. Multi-environment QTL analysis using composite interval mapping (CIM) in the $F_{2:3}$ maize mapping population 1 (MP1) for grain yield without cofactors (GY) and including plant height (GY(PH)), anthesis-silking interval (GY(ASI)) and both (GY(PH,ASI)) as cofactors (top of the figure) and multi-environment QTL analysis for plant height (PH) and anthesis-silking interval (ASI) (bottom of the figure). -$\log_{10}$(p-value) = 2 was considered as threshold to identify significant QTLs.

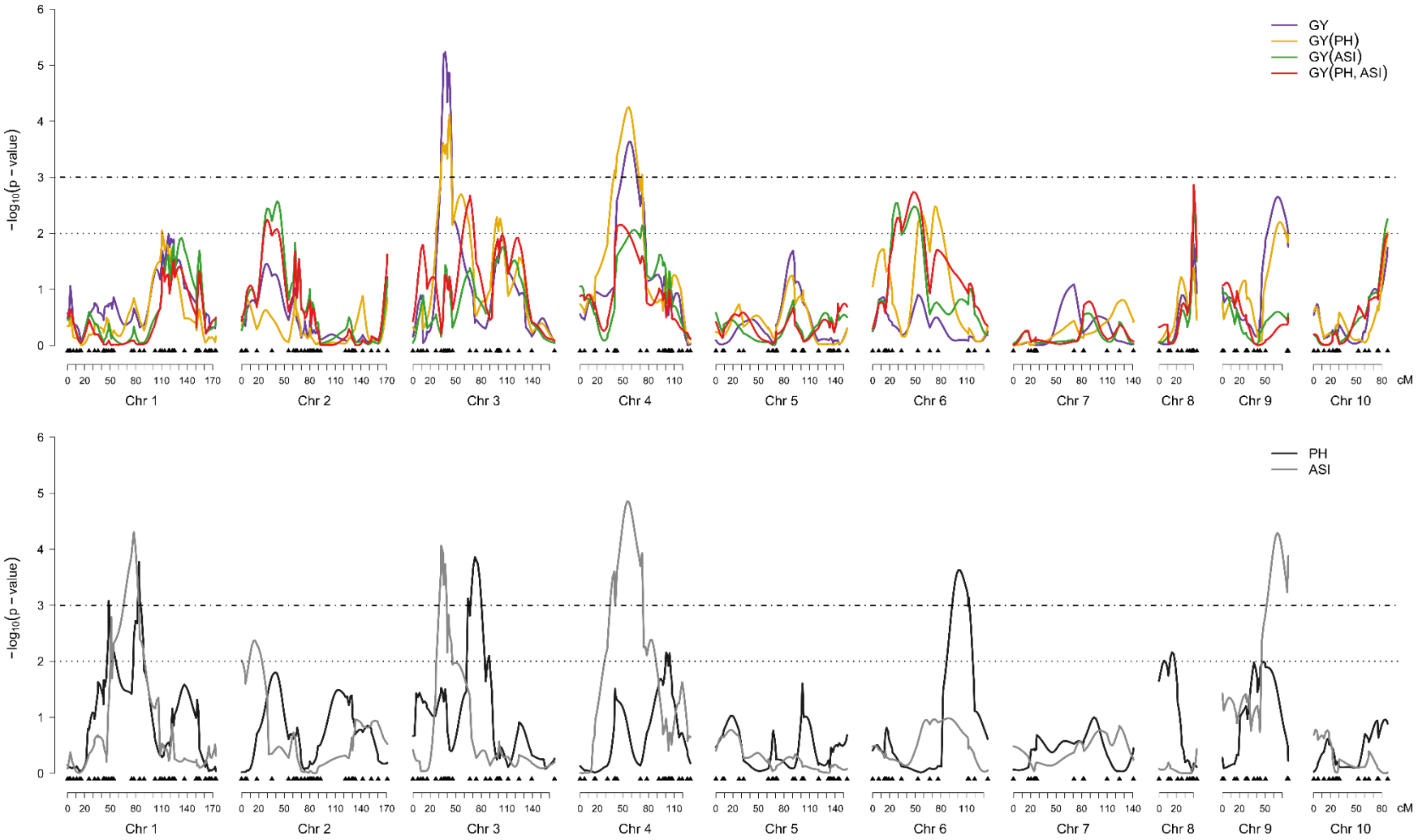

Figure 4. Multi-environment QTL analysis using composite interval mapping (CIM) in the $F_{2:3}$ maize mapping population 2 (MP2) for grain yield without cofactors (GY) and including plant height (GY(PH)), anthesis-silking interval (GY(ASI)) and both (GY(PH,ASI)) as cofactors (top of the figure) and multi-environment QTL analysis for plant height (PH) and anthesis-silking interval (ASI) (bottom of the figure). -$\log_{10}$(p-value) = 2 was considered as threshold to identify significant QTLs.

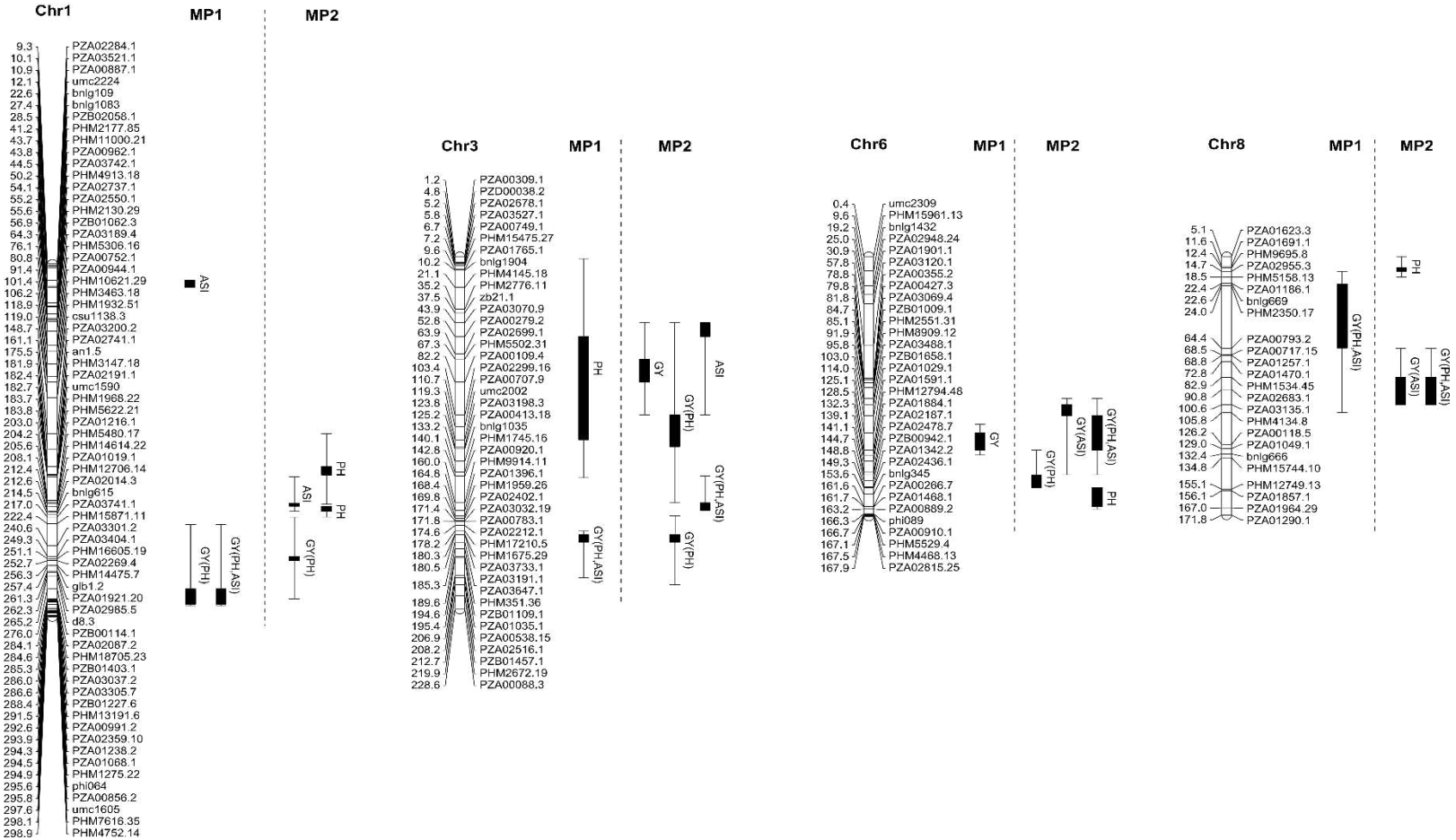

Figure 5. Projection of the QTLs found for plant height (PH), anthesis-silking interval (ASI), grain yield (GY), and grain yield including cofactors for plant height GY(PH), anthesis-silking interval GY(ASI) and both GY (PH,ASI) for mapping population 1 (MP1) and mapping population 2 (MP2). The chromosome 1, 3, 6 and 8 were depicted by display colocalization between both mapping populations. The position of markers are in mega base pair scale. The black boxes represent the region between markers flanking the QTL maximum peak and the projected line the confidence interval.

Supplemental materials

Table S1. Pearson´s correlation for grain yield (GY), plant height (PH) and anthesis-silking interval (ASI) evaluated under water stress (WS) and well-watered (WW) conditions in the years 2006 (06) and 2007 (07) for MP1.

Trait	GY WS06	GY WW06	GY WS07	GY WW07	PH WS06	PH WW06	PH WS07	PH WW07	ASI WS06	ASI WW06	ASI WS07
GY WW06	0.54**										
GY WS07	0.52**	0.30**									
GY WW07	0.29**	0.39**	0.39**								
PH WS06	0.39**	0.42**	0.18*	0.25**							
PH WW06	0.18*	0.40**	0.08	0.20*	0.47**						
PH WS07	0.21**	0.25**	0.51**	0.24**	0.50**	0.35**					
PH WW07	0.08	0.21**	0.14	0.49**	0.50**	0.43**	0.49**				
ASI WS06	-0.06	0.04	-0.04	-0.04	0.00	0.02	0.07	0.12			
ASI WW06	-0.18*	-0.05	-0.16*	-0.14	-0.10	-0.11	-0.07	0.00	0.19*		
ASI WS07	-0.04	0.00	-0.32**	-0.11	0.08	0.01	-0.09	0.08	0.21**	0.21**	
ASI WW07	0.01	0.07	-0.06	-0.16	0.05	0.01	-0.02	-0.06	0.21**	0.16	0.46**

* $\alpha \leq 0.01$; ** $\alpha \leq 0.001$

Table S2. Pearson´s correlation for grain yield (GY), plant height (PH) and anthesis-silking interval (ASI) evaluated under water stress (WS) in the years 2012 (12) and 2013 (13) for MP2.

Trait	GY WS12	GY WS13	PH WS12	PH WS13	ASI WS12
GY WS13	0.32**				
PH WS12	0.28**	-0.02			
PH WS13	0.16*	0.28**	0.39**		
ASI WS12	-0.36**	-0.24**	-0.07	-0.10	
ASI WS13	-0.22**	-0.61**	0.07	-0.13	0.47**

* $\alpha \leq 0.01$; ** $\alpha \leq 0.001$

Figure S1. Climate date of precipitation, minimum temperature (Min temp) and maximum temperature (Max temp) from June to October in 2012 and 2013. Data from Janauba experimental station (15°8’ S, 43°3’ W, 516 m) (Source: INMET Network Data).

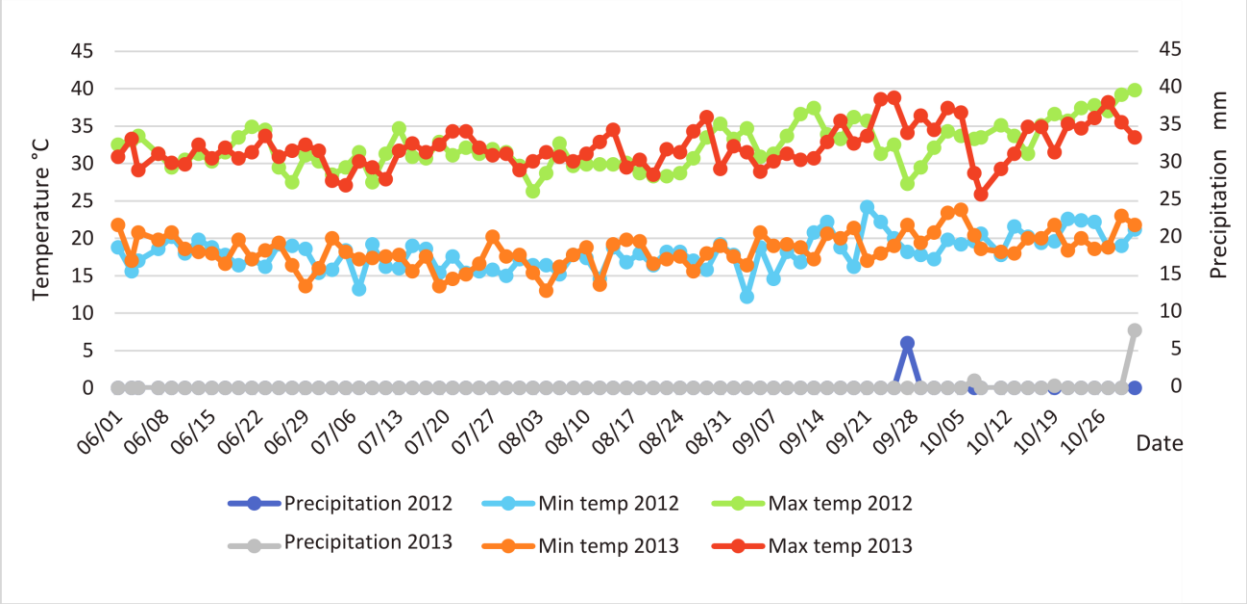

CAPÍTULO 2

Genome-wide association studies for root morphology and phosphorus acquisition efficiency in maize seedlings

Carlos Alexandre Gomes Ribeiro[1,4], Everaldo Gonçalves de Barros[1,2], Christy Gault[3], Jurandir Vieira Magalhaes[4], Sylvia Morais de Sousa[4,5], Maria Marta Pastina[4], Edward S Buckler[3,7,8], Claudia Teixeira Guimaraes[4,6*]

[1]Departamento de Genética e Melhoramento, Universidade Federal de Viçosa, Viçosa, Minas Gerais, 36570-000, Brazil (C.A.G.R., E.G.B)

[2]Programa de Pós-Graduação em Ciências Genômicas e Biotecnologia, Universidade Católica de Brasília, Brasília, Distrito Federal, 70330-710, Brazil (E.G.B)

[3]Institute for Genomic Diversity, Cornell University, Ithaca, New York 14853, USA (C.G., E.S.B)

[4]Embrapa Maize and Sorghum, Sete Lagoas, Minas Gerais, 35701–970, Brazil (C.A.G.R., J.V.M., S.M.d.S., M.M.P., C.T.G)

[5]Departamento de Bioengenharia, Universidade Federal de São João del-Rei, Praça São João del-Rei, Minas Gerais, 36301–160, Brazil (S.M.d.S)

[6]Departamento de Biologia Geral, Universidade Federal de Minas Gerais, Belo Horizonte, Minas Gerais, 31270–901, Brazil (C.T.G)

[7]United States Department of Agriculture-Agricultural Research Service (USDA-ARS) (E.S.B)

[8]Department of Plant Breeding and Genetics, Cornell University, Ithaca, New York 14853, USA (E.S.B)

*Corresponding author: claudia.guimaraes@embrapa.br, phone: +55 31 3027 1300, fax: +55 31 3027 1279

Abstract

Phosphorus (P) bioavailability is a recurrent problem in tropical soils. Maximizing soil exploration through proliferation and extension of the root system is a strategy for plants to overcome P deficiency. Genome-wide association with 561 tropical maize inbreed lines was undertaken for root morphology and P acquisition traits under low- and high-P concentrations, based on SNP markers obtained through Genotyping-by-Sequencing. Population structure was assessed through principal component and clustering analyses suggesting two subgroups formation within the panel, and the five first principal components were used for type I error correction. Linkage disequilibrium in this population decayed fast, reaching r^2 of 0.2 when two SNPs were separated on average by 1 kbp. A total of 136 SNPs were significantly associated with the phenotypic traits based on mixed linear model (-log(P-value) ≥ 5). Significant SNPs were well distributed across all chromosomes, corroborating with the genetic complexity of root morphology and P acquisition traits. Among these SNPs, the SNP S8_89092905 was found within the predicted gene GRMZM2G044531 in the chromosome 8, which encodes a putative AGC kinase family protein. Its C allele enhanced significantly root length under low-P condition, showing a trend towards improving root surface area, total seedling dry weight and total P content, and reducing total P concentration, with minimum influence on root diameter. Another SNP, S8_88964594, ~127 kbp away from the SNP S8_89092905 was detected with high linkage disequilibrium (r^2 = 0.77), it was placed within the candidate gene GRMZM2G057116, which encodes a putative WRKY transcription factor, making this region relevant for further studies. Comprehensive genome association analysis in the current study revealed potential candidate genes that can be used as target for marker-assisted breeding to develop P acquisition efficient maize genotypes.

Keywords: GWAS, GBS, root related traits, P uptake

Introduction

The food requirement facing the population increase is a great challenge for agricultural production. Abiotic stresses are important constraints for global food security, including phosphorus (P) as the second most limiting nutrient for grain yield after nitrogen (Vance and Chiou, 2011). P is a molecular component of nucleic acids and phospholipids, as well as it is involved in several metabolic processes (Plaxton, 1999; Hammond et al., 2004; Raghothama and Karthikeyan, 2005), being a mineral nutrient highly required for plant growth and development. In addition, P has one of the lowest use efficiency among the plant macronutrients and even with well-fertilized conditions, P deficiency can occurs in soils where P is strongly bound to soil clays (Wissuwa et al., 2005). Thus, high amount of chemical P fertilizers are required for a high-yield farming system, where the crops acquire less than 10% of the applied fertilizers (Baligar et al., 2001). In tropical soils, which are acid by nature, the P fixation by aluminum and iron oxides in clay minerals forms insoluble complexes, leading to a very low mobility of P (Shen et al., 2011). Beside the low-P bioavailability, the P is a non-renewable mineral, which may run out in less than 100 years (Vance et al., 2003; Vance and Chiou, 2011), justifying the studies on P use efficiency and adaptation mechanisms of plants under low-P conditions.

Plants have several physiological strategies to withstand P deficiency (Hammond et al., 2004) that can be classified in two general mechanisms: P internal utilization efficiency and P acquisition efficiency (Vance et al., 2003; Parentoni and Souza Júnior, 2008). P internal efficiency is related to the yield produced by the plants per nutrient applied (Good et al., 2004), involving mechanisms of P recycling, translocation and storage (Schachtman et al., 1998; Raghothama, 1999; Baligar et al., 2001; Vance et al., 2003; Shenoy and Kalagudi, 2005). P acquisition efficiency mechanisms are associated with chemical modifications of the rhizosphere (Schachtman et al., 1998; Dakora and Phillips, 2002), interactions with microorganisms (Schachtman et al., 1998; Rai et al., 2013) and changes in the root system (Lopez-Bucio et al., 2003; Zhu and Lynch, 2004; Lynch, 2007; Haling et al., 2013). The low concentration and mobility of P in the soil makes the proliferation and extension of the root system one of the main strategy to maximize P acquisition efficiency (Ramaekers et al., 2010). Additionally, P acquisition efficiency exerted higher effect in P use efficiency compared with P internal efficiency in tropical maize genotypes (Parentoni and Souza Júnior, 2008).

One promising approach to overcome P deficiency in plants is to explore the diversity in root morphology and theirs mechanisms of adaptation (Wissuwa et al., 2009). Despite useful, root traits are rarely applied as selection criteria in plant breeding due to the difficult of evaluation, mainly under field conditions. Several studies detected genetic variation for phosphorus efficiency among maize genotypes (Zhu et al., 2005, 2005; Parentoni et al., 2010; Calderon-Vazquez et al., 2011). However, a few genes were related to P efficiency in plants, one notable example is the Phosphorus-starvation tolerance 1 (PSTOL1), which encodes a serine/threonine kinase responsible to enhance early root growth and P acquisition in rice (Gamuyao et al., 2012). In maize, at least four candidate genes sharing high sequence identity and a conserved serine/threonine kinase domain with OsPSTOL1were co-localized with QTLs for root morphology and P acquisition traits (Azevedo et al., 2015). Additionally, these genes expressed preferentially in roots of the parental lines that contributed the alleles enhancing the respective phenotypes (Azevedo et al., 2015). Other protein kinases were related to root development, and also involved in nutrient acquisition (Santner and Watson, 2006; Zegzouti et al., 2006; Ma et al., 2012). For instance, the gene IRE (incomplete root hair elongation), encoding a serine/threonine kinase domain protein, was responsible to reduce the root hair in 40% compared to wild types in Arabidopsis (Oyama et al., 2002). OXI1 (Oxidative Signal Inducible1) encodes an AGC protein kinase responsible to improve root growth in response to mycorrhizal fungal infection in Arabidopsis (Camehl et al., 2011). Another AGC2-1 protein kinase is involved in root hair growth and development in Arabidopsis (Anthony et al., 2004).

Maize is the most widely cultivated cereal in the world with an extensive use, ranging from animal feed to biofuels industries. Maize is also highly genetic diverse, with a genome size of more than 2,000 Mbp, composed by approximately 85% of transposable elements and over 32,000 predicted genes in the reference genome (Schnable et al., 2009; Law et al., 2015). Association mapping emerged as a powerful approach to dissect complex traits controlled by many quantitative trait loci (QTL), by exploring the historical and evolutionary recombination within a collection of individuals (Yu and Buckler, 2006; Yan et al., 2011). Association mapping evaluates a broader number of alleles, requires a reduced time to generate a mapping population and offers a higher mapping resolution compared to linkage mapping (Yu and Buckler, 2006). Although both approaches can be complementary, and used for cross-validation. However, the linkage disequilibrium (LD) decay is critical to determine the mapping resolution and the marker density

required to cover the whole genome, which is highly variable among species and populations (Yan et al., 2011). In maize, the patterns of LD vary substantially regarding to the genome region and to the genetic variability within the target population, which ranges from a several hundred bp to few hundred kbp (Flint-Garcia et al., 2003; Chia et al., 2012). The current work aimed to identify SNP markers associated with genomic regions controlling root morphology and P acquisition in nutrient solution using a panel of tropical maize inbred lines.

Results

Phenotypic evaluation of the tropical maize association panel

A panel composed of 561 tropical maize inbred lines, including 363 from Embrapa and 198 from DTMA (Drought Tolerant Maize for Africa), was characterized for root morphology and P acquisition related traits. A total of 20 root morphology traits were assessed in nutrient solution under low- and high-P concentrations according to de Sousa et al. (2012), as well as three components of seedling dry weight, three of P concentration and three of P content. The association panel was evaluated in hydroponic solution containing the essential nutrients except for phosphorus, which was divided in two conditions, under low P availability and a control condition, here designated as high P. The correlations among all traits are depicted in the figure 1. High genetic variation and moderate to high broad sense heritability was observed for all traits (Table 1), corroborating previous results using a reduced number of maize genotypes (de Sousa et al., 2012; Azevedo et al., 2015). The heritability range was 0.381 for SPCont to 0.748 for ProjArea and SurfArea in low P condition and under high P the range was 0.461 for RPCont to 0.791 for AvgDiam. In general, root morphology traits showed higher heritability when compared with P concentration and P content. Traits evaluated under low and high P conditions showed similar profiles when the correlation among them was compared (Figure 1). Out of the 29 root morphology and P acquisition traits, six well-representative traits were selected based on low coefficient of variation and high heritability values, which were: total root length, average root diameter, root surface area, total seedling weight, total seedling P concentration and total seedling P content. These traits followed the normal distribution with a slight right skew.

Total root length was highly correlated with root surface area under low P condition (r^2 = 0.75), with a little reduction under high P (r^2 = 0.67). Average root diameter showed intermediate

and positive correlation with root surface area under low P (0.6), which was reduced in high P (0.38). Average root diameter was not correlated with total root length in low P and negatively correlated under high P (r^2 = -0.36). The correlation coefficient between total seedling dry weight and total root length was intermediate, ranging from 0.34 (low P) to 0.54 (high P), whereas it showed low correlations with root surface area under low (0.13) and high P (0.18), reaching negative values with average root diameter under low (-0.18) and high P (-0.40). Total seedling P concentration was negatively correlated to total seedling dry weight under both low and high P. Total seedling P content is a result of total seedling dry weight times P concentration, presenting positive correlations as expected. Root surface area was negatively correlated under both conditions, compared to total seedling P concentration and content, presenting higher correlation under high P. Total root length was negatively correlated with total seedling P concentration under low (-0.5) and high P (-0.44), and the correlation was low between total root length and total seedling P content under both conditions. The correlation between average root diameter and total seedling P content under low P and high P was -0.27 and -0.29, respectively. Average root diameter presented a contrasting profile compared with total seedling P concentration in low P (r^2 = -0.1), being positively correlated in high P (0.19).

Corrections of type I error using population structure and kinship matrix

A subset of 12,700 random SNPs, selected based on minor allele frequency (MAF) ≥ 1% and 10% of missing data, were used for principal components analysis (PCA). The five first principal components were included as a covariate to control the population structure in the GWAS model. The same group of SNPs was used to calculate a pairwise dissimilarity matrix based on the simple matching coefficient and then converted to a similarity matrix (K matrix) (Bradbury et al., 2007). The population structure was mainly applied for type I error correction in the GWAS. After testing several models for type I error correction using mixed linear model (MLM) according to Bradbury et al. (2007), the model considering both PC + K showed the best fit for GWAS (Figure S1).

With the same SNP data, a distance matrix was calculated for clustering analysis, the maize lines were clustered in two major groups, composed by Embrapa and DTMA lines (Figure 2), with few lines overlapping between the groups. The population structure was consistent with their geographical and selection origin as expected. Moreover, the Embrapa lines showed subgroups

formation that were divided by the major heterotic groups, Flint and Dent, which were confirmed by the pedigree data.

Fast linkage disequilibrium decay within the panel

Linkage disequilibrium analysis (LD) was performed between pairs of another subset of markers containing 29,188 SNPs filtered by MAF ≥ 5% and 10% of missing data. The nonlinear regression trend line of the average LD (r^2) vs the physical distance in base pair (BP) showed an average LD considering $r^2 = 0.2$ of approximately 1 kbp (Figure 3). LD decay slightly varied among chromosomes, ranging from $r^2 = 0.182$ on chromosome 7 to $r^2 = 0.236$ on chromosome 5 for a 1 kbp distance between SNPs.

Genome wide association mapping

The GWAS was performed with 353,540 SNPs in 561 inbred lines for the six selected traits (total root length, average root diameter, root surface area, total seedling dry weight, total seedling P concentration and total seedling P content) evaluated in low P and high P conditions. A best linear unbiased estimator (BLUE) for all traits was used to obtain the adjusted means. Different matrices of variance and covariance were tested for the phenotypic model adjustment and 12 checks were used in each experiment to obtain the adjusted means for the GWAS analysis. A total of 136 and eight SNPs were significantly associated at $-\log_{10}$ (P-value) of 5 and 6, respectively, considering all traits and both P conditions. The significant SNPs were well distributed across all chromosomes, encompassing 55% of all bins with at least one significant SNP, supporting the genetic complexity of root morphology and P related traits (Figure 4). The eight significant SNPs with $-\log_{10}$ (P-value) ≥ 6 were described in Table 2.

SNPs significantly associated with root morphology traits and total seedling dry weight

Six SNPs were significant for total root length at ($-\log_{10}$ (P-value) ≥ 5), with five for low P condition and one for high P. One of these SNPs, S8_89092905, showed the highest $-\log_{10}$ (P-value), 6.30, under low P, and it is located within the gene GRMZM2G044531 that encodes a putative AGC kinase family protein. For the root surface area, 11 SNPs were significant ($-\log_{10}$ (P-value) ≥ 5), seven for low P and four for high P. For root diameter average, 16 SNPs were associated ($-\log_{10}$ (P-value) ≥ 5), being three under low P and 13 under high P conditions. The

SNP S4_3746664 was highly associated under high P ($-\log_{10}$ (P-value) = 6.44), and placed within the predicted gene GRMZM2G037472, still uncharacterized. For total seedling dry weight, 27 SNPs were found to be associated with $-\log_{10}$ (P-value) ≥ 5, being 14 under low P and 13 for high P. With $-\log_{10}$ (P-value) ≥ 6, two associated SNPs S6_34607259 ($-\log_{10}$ (P-value) = 6.37) that does not hit any coding region and S9_137492237 ($-\log_{10}$ (P-value) = 6.43), were found for low P, the second SNP is 57 bp upstream the gene GRMZM2G378852 that encodes a putative MAPKKK family protein kinase. In addition, one associated SNP for high P (S10_77271433) was found with a $-\log_{10}$ (P-value) = 6.41, which was mapped within the predicted gene GRMZM2G110145, a putative cellulose synthase-like family protein.

The maize lines were divided based on the alleles for each SNP and the phenotypic means for all traits were compared for the SNPs S4_3746664, S8_89092905 and S9_137492237 (Figures 6 and 7). The allele A of the SNP S4_3746664 reduced root diameter under high P, with no effect under low P. A slight increase was observed for this allele on root length, total seedling dry weight and total seedling P content under low and high P conditions. The allele C of SNP S8_89092905 improved root length and root surface area under low P, also favoring these root traits under high P conditions, as well as total seedling dry weight and P content under both conditions. Additionally, it tended to decrease the total seedling P concentration without affecting average root diameter. The allele A of SNP S9_137492237 increased the total seedling dry weight with a slight improvement on total root length under low P.

A genomic region of about 610 kbp on maize chromosome 8 encompasses the significantly SNPs S8_89092905, associated with total root length and root surface area under low P (Figure 8). Despite a pericentromeric region with an expected extensive LD, a low LD was observed, comparing the S8_89092905 with the others 29 SNPs within this region, except for the SNP S8_89085566 (6.4 kbp upstream) and a group of five SNPs, approximately 127 kbp upstream the SNP S8_89092905. Among these five SNPs the second most significant SNP within this region (S8_88964594) presented a high LD ($r^2 \sim 0.77$) with the S8_89092905, the most significant one. S8_88964594 is inside the predicted gene GRMZM2G057116 that encodes a WRKY transcription factor.

SNPs significantly associated with total seedling P concentration and total seedling P content

For total seedling P concentration trait based on $-\log_{10}$ (P-value) ≥ 5, 32 SNPs were associated, 20 for low P and 12 for high P. No SNP was significant associated with the $-\log_{10}$ (P-value) ≥ 6. For the total seedling P content trait, 45 SNPs were found to be associated with a $-\log_{10}$ (P-value) ≥ 5, being 28 for low P and 16 for high P. With a $-\log_{10}$ (P-value) ≥ 6 were associated three for high P, The SNPs S8_21321754 and S8_21321777, both with $-\log_{10}$ (P-value) = 6.34 but more than 20 kbp away from the closest gene and S9_142935696 ($-\log_{10}$ (P-value) = 6.11), within the gene model GRMZM2G104618. Manhattan plot for all traits and conditions were depicted in the figures S2 and S3.

Discussion

Morphology traits

We assessed root morphology traits, P concentration and P content in maize inbred lines of 13 days old seedlings, grown hydroponically using low and high P concentrations in a paper pouch system. Mean values of the phenotypic traits were similar to those found by de Sousa et al. (2012), with little difference observed in CV and heritability estimates, possibly attributed to a greater number of genotypes showing a larger variability for root morphology traits (Table 1). Most of the traits were not affected by the P concentration in the nutrient solution, which presented similar means under low and high P (Figure 1). Several traits were highly correlated both positively and negatively, which were grouped to select one representative trait of each group. It is important to notice that some traits were derived from other measurements, justifying their high correlations (Zobel, 2008; de Sousa et al., 2012). Traits as root length and root dry weight have been shown to be positive correlated with grain yield (Cai et al., 2012; Abdel-Ghani et al., 2013).

Linkage disequilibrium

Maize is a cross pollinated species that normally presents a fast LD decay, which varies depending on the genetic diversity within the panel (Flint-Garcia et al., 2003). LD extension can decay within a few hundred base pairs (100 – 400 bp) in exotic maize landraces (Tenaillon et al., 2001) up to hundreds of thousands bp, as found in a set of temperate panel (Ames panel) with an average LD decay close to 10 kbp (Romay et al., 2013; Pace et al., 2015). Most of the studies uses

$r^2 = 0.2$ as threshold to consider the LD decay of average distance between SNPs. Our maize panel includes tropical maize lines derived from different breeding programs, including Brazil, South America and Africa, which presented the LD decay of 1 kbp (Figure 3). A panel composed by 103 maize lines genotyped with 55 million SNPs in the HapMap2, the LD extension was 5.5 kbp, reaching 1 kbp when 19 wild ancestors were included in the analysis (Chia et al., 2012). Thus, we can infer that our current panel, composed by 561 tropical maize lines, represents a high genetic diversity.

The fast LD decay request a high density of markers to provide a reasonable genome coverage (Tenaillon et al., 2001; Yu and Buckler, 2006), but the associated markers are expected to locate close to the target gene (Yan et al., 2011). Thus, in order to improve the already high density of over 350,000 GBS-based SNPs, we projected the version 3.1 of the maize HapMap onto our GBS data. This maize HapMap version includes over 60 million SNPs in 916 maize lines (unpublished data, Bukowski et al. in preparation). Over 8 million SNPs filtered for 50% of missing data and MAF of 5% were tested using GLM model for all traits and conditions, but no gain in the additional genome coverage was achieved, probably due a lack of tropical founders lines in the imputation steps, mostly ones that are part of the genealogy of our association mapping panel.

Association studies and candidate genes

The ability to overcome the low P availability has been associated to the exploratory capacity of roots in the soil (Forde and Lorenzo, 2001; Lopez-Bucio et al., 2003; Zhu and Lynch, 2004; Lynch, 2007; Svistoonoff et al., 2007; Parentoni and Souza Júnior, 2008; Ramaekers et al., 2010; Haling et al., 2013). According to Parentoni and Souza Júnior (2008), P acquisition efficiency in maize was more relevant to explain the total variation for P use efficiency than P internal utilization efficiency in a tropical maize germplasm under low P soils. The increases in root length and root surface area have improved P acquisition in Sorghum bicolor (Hufnagel et al., 2014), Cucumis melo (Fita et al., 2012) and Brassica napus (Zhang et al., 2011). Hence, strategies to investigate the genetic basis underlying root morphology traits and P acquisition could help the identification of genes and their favorable alleles useful for breeding purpose.

The allele A of the SNP S9_137492237 improved significantly the total seedling dry weight as well as the total root length and the root surface area, and reduced the total seedling P

concentration under P deficiency (Figures 6 and 7). This SNP locates 57 base pairs upstream the gene GRMZM2G378852 that encodes a putative MAPKKK family protein kinase. Although its function have not been determined, MAPKKK kinases are highly expressed maize primary roots (Kong et al., 2013; Liu et al., 2013), are involved in adventitious root development in cucumber (Pagnussat et al., 2004), and participate in several signaling events during plant development, such as cell division and in response to various stresses in maize (Hardin and Wolniak, 2001).

The SNP S4_3746664 was highly associated with average root diameter ($-\log_{10}$(P-value) = 6.44), of which the allele A reduced the root diameter under high P, with a slight improvement in root length, total seedling biomass and total seedling P content (Figures 6 and 7). This SNP harbors within the candidate gene GRMZM2G037472, which encodes a kinesin motor domain containing protein, involved in microtubule motor, however still uncharacterized. A smaller diameter in seminal roots have been suggested as an advantage in nutrient acquisition (Lynch, 2013). Additionally, features such as large diameter of primary root, are fundamental to favor the water flux and facilitate the root penetration in hard soils contributing to increase drought tolerance and nitrogen acquisition (Clark et al., 2008; Bengough et al., 2011; Lynch, 2013). Here we evaluated the average diameter of the whole root system, without discriminating the specific root types, therefore, the selection of genes contributing to enhance a specific root trait could result in positive gains in a breeding context for tolerance to multiple stresses.

The SNP S8_89092905 was highly associated with total root length under P deficiency. The allele C improved the early development of root system, increasing the total biomass accumulation, without affecting root diameter (Figure 6). This allele also tended to increase the total seedling P content and to reduce the total seedling P concentration (Figure 7), which is also highly concordant with the improvement on P acquisition efficiency by increasing root system. Although the fast decay detected on average in our panel (Figure 3), substantial variation in LD extension among genes within the same population has been observed reflecting the effect of chromosomal regions (Remington et al., 2001; Yan et al., 2011). The SNP S8_89092905 was located in a pericentromeric region of the chromosome 8, and despite the high LD extension expected, the average of r^2 between nearby markers has not been very high ($r^2 \sim 0.18$) (Figure 8). The SNP S8_89092905 is within the gene model GRMZM2G044531, which encodes a putative AGC kinase family protein. Different kinases from AGC family have been described in Arabidopsis to modulate root hair growth and development (Anthony et al., 2004), to promote root

growth in response to mycorrhiza infection (Camehl et al., 2011) and to regulate root waving (Santner and Watson, 2006). The SNP S8_88964594 was in highly LD with the SNP S8_89092905 (r^2 = 0.77) although they are separated physically by ~127 kbp away. The former SNP is within the gene model GRMZM2G057116 that encodes a putative WRKY transcription factor, which is well documented to be related to abiotic stresses such as aluminum, cold, drought and salinity in Arabidopsis, barley and maize (Eulgem et al., 2000; Seki et al., 2002; Mare et al., 2004; Maron et al., 2008; Mattiello et al., 2010). The genes GRMZM2G044531 and GRMZM2G057116 both encode uncharacterized proteins, however they belong to protein families, with other known genes already described to be related to root development under stress conditions (Rentel et al., 2004; Zegzouti et al., 2006; Lan et al., 2013). Furthermore, both genes could be acting separately or perhaps synergistically enhancing root development mainly under low P condition, making them important candidate genes.

A comprehensive genome association analysis revealed SNPs significantly associated with root morphology and P acquisition related traits that can be targets for marker-assisted breeding to improve P efficiency in maize. Maize P acquisition efficiency is not an easy index to evaluate under field condition, but is often related to differences in root morphology (Lynch, 2011). This makes root morphology assessed in young plants a useful tool to identify putative candidate genes enhancing the agronomic performance under low P conditions (Hufnagel et al., 2014). Due to the complexity of root morphology traits, a high number of SNPs were well distributed across the maize genome, covering a large portion of bins (Figure 4), but only a few of them were detected with high significance level, which was also found for this type of traits by Pace et al. (2015). Although other significant SNPs were found, those three SNPs described (S4_3746664, S8_89092905, S9_137492237) were highlighted by being associated with candidate genes related to gene families described by are involved in root morphology under abiotic stress, where the genes GRMZM2G044531 and GRMZM2G378852 encode putative serine/threonine kinases. One of the most important gene described to enhance early root growth and P acquisition in rice, PSTOL1 (Gamuyao et al., 2012), also contains a serine/threonine kinase domain, although comparing all amino acid sequence it shares low sequence similarity with those two genes. Some other kinase proteins have been described to be directly or indirectly involved in pathways related to root development, especially related to nutrient acquisition (Oyama et al., 2002; Zegzouti et al., 2006;

Camehl et al., 2011; Ma et al., 2012), suggesting a relevant role of diverse protein kinases in regulation of root development.

Material and methods

Plant material

The association mapping panel was composed by 561 inbred lines, including 363 from Embrapa Maize and Sorghum, and 198 from Drought Tolerant Maize for Africa panel (DTMA panel). The lines from Embrapa contained materials from different heterotic groups and some groups directly applied for breeding purposes aiming P acquisition efficiency, whereas a random subset of DTMA lines were obtained from the International Maize and Wheat Improvement Center (CIMMYT). These inbred lines were selected to represent a large diversity of tropical maize lines.

Root morphology analysis and phosphorus quantification

A high throughput phenotyping system based on assisted imaging, hydroponic culturing and computer quantification of root growth has been developed for root morphology (de Sousa et al., 2012), and it was used for the proposed screening of AM panel. Maize seeds were surface sterilized with sodium hypochlorite 0.5% (v/v) for 5 min and germinated in moistened paper rolls. After four days, the endosperm was removed and seedlings transferred to moistened blotting paper in paper pouches (24 x 33 x 0.020 cm) (Hund et al., 2009). Three uniform seedlings representing each genotype composed each paper pouch. Each container unit consisted of 10 paper pouches whose bottom 3 cm immersed in containers filled with 5 L of modified Magnavaca´s nutrient solution (Magnavaca et al., 1987) with 2.5 μM P for the low P and 250 μM P for the high P condition. The nutrient solution were replaced every three days and pH was maintained at 5.65. The containers were maintained in a growth chamber at controlled day/night temperatures (27/20 °C) with 12 h of h photoperiod, light intensity of 330 μmol photons m^{-2} s^{-1}.

After 13 days the root images were captured with a digital photography setup and analyzed using RootReader2D (http://www.plantmineralnutrition.net/rootreader.htm) and WinRHIZO (http://www.regent.qc.ca/products/rhizo/rhizo.html) software. The root system of each plant was spread out in a translucent, water filled tray illuminated from below and individually imaged. The images were batch thresholded using the RootReader2D software. During thresholding, the pixel

intensities are inverted and the dark roots separated from the illuminated background using a double adaptive thresholding filter. The thresholded images were imported into the WinRHIZO software for root analysis and quantification. The images were analyzed using a calibration grid as a reference scale and changing the input settings to pale roots on a black background (de Sousa et al., 2012). Totalizing 20 root morphology traits: Total root length (Length); Length per volume (LenPerVol); Average root diameter (AvgDiam); Number of forks (Forks); Number of crossing (Crossings); Total projected root area (ProjArea); Root surface area (SurfArea); Root volume (Volume); Root length $0.0 < d \leq 1.0$ (L1); Root surface area $0.0 < d \leq 1.0$ (SA1); Root projected area $0.0 < d \leq 1.0$ (PA1); Root volume $0.0 < d \leq 1.0$ (V1); Root length $1.0 < d \leq 2.0$ (L2); Root surface area $1.0 < d \leq 2.0$ (SA2); Root projected area $1.0 < d \leq 2.0$ (PA2); Root volume $1.0 < d \leq 2.0$ (V2); Root length $2.0 < d \leq 4.5$ (L3); Root surface area $2.0 < d \leq 4.5$ (SA3); Root projected area $2.0 < d \leq 4.5$ (PA3); Root volume $4.0 < d \leq 4.5$ (V3).

Root and shoot tissues were dried separately at 65 °C in a forced-air oven until a constant weight to determine root and shoot dry weight and total seedling dry weight. For P analysis, root and shoot tissues were subjected to nitric perchloric acid digestion (da Silva, 2009). The total P content in the seedling was calculated as the sum of the P content in each seedling component, which was the product of the dry weight and the P concentration in the root and shoot. Resulting the following traits: Root dry weight (RDW); Shoot dry weight (SDW); Total seedling dry weight (TDW); Root P concentration (RPConc); Root P content (RPCont); Shoot P concentration (SPConc); Shoot P content (SPCont); Total seedling P concentration (TPConc); Total seedling P content (TPCont).

Experimental design and adjusted means

The panel containing 561 tropical maize inbred lines was divided in three separated experiments containing, 192, 181 and 212 genotypes, with 12 checks in each experiment. Each biological replicate corresponded to three seedling, which was evaluated in an identical but independent block performed on a seven-day interval. The experimental design was incomplete blocks with three biological replicates for each phosphorus condition (low and high P).

To minimize the environment effect, Best Linear Unbiased Estimates (BLUE) for each trait and condition were obtained using GenStat 16.1 (Payne et al., 2009) through a linear model:

$$y_{ijk} = \mu + G_{i(j)} + E_j + R_{k(j)} + \varepsilon_{ijk}$$

y_{ijk} is the phenotype of the i^{th} individual (i = 1…561), in the j^{th} experiment (j = 1, 2, 3), of replicate k (k = 1, 2, 3); μ is the overall mean; $G_{i(j)}$ is the fixed genotypic effect of individual i at experiment j; E_j is the fixed effect of experiments; $R_{k(j)}$ is the fixed effect of replicate k at experiment j; and ε_{ijk} is the random non-genetic effect $\varepsilon_{ijk} \sim N(0, \sigma_\varepsilon^2)$.

Different structures of variance-covariance (VCOV) matrices were compared and the matrix fit for heterogeneous variance and uniform covariance among experiments for the residual effect was best suited to the phenotypic data based on AIC (Akaike Information Criterion) (Akaike, 1974).

The Pearson correlation (Table S1) and broad sense heritability (Table 1) were calculated using GenStat 16.1 (Payne et al., 2009). The heritability was calculated according to the expression:

$$h^2 = \sigma_g^2/(\sigma_g^2 + \sigma_\varepsilon^2/r)$$

where σ_g^2 is the genetic variance component, σ_ε^2 is the error variance component and r the number of replicates. The variance components were obtained through the linear model described above, except that the genotypic effect was considered as random. The correlation, heritability and coefficients of variation were used to select a subset of trait for further GWAS analyses.

SNP data

DNA was isolated from young leaves using the CTAB method (Saghai-Maroof et al., 1984). All panel was genotyped for genotyping-by-sequencing (GBS) (Elshire et al., 2011) with 955,120 SNPs distributed across maize genome. The ApeK1 restriction enzyme was used for library preparation, performed in an Illumina platform. The raw sequence was processed according the production pipeline following the protocol proposed by Glaubitz et al. (2014) and then imputed for missing data. The imputation was performed using Fast Inbred Line Library Imputation (FILLIN) with default parameters (Swarts et al., 2014). Monomorphic markers and ones with minor allele frequency (MAF) ≤ 5% were eliminated from the data set, resulting in 353,540 SNPs for further association analysis. Additionally, the GBS markers were used for HapMap projection in order to increase the SNP number using the HapMap version 3.1 (unpublished data, Bukowski et al. in preparation). A total of 36,872,942 SNPs were generated and then filtered for 50% of missing data and MAF ≥ 5%, resulting in 8,235,148 SNPs tested using GLM for GWAS.

Population structure and Kinship matrix

Principal components analysis (PCA) and clustering analysis were calculated using the software TASSEL 5.0 (Bradbury et al., 2007) to estimate population structure. For this, 12,700 SNPs were selected randomly from the 955,120 SNPs filtered for MAF ≥ 1% and 90% of non-missing data. The first five principal components (PC) were used to control for population structure in the association analysis. Clustering of genotypes was done with the cladogram function in TASSEL 5.0 to produce a distance matrix. This matrix was imported by the software PowerMarker V3.25 (Liu and Muse, 2005) and the phylogenetic tree was calculated based on neighbor joining method. Finally, the software Mega 6.06 (Tamura et al., 2013) was used to draw the phylogenetic tree. The family relatedness or kinship (K) matrix was obtained using the same markers to compute a pairwise dissimilarity matrix based on the simple matching coefficient was then converted to a similarity matrix by subtracting all values from 2 and then scaling so that the minimum value in the matrix is 0 and the maximum value is 2 (Yu et al., 2006). Kinship matrix was calculated using TASSEL 5 (Bradbury et al., 2007).

Linkage disequilibrium (LD)

The expected distance between SNPs in LD (LD decay) was estimated by the squared correlation coefficients at pairwise SNP markers (r^2) in TASSEL 5 (Bradbury et al., 2007). 29,188 SNPs filtered for MAF ≥ 5% and ≤ 10% of missing data were selected, before imputation, to calculate the LD decay. Nonlinear models with r^2 as responses (y) and pairwise distances in base pair as predictors (x) associated with violin plot were fitted for each chromosome and as well as combining all chromosomes together using R 3.2 statistical software. The violin plot was calculate within each distance, taking the r^2 values of all chromosomes by package vioplot (Hintze and Nelson, 1998). A cutoff of 0.2 was used to determine the LD decay.

GWAS analysis and candidate genes

Different models for association analysis were evaluated for type I error inflation. In order to selected the best model, quantile-quantile plots (Q-Q plot) of estimated -$\log_{10}$(p-value) were constructed using the observed p-values and the expected p-values (Figure S1). A mixed linear model (MLM) approach including both population structure and kinship matrix as cofactors was used (Yu et al., 2006; Bradbury et al., 2007) following the mathematical model: $y = X\beta + Zu + e$,

where y is the vector of phenotypic values, β is an unknown vector containing fixed effects including marker and population structure (PC). X and Z are the known design matrices; u ~ N (0, $\sigma_G^2 K$), being an unknown vector of random additive genetic effects (σ_G^2) from multiple genetic background for inbreed lines including the kinship matrix (K) and e ~ N (0, $\sigma_e^2 I$), the unobserved vector of random residuals. The MLM including PC and K was the chosen model applied for all traits and conditions, which were analyzed in TASSEL 5 (Bradbury et al., 2007). Two arbitraries thresholds, $-\log_{10}$ (p-value) = 5 and 6 were set to seek for nearby genes and the average LD, leading to a distance of 1kbp up and downstream of the significant SNP, was used to determine the co-localization with candidate genes.

Acknowledgments

We thank the Conselho Nacional de Desenvolvimento Científico e Tecnológico (CNPq) and Coordenação de Aperfeiçoamento de Pessoal de Nível Superior (CAPES) for the PhD fellowship to the first author (CAGR); Gislene Rodrigues Braga Cristeli for technical managing of the growth chamber experiments; Embrapa Maize and Sorghum and Generation Challenge Programme for the research logistic and financial support.

References

Abdel-Ghani AH, Kumar B, Reyes-Matamoros J, Gonzalez-Portilla PJ, Jansen C, San Martin JP, Lee M, Lubberstedt T (2013) Genotypic variation and relationships between seedling and adult plant traits in maize (Zea mays L.) inbred lines grown under contrasting nitrogen levels. Euphytica **189:** 123-133

Akaike H (1974) New Look at Statistical-Model Identification. Ieee Transactions on Automatic Control **Ac19:** 716-723

Anthony RG, Henriques R, Helfer A, Meszaros T, Rios G, Testerink C, Munnik T, Deak M, Koncz C, Bogre L (2004) A protein kinase target of a PDK1 signalling pathway is involved in root hair growth in Arabidopsis. Embo Journal **23:** 572-581

Azevedo GC, Cheavegatti-Gianotto A, Negri BF, Hufnagel B, Silva LDE, Magalhaes JV, Garcia AAF, Lana UGP, de Sousa SM, Guimaraes CT (2015) Multiple interval QTL mapping and searching for PSTOL1 homologs associated with root morphology, biomass accumulation and phosphorus content in maize seedlings under low-P. Bmc Plant Biology **15**

Baligar VC, Fageria NK, He ZL (2001) Nutrient use efficiency in plants. Communications in Soil Science and Plant Analysis **32:** 921-950

Bengough AG, McKenzie BM, Hallett PD, Valentine TA (2011) Root elongation, water stress, and mechanical impedance: a review of limiting stresses and beneficial root tip traits. Journal of Experimental Botany **62:** 59-68

Bradbury PJ, Zhang Z, Kroon DE, Casstevens TM, Ramdoss Y, Buckler ES (2007) TASSEL: software for association mapping of complex traits in diverse samples. Bioinformatics **23:** 2633-2635

Cai HG, Chen FJ, Mi GH, Zhang FS, Maurer HP, Liu WX, Reif JC, Yuan LX (2012) Mapping QTLs for root system architecture of maize (Zea mays L.) in the field at different developmental stages. Theoretical and Applied Genetics **125:** 1313-1324

Calderon-Vazquez C, Sawers RJH, Herrera-Estrella L (2011) Phosphate Deprivation in Maize: Genetics and Genomics. Plant Physiology **156:** 1067-1077

Camehl I, Drzewiecki C, Vadassery J, Shahollari B, Sherameti I, Forzani C, Munnik T, Hirt H, Oelmuller R (2011) The OXI1 Kinase Pathway Mediates Piriformospora indica-Induced Growth Promotion in Arabidopsis. Plos Pathogens **7**

Chia JM, Song C, Bradbury PJ, Costich D, de Leon N, Doebley J, Elshire RJ, Gaut B, Geller L, Glaubitz JC, Gore M, Guill KE, Holland J, Hufford MB, Lai JS, Li M, Liu X, Lu YL, McCombie R, Nelson R, Poland J, Prasanna BM, Pyhajarvi T, Rong TZ, Sekhon RS, Sun Q, Tenaillon MI, Tian F, Wang J, Xu X, Zhang ZW, Kaeppler SM, Ross-Ibarra J, McMullen MD, Buckler ES, Zhang GY, Xu YB, Ware D (2012) Maize HapMap2 identifies extant variation from a genome in flux. Nature Genetics **44:** 803-U238

Clark LJ, Price AH, Steele KA, Whalley WR (2008) Evidence from near-isogenic lines that root penetration increases with root diameter and bending stiffness in rice. Functional Plant Biology **35:** 1163-1171

Dakora FD, Phillips DA (2002) Root exudates as mediators of mineral acquisition in low-nutrient environments. Plant and Soil **245:** 35-47

da Silva FC (2009) Manual of chemical analyzes of soil, plants and fertilizer (In Portuguese). Embrapa Comunicação para Transferência de Tecnologia, Brasília. 627 p.

de Sousa SM, Clark RT, Mendes FF, de Oliveira AC, de Vasconcelos MJV, Parentoni SN, Kochian LV, Guimaraes CT, Magalhaes JV (2012) A role for root morphology and related candidate genes in P acquisition efficiency in maize. Functional Plant Biology **39:** 925-935

Elshire RJ, Glaubitz JC, Sun Q, Poland JA, Kawamoto K, Buckler ES, Mitchell SE (2011) A Robust, Simple Genotyping-by-Sequencing (GBS) Approach for High Diversity Species. Plos One **6**

Eulgem T, Rushton PJ, Robatzek S, Somssich IE (2000) The WRKY superfamily of plant transcription factors. Trends in Plant Science **5:** 199-206

Fita A, Bowen HC, Hayden RM, Nuez F, Pico B, Hammond JP (2012) Diversity in Expression of Phosphorus (P) Responsive Genes in Cucumis melo L. Plos One **7**

Flint-Garcia SA, Thornsberry JM, Buckler ES (2003) Structure of linkage disequilibrium in plants. Annual Review of Plant Biology **54:** 357-374

Forde B, Lorenzo H (2001) The nutritional control of root development. Plant and Soil **232:** 51-68

Gamuyao R, Chin JH, Pariasca-Tanaka J, Pesaresi P, Catausan S, Dalid C, Slamet-Loedin I, Tecson-Mendoza EM, Wissuwa M, Heuer S (2012) The protein kinase Pstol1 from traditional rice confers tolerance of phosphorus deficiency. Nature **488:** 535-539

Glaubitz JC, Casstevens TM, Lu F, Harriman J, Elshire RJ, Sun Q, Buckler ES (2014) TASSEL-GBS: A High Capacity Genotyping by Sequencing Analysis Pipeline. Plos One **9**

Good AG, Shrawat AK, Muench DG (2004) Can less yield more? Is reducing nutrient input into the environment compatible with maintaining crop production? Trends in Plant Science **9:** 597-605

Haling RE, Brown LK, Bengough AG, Young IM, Hallett PD, White PJ, George TS (2013) Root hairs improve root penetration, rootsoil contact, and phosphorus acquisition in soils of different strength. Journal of Experimental Botany **64:** 3711-3721

Hammond JP, Broadley MR, White PJ (2004) Genetic responses to phosphorus deficiency. Annals of Botany **94:** 323-332

Hardin SC, Wolniak SM (2001) Expression of the mitogen-activated protein kinase kinase ZmMEK1 in the primary root of maize. Planta **213:** 916-926

Hintze JL, Nelson RD (1998) Violin plots: A box plot-density trace synergism. American Statistician **52:** 181-184

Hufnagel B, de Sousa SM, Assis L, Guimaraes CT, Leiser W, Azevedo GC, Negri B, Larson BG, Shaff JE, Pastina MM, Barros BA, Weltzien E, Frederick H, Rattunde W, Viana JH, Clark RT, Falcao A, Gazaffi R, Garcia AAF, Schaffert RE, Kochian LV, Magalhaes JV (2014) Duplicate and Conquer: Multiple Homologs of PHOSPHORUS-STARVATION TOLERANCE1 Enhance Phosphorus Acquisition and Sorghum Performance on Low-Phosphorus Soils. Plant Physiology **166:** 659-U323

Hund A, Trachsel S, Stamp P (2009) Growth of axile and lateral roots of maize: I development of a phenotying platform. Plant and Soil **325:** 335-349

Kong XP, Lv W, Zhang D, Jiang SS, Zhang SZ, Li DQ (2013) Genome-Wide Identification and Analysis of Expression Profiles of Maize Mitogen-Activated Protein Kinase Kinase Kinase. Plos One **8**

Lan P, Li WF, Schmidt W (2013) Genome-wide co-expression analysis predicts protein kinases as important regulators of phosphate deficiency-induced root hair remodeling in Arabidopsis. Bmc Genomics **14**

Law MY, Childs KL, Campbell MS, Stein JC, Olson AJ, Holt C, Panchy N, Lei JK, Jiao D, Andorf CM, Lawrence CJ, Ware D, Shiu SH, Sun YN, Jiang N, Yandell M (2015) Automated Update, Revision, and Quality Control of the Maize Genome Annotations Using MAKER-P Improves the B73 RefGen_v3 Gene Models and Identifies New Genes. Plant Physiology **167:** 25-39

Liu KJ, Muse SV (2005) PowerMarker: an integrated analysis environment for genetic marker analysis. Bioinformatics **21:** 2128-2129

Liu YK, Wang L, Zhang D, Li DQ (2013) Expression Analysis of Segmentally Duplicated ZmMPK3-1 and ZmMPK3-2 genes in Maize. Plant Molecular Biology Reporter **31:** 457-463

Lopez-Bucio J, Cruz-Ramirez A, Herrera-Estrella L (2003) The role of nutrient availability in regulating root architecture. Current Opinion in Plant Biology **6:** 280-287

Lynch JP (2007) Roots of the second green revolution. Australian Journal of Botany **55:** 493-512

Lynch JP (2011) Root Phenes for Enhanced Soil Exploration and Phosphorus Acquisition: Tools for Future Crops. Plant Physiology **156:** 1041-1049

Lynch JP (2013) Steep, cheap and deep: an ideotype to optimize water and N acquisition by maize root systems. Annals of Botany **112:** 347-357

Ma TL, Wu WH, Wang Y (2012) Transcriptome analysis of rice root responses to potassium deficiency. Bmc Plant Biology **12**

Magnavaca R, Gardner CO, Clark RB (1987) Inheritance of aluminum tolerance in maize. In WH Gabelman, BC Loughman, eds, Genetic Aspects of Plant Mineral Nutrition. Martinus Nijhoff Publishers, Dordrecht, The Netherlands, pp 201–212

Mare C, Mazzucotelli E, Crosatti C, Francia E, Stanca AM, Cattivelli L (2004) Hv-WRKY38: a new transcription factor involved in cold- and drought-response in barley. Plant Molecular Biology **55:** 399-416

Maron LG, Kirst M, Mao C, Milner MJ, Menossi M, Kochian LV (2008) Transcriptional profiling of aluminum toxicity and tolerance responses in maize roots. New Phytologist **179:** 116-128

Mattiello L, Kirst M, da Silva FR, Jorge RA, Menossi M (2010) Transcriptional profile of maize roots under acid soil growth. Bmc Plant Biology **10**

Oyama T, Shimura Y, Okada K (2002) The IRE gene encodes a protein kinase homologue and modulates root hair growth in Arabidopsis. Plant Journal **30:** 289-299

Pace J, Gardner C, Romay C, Ganapathysubramanian B, Lubberstedt T (2015) Genome-wide association analysis of seedling root development in maize (Zea mays L.). Bmc Genomics **16**

Pagnussat GC, Lanteri ML, Lombardo MC, Lamattina L (2004) Nitric oxide mediates the indole acetic acid induction activation of a mitogen-activated protein kinase cascade involved in adventitious root development. Plant Physiology **135:** 279-286

Parentoni SN, Souza Júnior CL (2008) Phosphorus acquisition and internal utilization efficiency in tropical maize genotypes. Pesquisa Agropecuaria Brasileira **43:** 893-901

Parentoni SN, Souza Júnior CL, Alves VMD, Gama EEG, Coelho AM, de Oliveira AC, Guimaraes PEO, Guimaraes CT, Vasconcelos MJV, Pacheco CAP, Meirelles WF, de Magalhaes JV, Guimaraes LJM, da Silva AR, Mendes FF, Schaffert RE (2010) Inheritance and Breeding Strategies for Phosphorus Efficiency in Tropical Maize (Zea Mays L.). Maydica **55:** 1-15

Payne RW (2009) GenStat. Wiley Interdiscip Rev Comput Stat **1:** 255–258

Plaxton WC (1999) Metabolic aspects of phosphate starvation in plants. Phosphorus in Plant Biology: Regulatory Roles in Molecular, Cellular, Organismic, and Ecosystem Processes **19:** 229-241

Rai A, Rai S, Rakshit A (2013) Mycorrhiza-mediated phosphorus use efficiency in plants. Environ Exp Biol **11:** 107-117

Raghothama KG (1999) Phosphate acquisition. Annual Review of Plant Physiology and Plant Molecular Biology **50:** 665-693

Raghothama KG, Karthikeyan AS (2005) Phosphate acquisition. Plant and Soil **274:** 37-49

Ramaekers L, Remans R, Rao IM, Blair MW, Vanderleyden J (2010) Strategies for improving phosphorus acquisition efficiency of crop plants. Field Crops Research **117:** 169-176

Remington DL, Thornsberry JM, Matsuoka Y, Wilson LM, Whitt SR, Doeblay J, Kresovich S, Goodman MM, Buckler ES (2001) Structure of linkage disequilibrium and phenotypic

associations in the maize genome. Proceedings of the National Academy of Sciences of the United States of America **98:** 11479-11484

Rentel MC, Lecourieux D, Ouaked F, Usher SL, Petersen L, Okamoto H, Knight H, Peck SC, Grierson CS, Hirt H, Knight MR (2004) OXI1 kinase is necessary for oxidative burst-mediated signalling in Arabidopsis. Nature **427:** 858-861

Romay MC, Millard MJ, Glaubitz JC, Peiffer JA, Swarts KL, Casstevens TM, Elshire RJ, Acharya CB, Mitchell SE, Flint-Garcia SA, McMullen MD, Holland JB, Buckler ES, Gardner CA (2013) Comprehensive genotyping of the USA national maize inbred seed bank. Genome Biology **14**

Saghai-Maroof MA, Soliman KM, Jorgensen RA, Allard RW (1984) Ribosomal DNA Spacer-Length Polymorphisms in Barley - Mendelian Inheritance, Chromosomal Location, and Population-Dynamics. Proceedings of the National Academy of Sciences of the United States of America-Biological Sciences **81:** 8014-8018

Santner AA, Watson JC (2006) The WAG1 and WAG2 protein kinases negatively regulate root waving in Arabidopsis. Plant Journal **45:** 752-764

Schachtman DP, Reid RJ, Ayling SM (1998) Phosphorus uptake by plants: From soil to cell. Plant Physiology **116:** 447-453

Schnable PS, Ware D, Fulton RS, Stein JC, Wei FS, Pasternak S, Liang CZ, Zhang JW, Fulton L, Graves TA, Minx P, Reily AD, Courtney L, Kruchowski SS, Tomlinson C, Strong C, Delehaunty K, Fronick C, Courtney B, Rock SM, Belter E, Du FY, Kim K, Abbott RM, Cotton M, Levy A, Marchetto P, Ochoa K, Jackson SM, Gillam B, Chen WZ, Yan L, Higginbotham J, Cardenas M, Waligorski J, Applebaum E, Phelps L, Falcone J, Kanchi K, Thane T, Scimone A, Thane N, Henke J, Wang T, Ruppert J, Shah N, Rotter K, Hodges J, Ingenthron E, Cordes M, Kohlberg S, Sgro J, Delgado B, Mead K, Chinwalla A, Leonard S, Crouse K, Collura K, Kudrna D, Currie J, He RF, Angelova A, Rajasekar S, Mueller T, Lomeli R, Scara G, Ko A, Delaney K, Wissotski M, Lopez G, Campos D, Braidotti M, Ashley E, Golser W, Kim H, Lee S, Lin JK, Dujmic Z, Kim W, Talag J, Zuccolo A, Fan C, Sebastian A, Kramer M, Spiegel L, Nascimento L, Zutavern T, Miller B, Ambroise C, Muller S, Spooner W, Narechania A, Ren LY, Wei S, Kumari S, Faga B, Levy MJ, McMahan L, Van Buren P, Vaughn MW, Ying K, Yeh CT, Emrich SJ, Jia Y, Kalyanaraman A, Hsia AP, Barbazuk WB, Baucom RS, Brutnell TP, Carpita NC, Chaparro C, Chia JM, Deragon JM, Estill JC, Fu Y, Jeddeloh JA, Han YJ, Lee H, Li PH, Lisch DR, Liu SZ, Liu ZJ, Nagel DH, McCann MC, SanMiguel P, Myers AM, Nettleton D, Nguyen J, Penning BW, Ponnala L, Schneider KL, Schwartz DC, Sharma A, Soderlund C, Springer NM, Sun Q, Wang H, Waterman M, Westerman R, Wolfgruber TK, Yang LX, Yu Y, Zhang LF, Zhou SG, Zhu Q, Bennetzen JL, Dawe RK, Jiang JM, Jiang N, Presting GG, Wessler SR, Aluru S, Martienssen RA, Clifton SW, McCombie WR, Wing RA, Wilson RK (2009) The B73 Maize Genome: Complexity, Diversity, and Dynamics. Science **326:** 1112-1115

Seki M, Narusaka M, Ishida J, Nanjo T, Fujita M, Oono Y, Kamiya A, Nakajima M, Enju A, Sakurai T, Satou M, Akiyama K, Taji T, Yamaguchi-Shinozaki K, Carninci P, Kawai J, Hayashizaki Y, Shinozaki K (2002) Monitoring the expression profiles of 7000 Arabidopsis genes under drought, cold and high-salinity stresses using a full-length cDNA microarray. Plant Journal **31:** 279-292

Shen JB, Yuan LX, Zhang JL, Li HG, Bai ZH, Chen XP, Zhang WF, Zhang FS (2011) Phosphorus Dynamics: From Soil to Plant. Plant Physiology **156:** 997-1005

Shenoy VV, Kalagudi GM (2005) Enhancing plant phosphorus use efficiency for sustainable cropping. Biotechnology Advances **23:** 501-513

Svistoonoff S, Creff A, Reymond M, Sigoillot-Claude C, Ricaud L, Blanchet A, Nussaume L, Desnos T (2007) Root tip contact with low-phosphate media reprograms plant root architecture. Nature Genetics **39:** 792-796

Swarts K, Li HH, Navarro JAR, An D, Romay MC, Hearne S, Acharya C, Glaubitz JC, Mitchell S, Elshire RJ, Buckler ES, Bradbury PJ (2014) Novel Methods to Optimize Genotypic Imputation for Low-Coverage, Next-Generation Sequence Data in Crop Plants. Plant Genome **7**

Tamura K, Stecher G, Peterson D, Filipski A, Kumar S (2013) MEGA6: Molecular Evolutionary Genetics Analysis Version 6.0. Molecular Biology and Evolution **30:** 2725-2729

Tenaillon MI, Sawkins MC, Long AD, Gaut RL, Doebley JF, Gaut BS (2001) Patterns of DNA sequence polymorphism along chromosome 1 of maize (Zea mays ssp mays L.). Proceedings of the National Academy of Sciences of the United States of America **98:** 9161-9166

Vance CP, Chiou TJ (2011) Phosphorus Focus Editorial. Plant Physiology **156:** 987-988

Vance CP, Uhde-Stone C, Allan DL (2003) Phosphorus acquisition and use: critical adaptations by plants for securing a nonrenewable resource. New Phytologist **157:** 423-447

Wissuwa M, Gamat G, Ismail AM (2005) Is root growth under phosphorus deficiency affected by source or sink limitations? Journal of Experimental Botany **56:** 1943-1950

Wissuwa M, Mazzola M, Picard C (2009) Novel approaches in plant breeding for rhizosphere-related traits. Plant and Soil **321:** 409-430

Yan JB, Warburton M, Crouch J (2011) Association Mapping for Enhancing Maize (Zea mays L.) Genetic Improvement. Crop Science **51:** 433-449

Yu JM, Buckler ES (2006) Genetic association mapping and genome organization of maize. Current Opinion in Biotechnology **17:** 155-160

Yu JM, Pressoir G, Briggs WH, Bi IV, Yamasaki M, Doebley JF, McMullen MD, Gaut BS, Nielsen DM, Holland JB, Kresovich S, Buckler ES (2006) A unified mixed-model method for association mapping that accounts for multiple levels of relatedness. Nature Genetics **38:** 203-208

Zegzouti H, Li W, Lorenz TC, Xie MT, Payne CT, Smith K, Glenny S, Payne GS, Christensen SK (2006) Structural and functional insights into the regulation of Arabidopsis AGC VIIIa kinases. Journal of Biological Chemistry **281:** 35520-35530

Zhang HW, Huang Y, Ye XS, Xu FS (2011) Genotypic variation in phosphorus acquisition from sparingly soluble P sources is related to root morphology and root exudates in Brassica napus. Science China-Life Sciences **54:** 1134-1142

Zhu JM, Kaeppler SM, Lynch JP (2005) Mapping of QTL controlling root hair length in maize (Zea mays L.) under phosphorus deficiency. Plant and Soil **270:** 299-310

Zhu JM, Kaeppler SM, Lynch JP (2005) Mapping of QTLs for lateral root branching and length in maize (Zea mays L.) under differential phosphorus supply. Theoretical and Applied Genetics **111:** 688-695

Zhu JM, Lynch JP (2004) The contribution of lateral rooting to phosphorus acquisition efficiency in maize (Zea mays) seedlings. Functional Plant Biology **31:** 949-958

Zobel RW (2008) Hardware and software efficacy in assessment of fine root diameter distributions. Computers and Electronics in Agriculture **60:** 178-189

Tables

Table 1. Mean, minimum (Min), maximum (Max), standard deviation (SD), coefficient of variation (CV) and heritability (h^2) for all traits evaluated under low and high phosphorus conditions in a 561 tropical maize panel.

		Low P						High P					
Trait	Abbreviation	Mean	Min	Max	SD	CV	h^2	Mean	Min	Max	SD	CV	h^2
Total root length (cm)	**Length**	**167.1**	**32.4**	**479.4**	**66.2**	**39.7**	**0.75**	**169.3**	**20.8**	**515.5**	**75.7**	**44.7**	**0.75**
Length per volume (cm/m^3)	LenPerVol	167.1	32.4	479.4	66.2	39.7	0.75	169.3	20.8	515.5	75.7	44.7	0.75
Average root diameter (mm)	**AvgDiam**	**0.97**	**0.37**	**2.15**	**0.32**	**33.4**	**0.74**	**0.98**	**0.43**	**2.25**	**0.32**	**32.5**	**0.79**
Number of forks	Forks	234.3	16	924.7	132.2	56.4	0.74	300.5	5	1167	175.0	58.3	0.70
Number of crossing	Crossings	18.5	0	153.7	16.4	88.4	0.68	22.3	0	187	19.9	89.2	0.65
Total projected root area (cm^2)	ProjArea	16.0	3.8	63.9	8.8	55.0	0.75	15.7	2.9	49	7.6	48.4	0.74
Root surface area (cm^2)	**SurfArea**	**50.3**	**12**	**200.8**	**27.7**	**55.0**	**0.75**	**49.3**	**9.2**	**154**	**23.8**	**48.4**	**0.74**
Root volume (cm^3)	Volume	1.35	0.19	6.73	1.07	79.3	0.74	1.28	0.21	5.03	0.90	70.3	0.73
Root length $0.0 < d \leq 1.0$ *	L1	109.2	1.3	382.9	57.6	52.8	0.73	114.4	1.8	486.3	74.0	64.7	0.74
Root surface area $0.0 < d \leq 1.0$ *	SA1	18.1	0.2	65.1	8.4	46.5	0.74	18.8	0.4	61.1	9.8	52.1	0.74
Root projected area $0.0 < d \leq 1.0$ *	PA1	5.77	0.07	20.73	2.68	46.5	0.74	5.99	0.14	19.43	3.12	52.1	0.74
Root volume $0.0 < d \leq 1.0$ *	V1	0.29	0	1.04	0.14	46.5	0.74	0.30	0.01	0.88	0.14	47.0	0.73
Root length $1.0 < d \leq 2.0$ *	L2	49.5	1.2	211.5	40.5	81.9	0.74	47.5	2	193.5	34.2	72.1	0.72
Root surface area $1.0 < d \leq 2.0$ *	SA2	21.1	0.5	95.8	18.0	85.6	0.73	20.4	0.8	87	15.5	75.9	0.71
Root projected area $1.0 < d \leq 2.0$ *	PA2	6.69	0.16	30.49	5.75	85.9	0.73	6.50	0.24	27.71	4.94	75.9	0.71
Root volume $1.0 < d \leq 2.0$ *	V2	0.74	0.02	3.57	0.66	89.5	0.72	0.72	0.02	3.23	0.58	80.2	0.71
Root length $2.0 < d \leq 4.5$ *	L3	8.26	0.27	63.06	9.94	120.3	0.70	7.24	0.19	63.79	9.18	126.7	0.67
Root surface area $2.0 < d \leq 4.5$ *	SA3	7.47	0.5	52.62	8.36	111.9	0.71	6.50	0.2	51.95	7.58	116.6	0.68
Root projected area $2.0 < d \leq 4.5$ *	PA3	2.38	0.16	16.75	2.66	111.9	0.71	2.07	0.06	16.54	2.41	116.6	0.68
Root volume $4.0 < d \leq 4.5$ *	V3	0.66	0.04	3.85	0.69	104.5	0.70	0.57	0.02	3.98	0.61	107.4	0.66
Root dry weight (mg)	RDW	31.5	4	87	10.2	32.5	0.73	32.9	7.3	150	13.1	39.9	0.66
Shoot dry weight (mg)	SDW	34.3	3	120	16.0	46.5	0.72	40.5	4	132.7	19.0	46.9	0.71
Total seedling dry weight (mg)	**TDW**	**65.8**	**11.5**	**166.3**	**23.9**	**36.3**	**0.73**	**73.5**	**15.3**	**220.3**	**30.0**	**40.9**	**0.72**
Root P concentration (mgg^{-1})	RPConc	7.98	0.9	26.6	3.57	44.8	0.63	7.22	0.6	38.3	3.39	46.9	0.57
Root P content (mg)	RPCont	0.24	0.03	0.88	0.12	50.0	0.53	0.23	0.02	1.59	0.12	53.2	0.46
Shoot P concentration (mgg^{-1})	SPConc	6.84	0.8	16	2.05	29.9	0.65	6.89	1	19.5	2.01	29.2	0.51
Shoot P content (mg)	SPCont	0.22	0.02	0.95	0.10	43.4	0.38	0.27	0.03	1.16	0.13	49.0	0.61
Total seedling P concentration (mgg^{-1})	**TPConc**	**7.45**	**2.84**	**20.32**	**2.53**	**33.9**	**0.69**	**7.09**	**2.09**	**20.63**	**2.24**	**31.6**	**0.63**
Total seedling P content (mg)	**TPCont**	**0.46**	**0.1**	**1.32**	**0.17**	**36.4**	**0.43**	**0.50**	**0.07**	**2.39**	**0.20**	**41.1**	**0.55**

***** The symbol " $< d \leq$ " represents an interval of a specific diameter, being: $0.0 < d \leq 1.0$ for super fine roots; $1.0 < d \leq 2.0$ for fine roots and $2.0 < d \leq 4.5$ for thick roots. Data in bold are representing the selected traits for GWAS analysis.

Table 2. Significant SNPs identified through MLM analysis for root morphology traits, concentration and content of P, for low, high and low/high P conditions, based on a $-\log_{10}$ (P-value) ≥ 6, and their bin, position, alleles, minor allele frequency (MAF) and nearby candidate genes with a maximum distance of 1 kbp.

Trait	Condition	SNP	Chr (bin)	Position (BP)	$-\log_{10}$ (P-value)	Allele 1/2	MAF	Putative Candidate Gene
AvgDiam	high P	S4_3746664	4.01	12,312,455	6.44	A/C	0.21	GRMZM2G037472
Length	low P	S8_89092905	8.03	89,092,905	6.30	C/A	0.13	GRMZM2G044531
TDW	low P	S6_34607259	6.01	34,607,259	6.37	T/C	0.25	-
	low P	S9_137492237	9.06	137,492,237	6.43	G/A	0.48	GRMZM2G078933
	high P	S10_77271433	10.03	77,271,433	6.41	G/C	0.09	GRMZM2G110145
TPCont	high P	S8_21321754	8.03	21,321,754	6.34	G/A	0.22	-
	high P	S8_21321777	8.03	21,321,777	6.34	A/G	0.22	-
	high P	S9_142935696	9.06	142,935,696	6.11	T/A	0.47	GRMZM2G104618

Figures

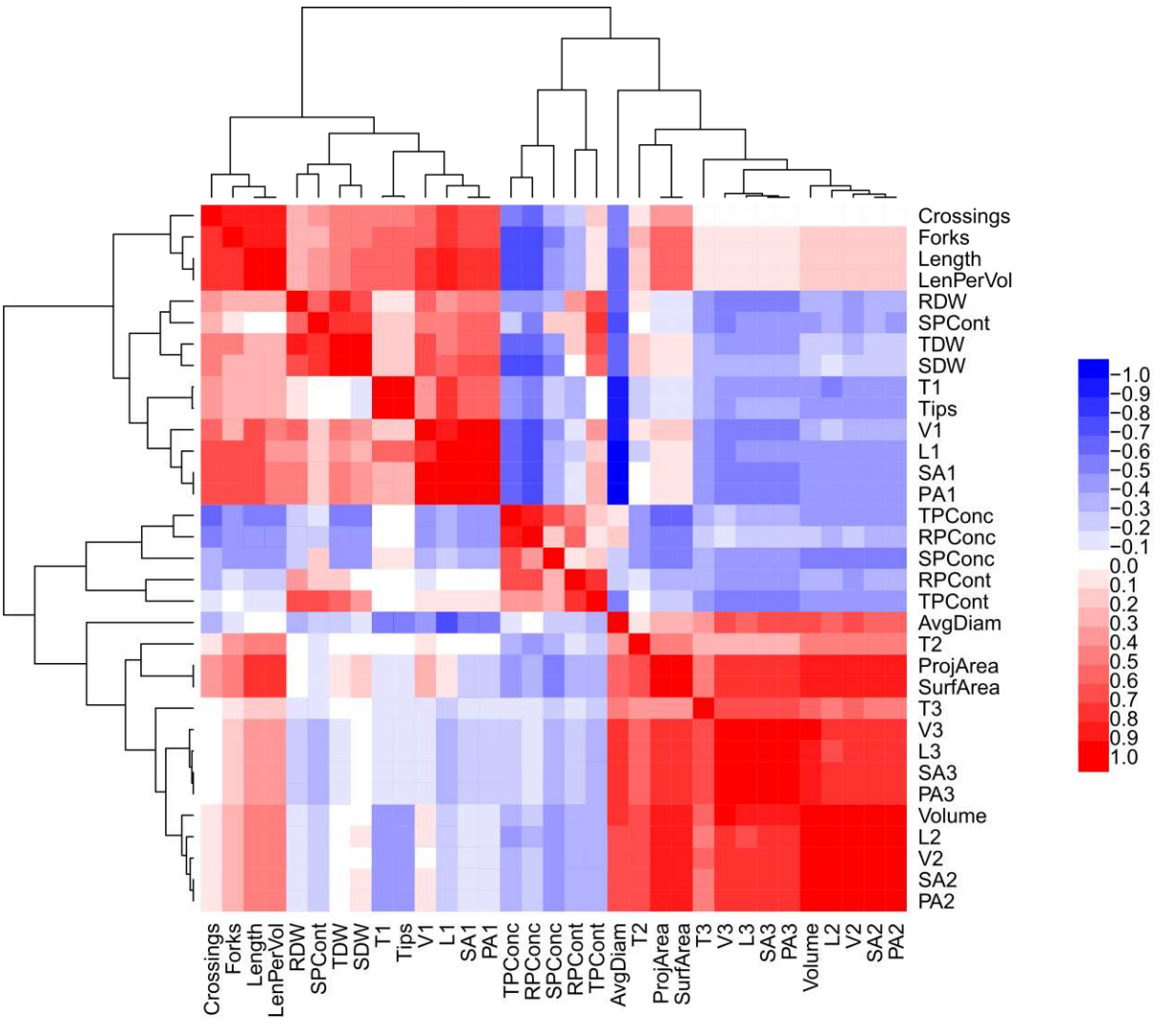

Figure 1. Pearson´s correlation among root morphology, P concentration and P content traits. Lower diagonal are the correlation of those traits evaluated under low P condition and upper diagonal are the correlation under high P conditions.

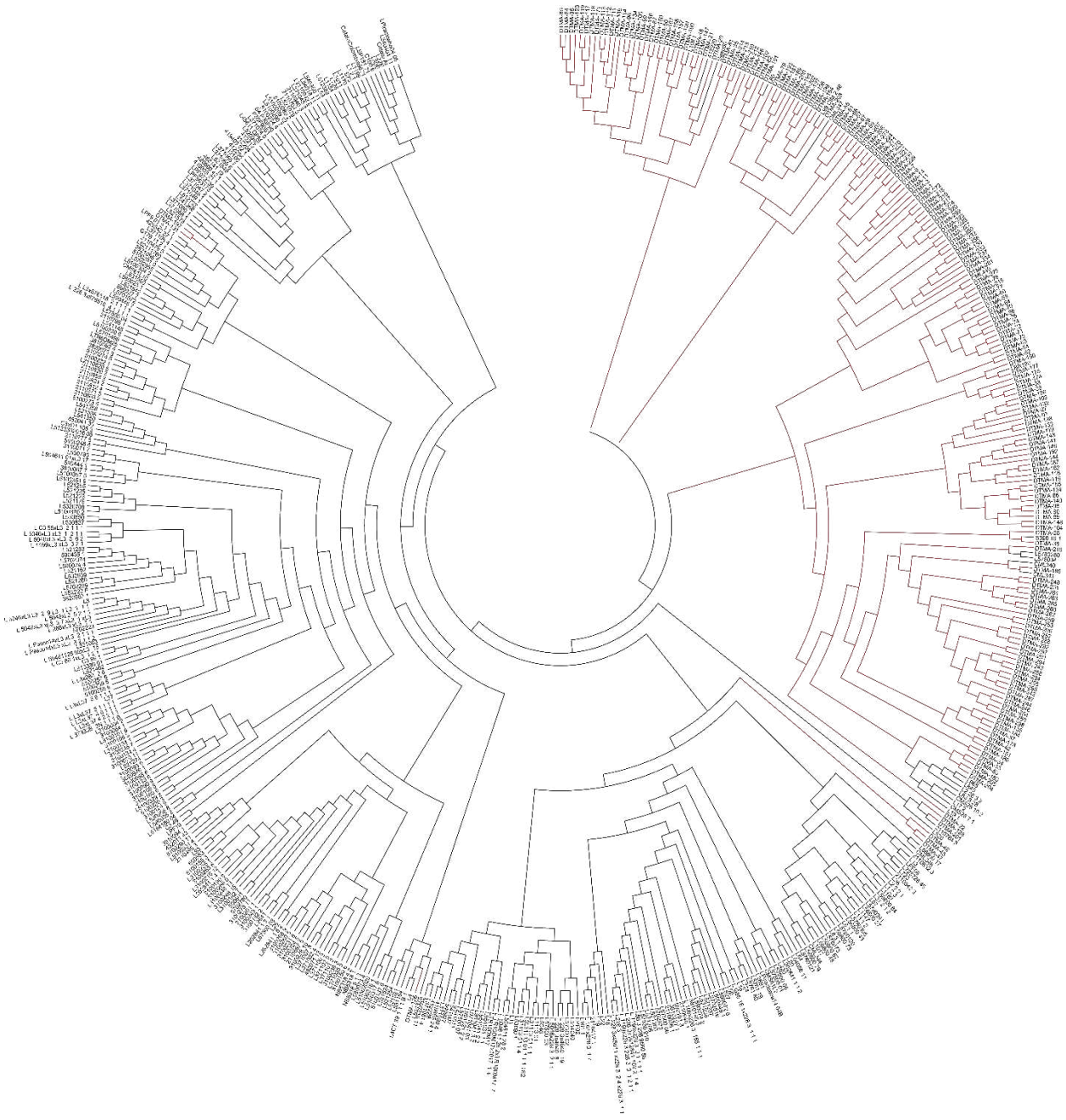

Figure 2. Clustering analysis of the association panel showing the genetic relationship among the 561 tropical maize inbred lines. The Embrapa and DTMA lines are represented by black and red color respectively.

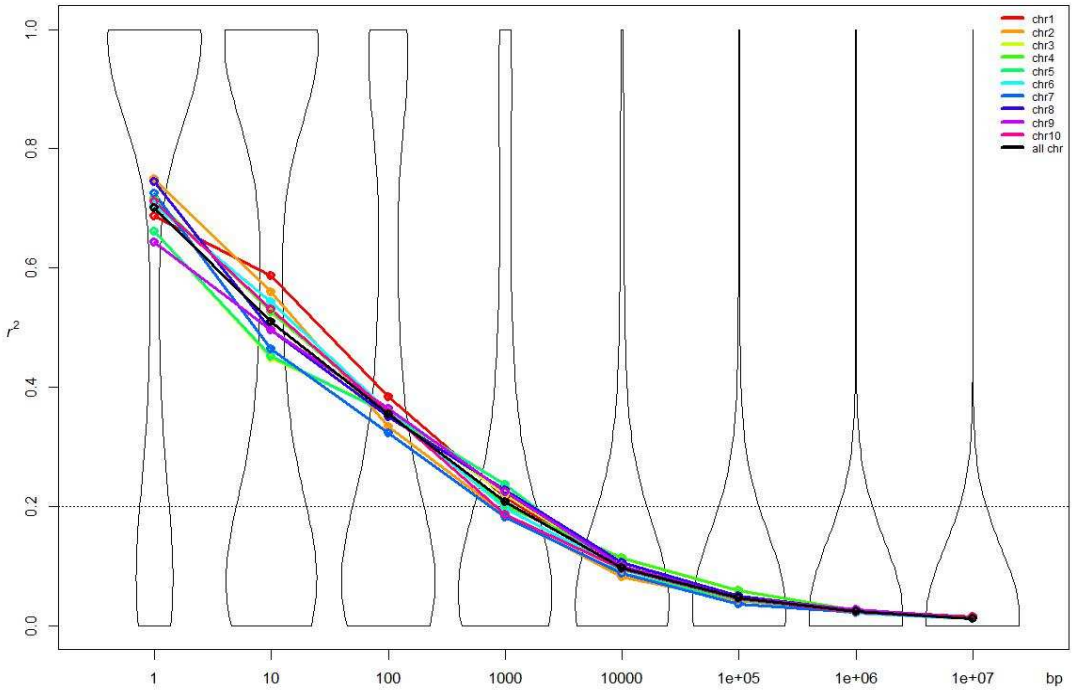

Figure 3. Linkage disequilibrium decay across the 10 maize chromosomes with 29,188 SNPs. The black line represents the average of all chromosomes, in the background is depicted the violin plot showing the distribution of all r^2 values. Dotted lines represent the threshold of 0.2.

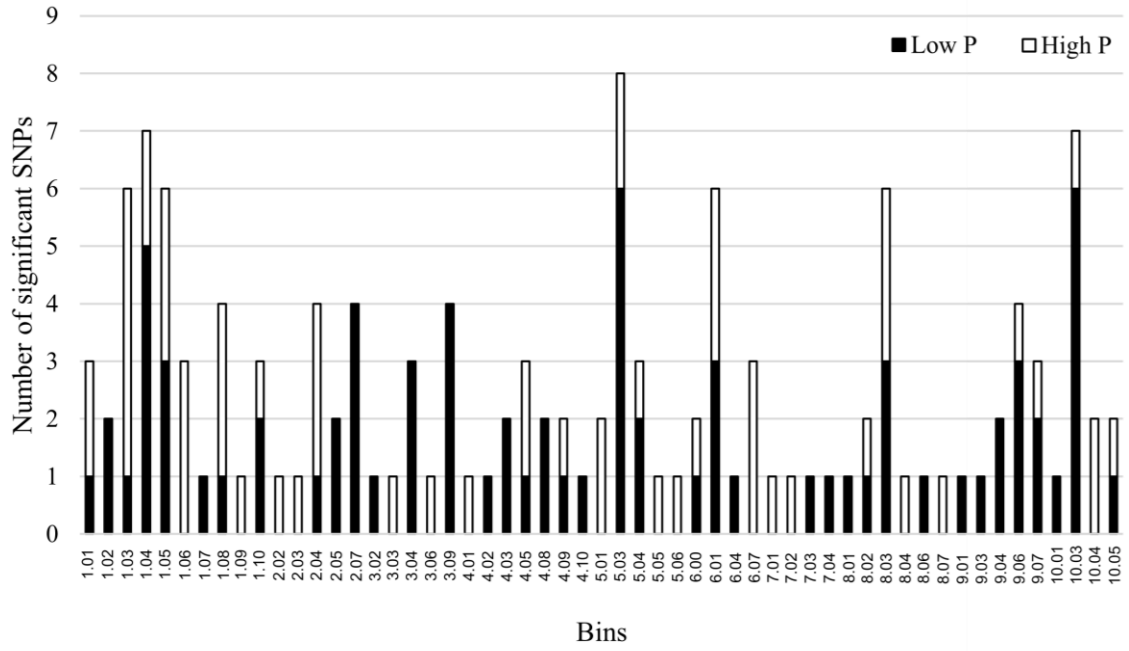

Figure 4. Distribution of significant SNPs (136), with $-\log_{10}$(P-value) ≥ 5, for low (black) and high (white) P conditions through the bins of each chromosome. The y axis shows the number of significant SNPs.

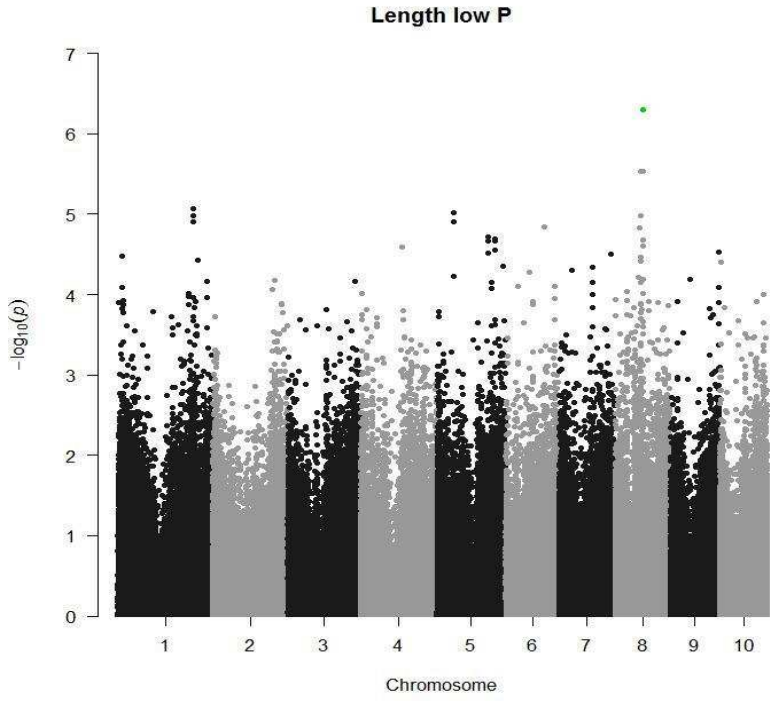

Figure 5. Manhattan plot for the total root length trait under low P condition using MLM (PC + K) in a panel of 561 tropical maize inbred lines with a total of 353,540 SNP markers. The green point represents the significant SNP S8_89092905.

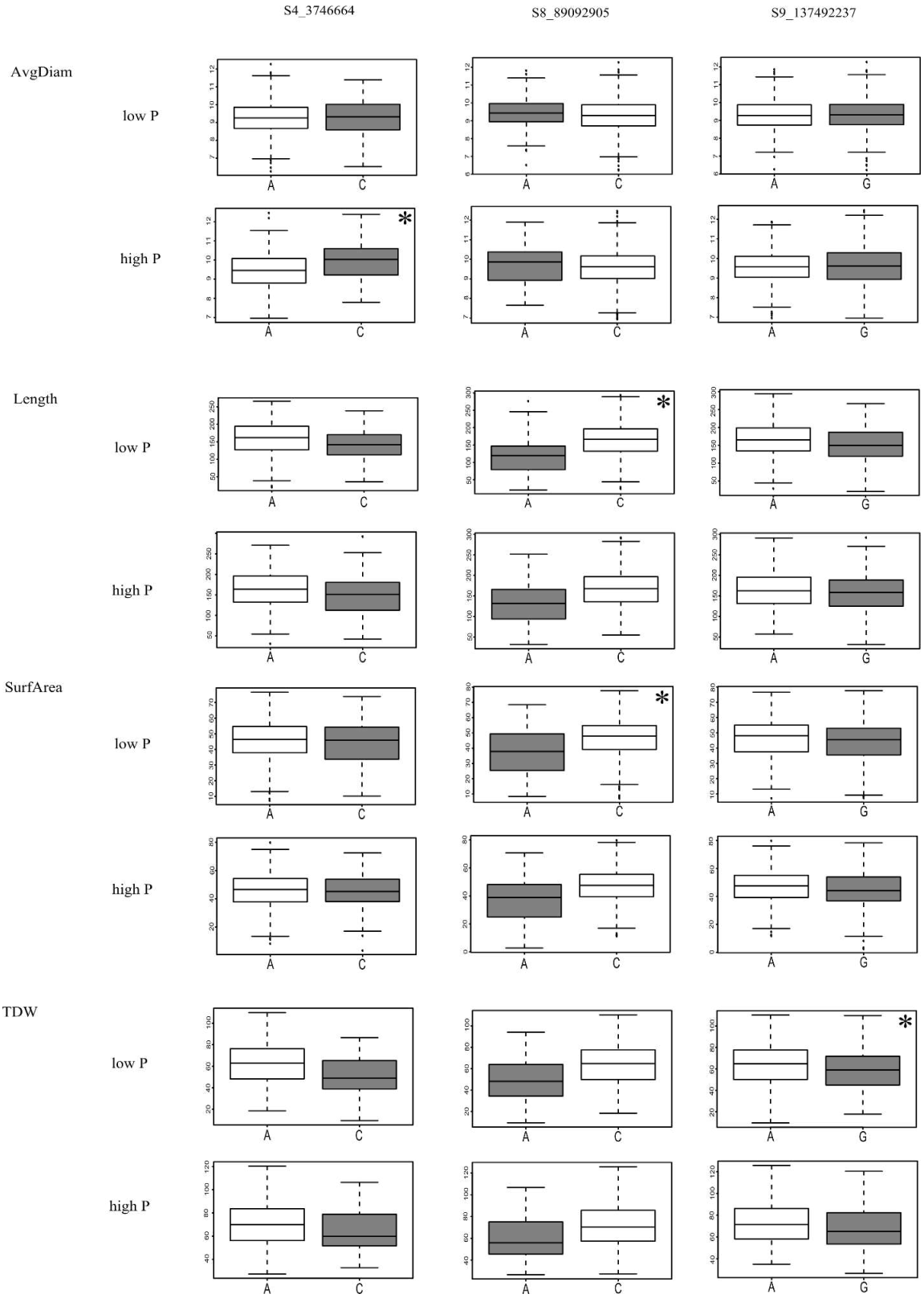

Figure 6. Boxplot of the significant SNPs S4_3746664, S8_89092905 and S9_137492237 associated with morphological traits under low and high P conditions. The asterisk represents wherein trait/condition, the SNP was significant. The white boxes show the favorable allele for enhance P acquisition.

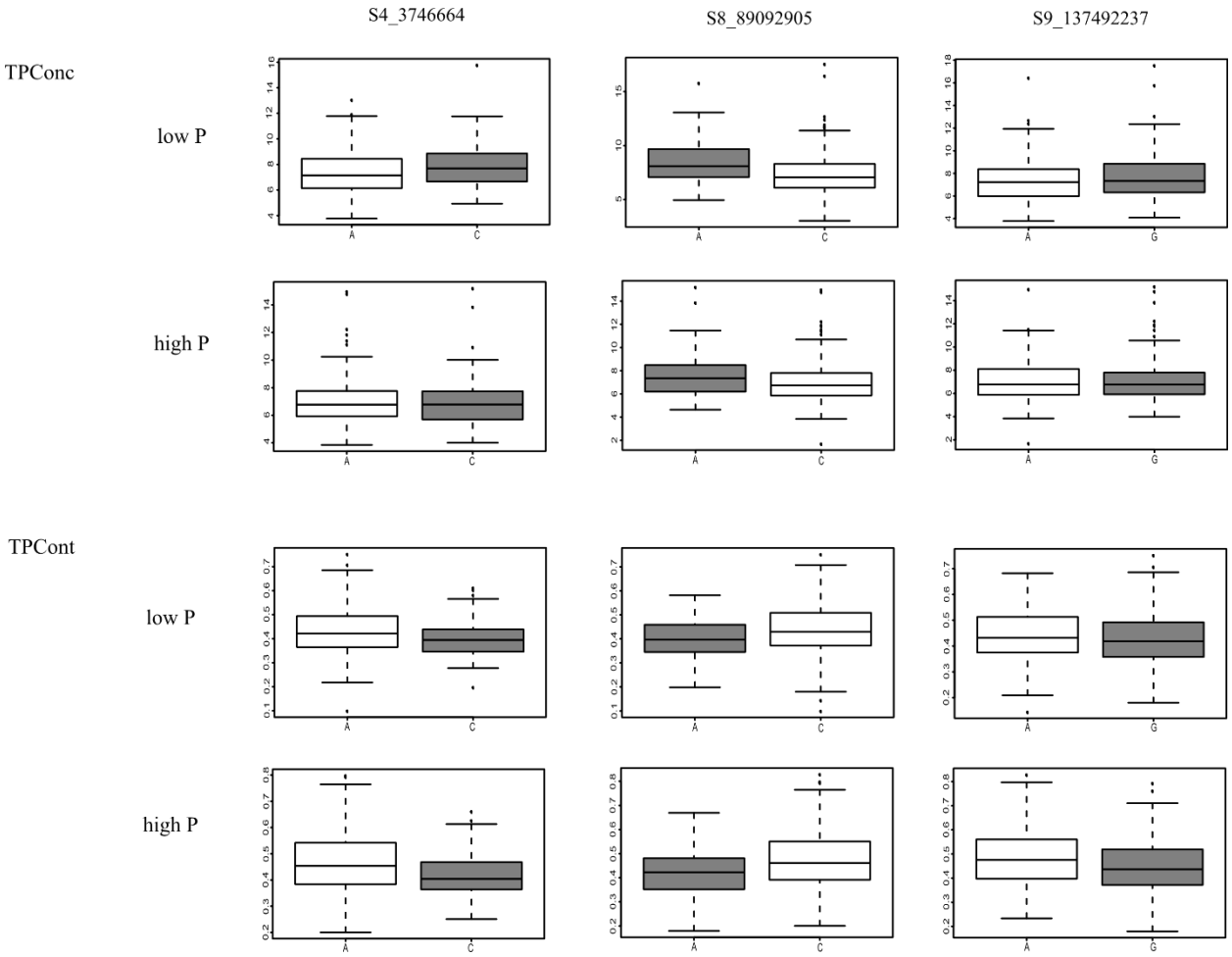

Figure 7. Boxplot of the significant SNPs S4_3746664, S8_89092905 and S9_137492237 for total seedling P concentration (TPConc) and content (TPCont) traits under low and high P conditions. The white boxes show the favorable allele for enhance P acquisition.

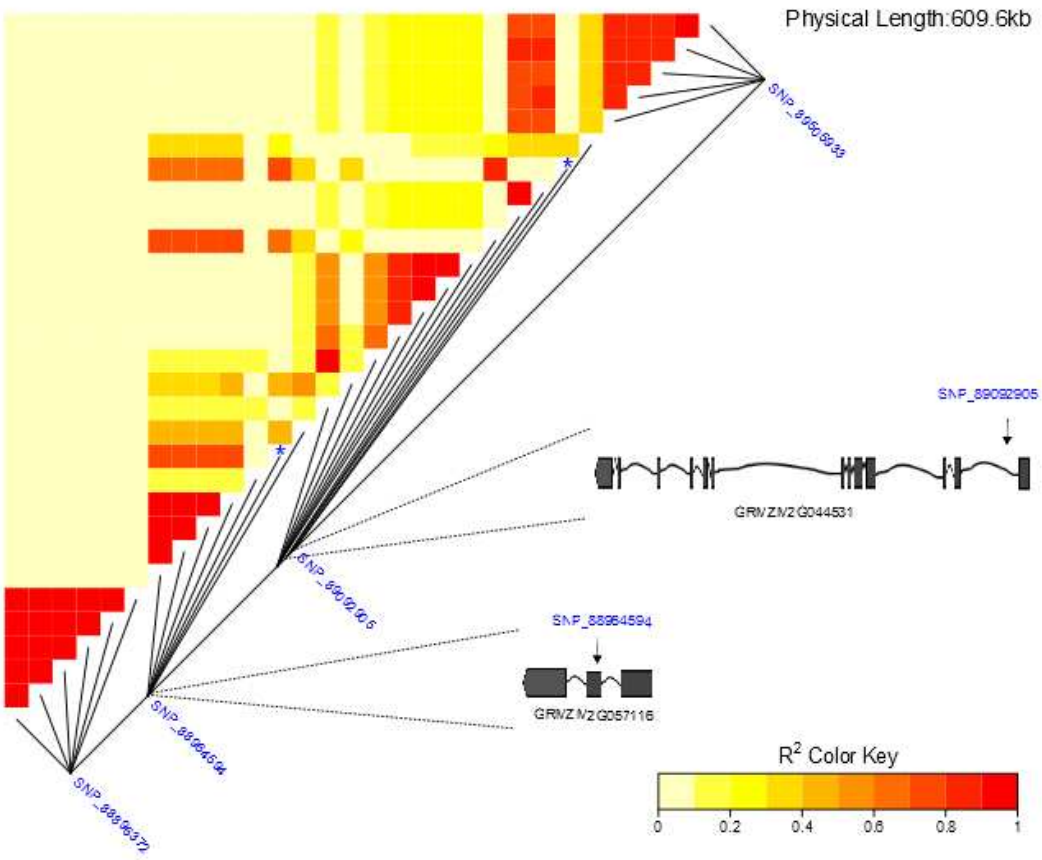

Figure 8. Linkage disequilibrium in a 609.6 kbp region within the bin 8.03 of the chromosome 8. The black lines represent each SNP and the blue asterisks depict the two most significant SNPs of this region for total root length under low P condition. The position of the genes GRMZM2G044531 and GRMZM2G057116 are illustrated in the figure and the position of the significant SNPs (S8_89092905 and S8_88964594).

Supplemental Materials

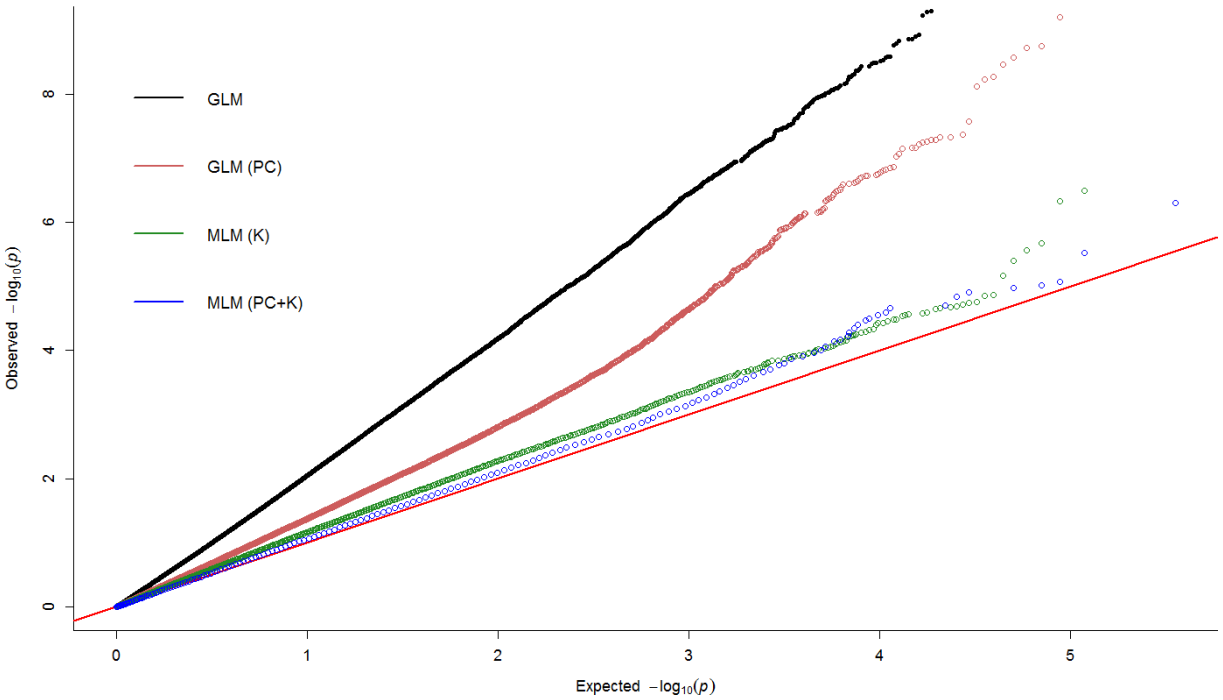

Figure S1. Q-Q plot for total root length under low P conditions using GLM, GLM (PC), MLM (K) and MLM (PC+K) in a panel of 561 tropical maize inbred lines with a total of 353,540 SNP markers.

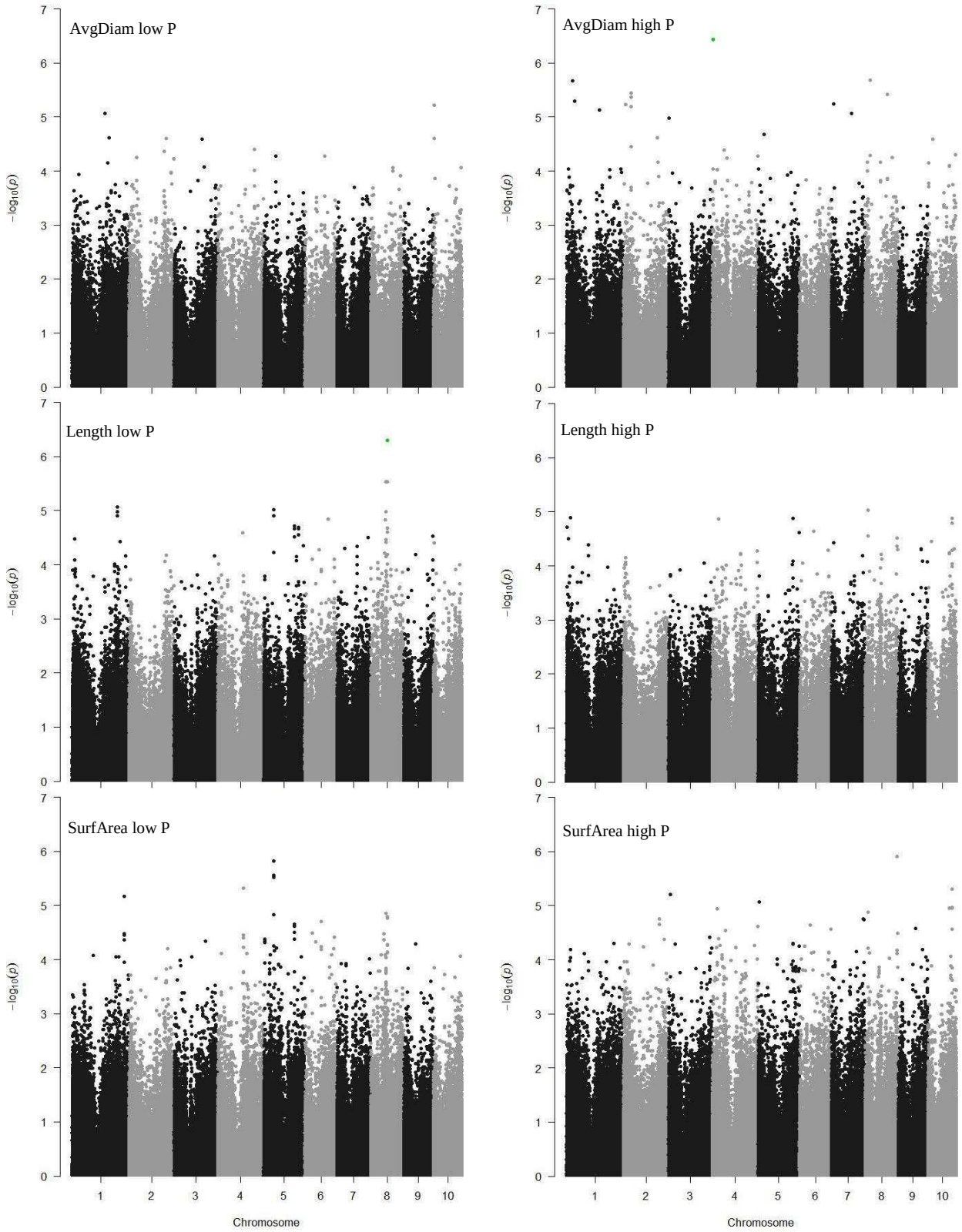

Figure S2. Manhattan plot for AvgDiam, Length and SurfArea for low and high P conditions using MLM (PC + K) in a panel of 563 inbred lines with a total of 353,540 SNP markers. The green points represent the significant SNPs with $-\log_{10}$(P-value) ≥ 6.

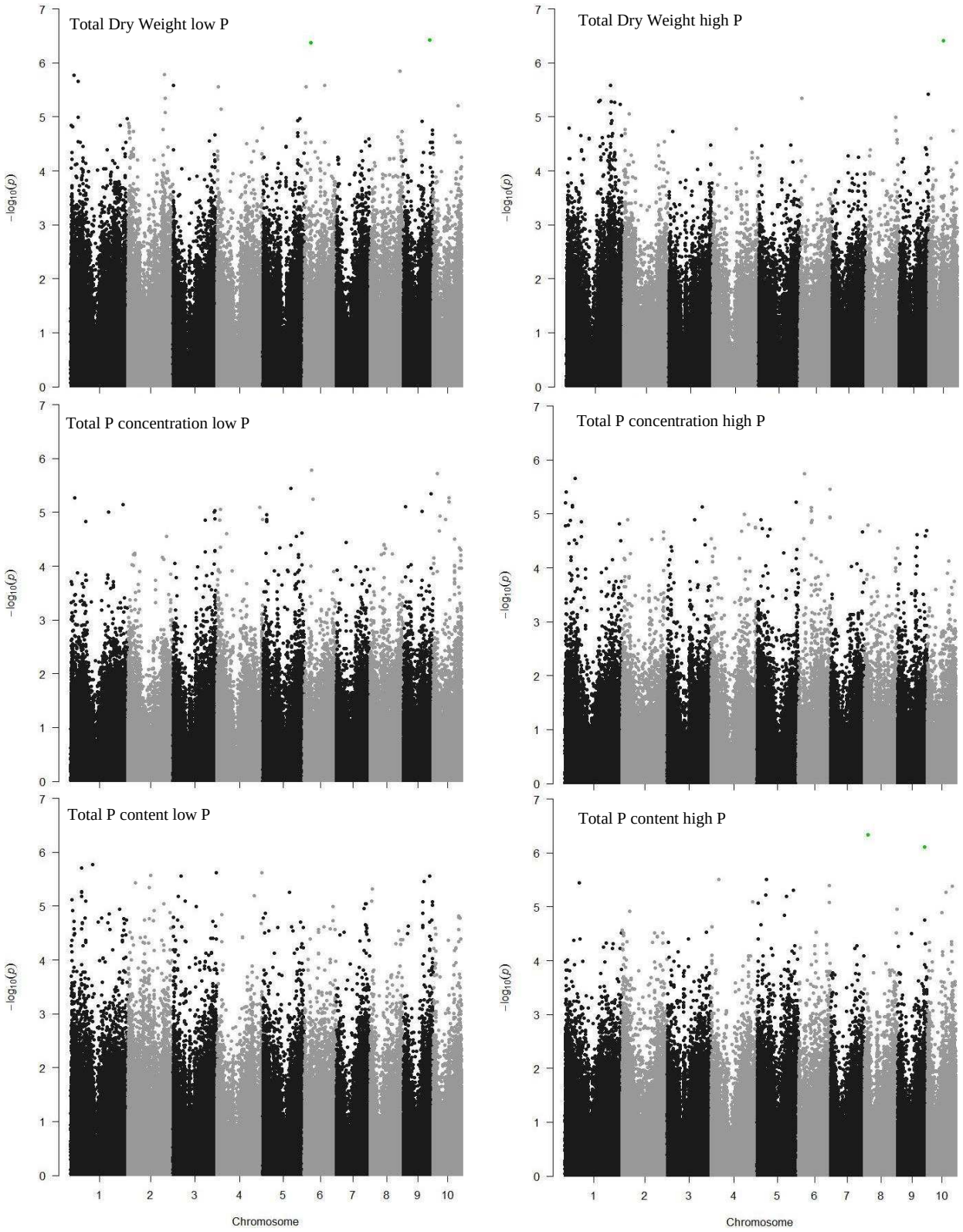

Figure S3. Manhattan plot for total seedling dry weight, total seedling P concentration and total seedling P Content for low and high P conditions using MLM (PC + K) in a panel of 563 inbred lines with a total of 353,540 SNP markers. The green points represent the significant SNPs with $-\log_{10}$(P-value) ≥ 6.

CONCLUSÃO GERAL

O mapeamento de QTL foi realizado em duas populações bi-parentais ($F_{2:3}$) de milho tropical, sendo identificadas 52 regiões genômicas relacionadas com a produção de grãos, altura de planta e intervalo de florescimento sob estresse hídrico e irrigação plena. Por meio da abordagem de modelos mistos, as características fenológicas de altura de planta e intervalo de florescimento foram utilizadas como covariáveis no mapeamento de QTLs para produção de grãos. Alguns dos QTLs para produção de grãos foram co-localizados com os QTLs para altura de planta e intervalo de florescimento, indicando um efeito das características fenológicas na produção de grãos. Com isso, o uso das covariáveis fenológicas possibilitou uma maior acurácia na detecção dos QTLs para produção de grãos com e sem estresse hídrico. Várias dessas regiões apresentaram efeito constante entre diferentes ambientes. Combinando todas as informações, quatro regiões genômicas apresentaram QTLs para produção de grãos coincidentes nas duas populações, sendo todas confirmadas pela identificação de QTLs e de genes candidatos associados com tolerância ao estresse hídrico em outros estudos. A estabilidade dessas regiões em diferentes ambientes e backgrounds genéticos, demonstra uma potencial utilização em programas de seleção assistida visando a obtenção de cultivares de milho com maior estabilidade de produção sob deficiência hídrica.

Um estudo de associação genômica ampla foi realizado em um painel contendo 561 linhagens de milho tropical da Embrapa Milho e Sorgo e do CIMMYT, genotipado com mais de 350.000 SNPs e avaliado para características de morfologia radicular e de aquisição de fósforo (P) em solução nutritiva sob alta e baixa concentração de P. O desequilíbrio de ligação apresentou um rápido decaimento médio (1.000 pb), demonstrando uma alta diversidade genética no painel. Um total de 136 SNPs foram significativamente associados com seis características fenotípicas mais relevantes, distribuídos ao longo de todo o genoma do milho. O SNP S8_89092905, altamente associado com comprimento total radicular e área superficial de raiz sob baixo P, foi localizado dentro do gene predito GRMZM2G044531, que codifica uma provável proteína da família AGC quinase. Outro SNP significativamente associado com as mesmas características radiculares (S8_88964594), foi localizado dentro do gene GRMZM2G057116, que codifica um fator de transcrição da família WRKY. Apesar dos SNPs estarem a mais de 120 kbp de distância física, eles possuem um elevado desequilíbrio de ligação ($r^2 = 0,77$), sugerindo fortemente que essa região

genômica (bin 8.03) esteja associada com a morfologia radicular e com potencial aumento na eficiência de aquisição de P.

Interessantemente, as duas estratégias utilizadas para dissecar componentes genéticos de características complexas como tolerância à seca e eficiência no uso de fósforo em milho, apontaram uma região genômica comum - bin 8.03 - no cromossomo 8. Nessa região foram identificados, além dos genes candidatos citados anteriormente, QTLs para produção de grãos coincidentes nas duas populações de milho tropical avaliadas sob regimes hídricos contrastantes, o que sugere a necessidade de uma investigação mais aprofundada dessa região, em nível tanto de mapeamento fino, visando identificar mais precisamente os genes relacionados à produção de grãos, quanto na caracterização dos potenciais genes candidatos identificados para morfologia radicular.